A survey to the NuTeV anomaly: significance of the nuclear parton distributions

Hannu Paukkunen[1]

University of Jyväskylä
Department of Physics

Pro Gradu Thesis

December 2005

[1]htpaukku@st.jyu.fi

Prologue

Do not keep saying to yourself, if you can possibly avoid it, "But how can it be like that?" because you will get "down the drain," into a blind alley from which nobody has yet escaped. Nobody knows how it can be like that.

Feynman

As I am interested in the theory of the particle physics, I find it very annoying to take any formulas as "God's gift" without knowing how they exactly come about, and just feed them on numbers. Occasionally, to make any progress with a physical problem, one cannot, however, avoid it. But doing such, bothers me and this is the reason why this thesis became quite long: I wanted to explicitly include many nontrivial calculations and the field theory related calculations are usually not the shortest ones.

I am most grateful to my supervisor Kari J. Eskola for a fruitful collaboration and being patient enough as I have took my time really digging into the subject. My special thanks goes also to the professor Vesa Ruuskanen for pointing out some of my mistakes that are now absent from this thesis. For the financial support, I acknowledge the grants from the URHIC project at the Helsinki Institute of Physics and from the Academy of Finland, project 206024.

Finally, I wish to thank my parents and all my sisters for their love and care on the road I have chosen.

At Kortepohja, Jyväskylä just before Christmas 2005

Hannu Paukkunen

Contents

1 Introduction **7**
- 1.1 Strange result from Fermilab! . . . 7
- 1.2 Experiment . . . 7
- 1.3 Possible explanations . . . 9

2 Electroweak Lagrangian **11**
- 2.1 Gauge transformation . . . 12
- 2.2 Covariant derivative . . . 12
- 2.3 Field strengths . . . 13
- 2.4 Particle content . . . 14
- 2.5 Charged-current interactions . . . 15
- 2.6 Neutral-current interactions . . . 15
- 2.7 Gauge boson self-interactions . . . 17
- 2.8 The Higgs mechanism . . . 17
- 2.9 Gauge boson masses . . . 18
- 2.10 Fermion masses . . . 19

3 Tree-level quantization **21**
- 3.1 Correlation functions in path integral formalism . . . 21
- 3.2 Change of representation . . . 22
- 3.3 Choice of gauge . . . 23
- 3.4 Heavy boson propagator . . . 24
- 3.5 Goldstone propagator . . . 28
- 3.6 Fermion propagator . . . 28
- 3.7 Interacting theory . . . 31

4 Deep inelastic scattering **35**
- 4.1 Deep inelastic scattering in a nutshell . . . 35
  - 4.1.1 Kinematics . . . 36
  - 4.1.2 General cross-section formula . . . 37
- 4.2 Charged current neutrino DIS . . . 37
  - 4.2.1 General charged current matrix element . . . 37
  - 4.2.2 Leptonic tensor . . . 39
  - 4.2.3 Hadronic tensor . . . 40
  - 4.2.4 Contraction $L^{\mu\nu}W_{\mu\nu}$ . . . 41
  - 4.2.5 Antineutrino scattering . . . 43
  - 4.2.6 DIS in the parton model . . . 44
  - 4.2.7 Accommodating antiquarks . . . 48

4.2.8 $\overline{\nu}h$ DIS in the parton model . . . 49
4.3 Neutral current DIS . . . 50
4.3.1 General neutral current cross-section . . . 50
4.3.2 Connection to the parton model . . . 51
4.4 QED DIS . . . 52
4.4.1 Parton model DIS in QED . . . 53
4.5 Drell-Yan process . . . 54
4.5.1 The quark sub-process . . . 54
4.5.2 Embedding to hadronic level . . . 57
4.6 Phenomenology: from free proton to the bound nucleus . . . 58
4.6.1 Structure function ${}^{EM}F_2$ for free proton . . . 58
4.6.2 Nuclear effects . . . 62
4.6.3 EKS98 parametrization . . . 63

5 nPDFs and NuTeV anomaly 67
5.1 Observables R^ν, $R^{\overline{\nu}}$ and R^- . . . 67
5.1.1 Sophistications to structure functions . . . 67
5.1.2 Observables R^ν and $R^{\overline{\nu}}$ and Llewellyn Smith formula . . . 68
5.1.3 Observable R^- and Paschos-Wolfenstein formula . . . 70
5.2 Can $R^A_{d/V} \neq R^A_{u/V}$ cause NuTeV anomaly? . . . 71
5.2.1 The procedure . . . 72
5.2.2 Results . . . 73
5.2.3 Consequences in R_{DY} and R_{F_2} . . . 76
5.3 Conclusion an outlook . . . 77

Chapter 1

Introduction

1.1 Strange result from Fermilab!

The Weinberg weak mixing angle $\sin^2\theta_{\mathrm{W}}$ is one of the most crucial parameters in The Standard Model of particle physics. The current world average of this quantity combined from several experiments is [1]

$$\left\langle \sin^2\theta_{\mathrm{W}} \right\rangle = 0.2227 \pm 0.00037.$$

A few years ago, the NuTeV collaboration announced [2] that their measurements in deep inelastic neutrino-nucleus scattering indicated the value of Weinberg weak mixing angle

$$\sin^2\theta_{\mathrm{W}}^{\mathrm{NuTeV}} = 0.2277 \pm 0.0013(stat) \pm 0.0009(syst).$$

The result was surprising and unexpected being about 3σ apart from the world average value. Today, this deviation — the NuTeV anomaly — still remains as an open question without a unique explanation.

1.2 Experiment

Neutrino and antineutrino beams needed in the experiment were produced as follows (see also fig. 1.1): High energy (800 GeV) protons from the Tevatron were first impinged on a BeO target. The subsequent shower of hadrons entered in the Sign Selected Quadrupole Train (SSQT) — a group of dipole magnets that selected the pions and kaons of a particular charge to a secondary beam toward the NuTeV target. These subsequently decayed producing muons and either neutrinos or antineutrinos depending of the charge of the meson:

$$\pi^+, K^+ \to \mu^+ + \nu_\mu$$

$$\pi^-, K^- \to \mu^- + \overline{\nu}_\mu.$$

At the last stage, the residual muons were removed from the beam by the muon shield — a huge block of lead and steel.

The actual NuTeV target shown in fig. 1.2 consisted of steel (mainly iron ^{56}Fe) plates interspersed with scintillation counters and drift chambers. At the

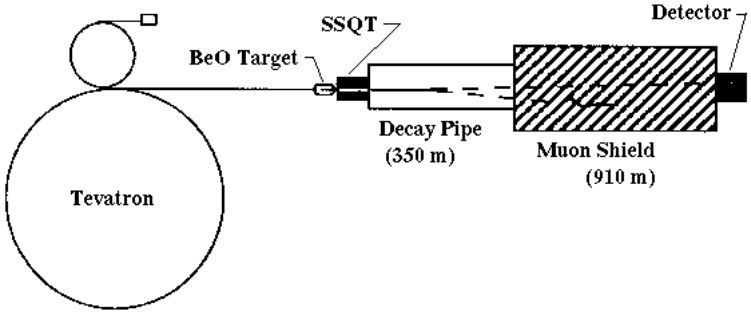

Figure 1.1: Conceptual sketch from the NuTeV beamline [3].

end of the detector there was a muon detector. Every now and then a neutrino interacted with a iron nucleus producing a shower of hadrons. The events were classified to the charged current (CC) and neutral current (NC) events according to whether there was a muon in the final state or not, as illustrated in fig. 1.3.

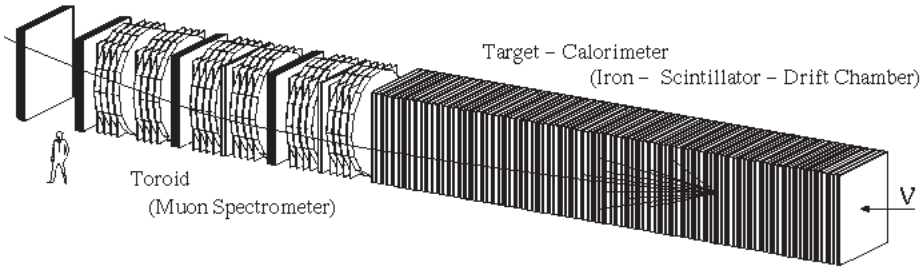

Figure 1.2: The target used in the NuTeV experiment [3].

From the number of counted NC and CC events the NuTeV collaboration extracted the cross-section ratios

$$R^{\nu} \equiv \frac{\sigma^{NC}(\nu N)}{\sigma^{CC}(\nu N)} \tag{1.1}$$

$$R^{\overline{\nu}} \equiv \frac{\sigma^{NC}(\overline{\nu} N)}{\sigma^{CC}(\overline{\nu} N)}. \tag{1.2}$$

for ν and $\overline{\nu}$ beams. Both of these can be separately related to the weak mixing angle $\sin^2\theta_{\mathrm{W}}$ but to reduce the amount of uncertainties arising from the nuclear parton distributions, they were combined to a single observable

$$R^{-} \equiv \frac{\sigma^{NC}(\nu N) - \sigma^{NC}(\overline{\nu} N)}{\sigma^{CC}(\nu N) - \sigma^{CC}(\overline{\nu} N)} \tag{1.3}$$

which is also related to $\sin^2\theta_{\mathrm{W}}$. The actual extraction of the value of $\sin^2\theta_{\mathrm{W}}$ trusted on a sophisticated Monte Carlo simulation which is needed to predict the

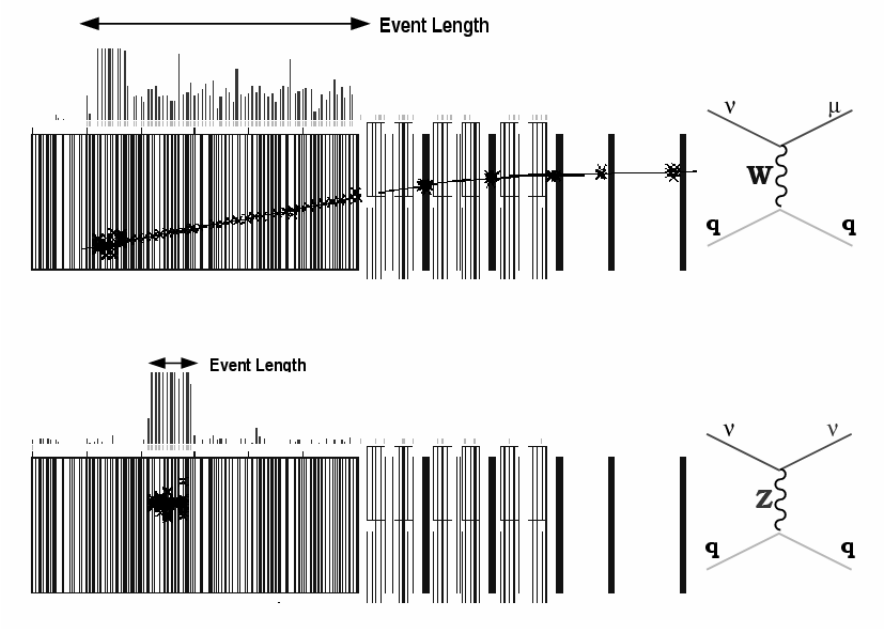

Figure 1.3: Example of CC and NC events in the NuTeV detector. In the CC reaction there is muon in the final state and the energy deposited in the detector is distributed along the muon track. NC event is distinguished from the CC one since there is no muon in the final state and the energy is deposited in a much smaller volume [3].

actual flux and energy distribution of the incoming neutrinos. Having considered and examined various sources of errors the NuTeV group then reported their astonishing result which has thereafter caught a great deal of attention by the particle physics community.

1.3 Possible explanations

A number of proposed resolutions extending from the conventional explanations within the Standard Model [4, 5] to the more exotic ones that would require novel physics outside the Standard Model [6, 5], has emerged.

As intriguing as it would be to see some new physics appearing in the result it has turned out to be quite difficult to find beyond-Standard-Model physics that would explain the NuTeV anomaly while agreeing with other precision electroweak measurements. Exotics like extra Z vector bosons or Leptoquarks would need to be precisely 'fine-tuned' in order to reconcile the anomaly while the loop corrections from Supersymmetric models tend to be in wrong direction [7]. Question about varying coupling constant G_F and mixing angle $\sin^2\theta_{\mathrm{W}}$ from a process to another has also been posed [8] and even the possibility of magnetic monopoles has been proposed [9] to be hiding behind the anomaly! This just illustrates how amazing the result in question is.

However, it is important to carefully investigate whether the NuTeV anomaly

could be explained within the current framework of Standard Model. The possible effects of the next-to-leading-order QCD [6, 10] and the radiative electroweak corrections [11, 12] are supposed to be under control. But all relevant contributions were not implemented in the original NuTeV analysis and there is still a question mark about the issue.

Another thing that has to be taken into account is that the NuTeV target is mainly iron and some consequences from the non-isoscalar nature of a fairly heavy nucleus can arise. Indeed, the recent discussion implies that considerable part of the NuTeV anomaly can be simply due to our insufficient knowledge of the parton structure of the heavy nucleus! Although still uncertain at this stage, the possible asymmetry between strange and antistrange quark distributions $S^- \equiv \int x[s(x) - \overline{s}(x)]dx \neq 0$ [13, 14, 15] and isospin violating PDFs [13, 15] may both be viable in interpreting the anomaly.

The main purpose of this thesis is to study the NuTeV anomaly from the point of view of nuclear parton distributions (nPDFs). Particularly, we point out that the possible difference between the nuclear corrections for the valence-u and valence-d distributions in a bound proton compared to to the free proton ones contributes to the anomaly. This difference may, as we show, be significant enough to explain the NuTeV anomaly without disagreeing with other experimental data constraining the nPDFs.

Before we attack this issue, we need to do some preparations. First, we briefly review the electroweak Lagrangian and then quantize it to such extent that simple tree-level contributions to scattering events can be computed. We go on and work out the cross-sections for deep inelastic scattering and Drell-Yan processes and after these preliminaries we are ready to discuss the NuTeV experiment.

We will derive some simple expressions for R^ν, $R^{\overline{\nu}}$ and R^- — often mentioned when these observables are discussed — that relate them to $\sin^2\theta_{\mathrm{W}}$. At the end we present the results of our numerical calculations [16] that demonstrate the chance that the NuTeV anomaly could be due to the different nuclear effects between u-valence and d-valence quark distributions.

Chapter 2

Electroweak Lagrangian

The Standard Model of the electroweak interactions is a beautiful example of close interplay between experiments and theoretical notions. On the one hand there is a deep theoretical principle of gauge invariance that fixes the framework and constrains the possible interactions. The remaining freedom is then fixed in such a way that the phenomenology observed in the experiments is correctly reproduced. The most important underlying experimental facts are:

- Only left-handed fermions and right-handed antifermions participate in weak processes such as β-decays $n \to p\,\overline{\nu}_e\,e^-$ or $\mu^- \to e^-\,\overline{\nu}_e\,\nu_\mu$. Thus, parity is broken in weak interactions. The strength of the interaction appears to be universal in such processes.

- Only left-handed neutrinos and right-handed antineutrinos exist.

- Fermions come in three families.

- Lepton number is conserved.

Such facts were good enough for Steven Weinberg and Abdus Salam to formulate the unified electroweak theory that describes the electrodynamics and weak phenomena [17, 18]. It was originally an idea of Sheldon Glashow that the weak phenomena are mediated by heavy intermediate bosons. But such a theory was ill-defined: it was not renormalizable. In the Weinberg model the intermediate bosons are originally massless but become massive due to the spontaneous symmetry breaking — the Higgs mechanism. As Geradus 't Hooft later showed, such a theory is indeed renormalizable. This theory has been hugely successfull and at present the only missing piece is the experimental evidence of the Higgs boson that emerges from the spontaneous symmetry breaking and gives all fermions and heavy bosons their masses.

In what follows, we will review how the Lagrangian of the Glashow-Weinberg-Salam model (GWS-model for short) emerges from the requirement of gauge invariance and how parity breaking is introduced.

2.1 Gauge transformation

The underlying principle fo the GWS theory is to require Lagrangian to remain invariant under local $SU(2) \times U(1)$ gauge transformations

$$V(x) \equiv e^{iY\beta(x)} e^{iT^i \alpha^i(x)} \tag{2.1}$$

where Y is the *weak hypercharge* operator and T^i's are hermitian *weak isospin* generators satisfying the $SU(2)$ algebra

$$[T^i, T^j] = i\epsilon^{ijk}\, T^k, \tag{2.2}$$

where ϵ^{ijk} is completely antisymmetric Levi-Civita symbol

$$\epsilon^{ijk} = \begin{cases} +1 & \text{if } ijk \text{ is even permutation of 123,} \\ -1 & \text{if } ijk \text{ is odd permutation of 123,} \\ 0 & \text{otherwise.} \end{cases} \tag{2.3}$$

2.2 Covariant derivative

To include fermions we should have the kinetic term

$$i\overline{\Psi}\gamma^\mu \partial_\mu \Psi, \tag{2.4}$$

where Ψ is a four-component spinor and $\overline{\Psi} \equiv \Psi^\dagger \gamma^0$, where γ^0 is one of the four Dirac-matrices γ^μ. Such terms gives the Dirac equation as a equation of motion for massless fermions. This includes the derivative ∂_μ. The problem is that the usual definition of the derivative

$$n^\mu \partial_\mu \Psi(x) = \lim_{\epsilon \to 0} \frac{1}{\epsilon} \left[\Psi(x + \epsilon n) - \Psi(x)\right] \tag{2.5}$$

makes no sense since the two terms in square brackets transform in a different way. To solve this problem we define unitary *comparator* $U(y, x)$ between two space-time points with a transformation property

$$U(y, x) \to V(y) U(y, x) V^\dagger(x). \tag{2.6}$$

Now the quantity $U(y, x)\Psi(x)$ transforms as

$$U(y, x)\Psi(x) \to V(y) U(y, x) \Psi(x), \tag{2.7}$$

which is exactly how $\Psi(y)$ transforms. Thus, it makes sense to define the *covariant derivative*

$$n^\mu D_\mu \Psi(x) = \lim_{\epsilon \to 0} \frac{1}{\epsilon} \left[\Psi(x + \epsilon n) - U(x + \epsilon n, x)\Psi(x)\right]. \tag{2.8}$$

Due to the unitarity and natural requirement $U(y, y) = 1$, $U(y, x)$ can be taken as pure phase

$$U(x, y) = e^{if(x,y)}$$

where $f(x, y)$ is a smooth function constructed out of operators Y and T^i. Expanding this for infinitesimal ϵ gives

$$U(x + \epsilon n) = 1 + i\epsilon n^\mu \left[g A^i_\mu(x) T^i + g' B_\mu(x) Y\right], \tag{2.9}$$

where g and g' are real constants and $B_\mu(x)$ and $A^i_\mu(x)$ are real *vector fields*. Using this expansion in 2.8 we end up with

$$D_\mu\Psi(x) = \left[\partial_\mu - igA_\mu(x) - ig'B_\mu(x)Y\right]\Psi(x), \tag{2.10}$$

where $A_\mu(x) \equiv A^i_\mu(x)T^i$. The transformation properties of $A^i_\mu(x)$ and $B_\mu(x)$ can be inferred from (2.6) as

$$igA_\mu(x) + ig'B_\mu(x)Y \to V(x)\left[-\partial_\mu + igA_\mu(x) + ig'B_\mu(x)Y\right]V^\dagger(x), \tag{2.11}$$

or for an infinitesimal transformation

$$\begin{aligned} B_\mu(x) &\to B_\mu(x) + \frac{1}{g'}\,\partial_\mu\beta(x) \\ A^i_\mu(x) &\to A^i_\mu(x) + \frac{1}{g}\partial_\mu\alpha^i(x) + \epsilon^{ijk}A^j_\mu\alpha^k(x). \end{aligned} \tag{2.12}$$

With these transformation properties the covariant derivative $D_\mu\Psi$ transforms as the field on which it acts:

$$D_\mu\Psi(x) \to V(x)D_\mu\Psi(x),$$

and the kinetic term

$$\mathcal{L}_\Psi \equiv i\overline{\Psi}\gamma^\mu D_\mu\Psi \tag{2.13}$$

is invariant under the gauge transformation $V(x)$.

2.3 Field strengths

As we introduced 4 vector fields we should then add also the kinetic terms

$$-\frac{1}{4}\left(\partial_\mu B_\nu - \partial_\nu B_\mu\right)\left(\partial^\mu B^\nu - \partial^\nu B^\mu\right)$$

in order to interpret them as true propagating gauge bosons. Such terms give a massless Klein-Gordon equation as a equation of motion. For B_μ singlet this works as such but for A^i_μ triplet the kinetic term alone would break the gauge invariance! Thus, we need some additional terms to ensure the gauge invariance.

The general procedure for obtaining kinetic terms for gauge bosons is to compute the commutator of covariant derivatives

$$\begin{aligned} [D_\mu, D_\nu] &= -ig\left(\partial_\mu A_\nu - \partial_\nu A_\mu - ig[A_\mu, A_\nu]\right) \\ &\quad -ig'\left(\partial_\mu B_\nu - \partial_\nu B_\mu\right), \end{aligned} \tag{2.14}$$

from which we can read the *field strengths* $\tilde{B}_{\mu\nu}$ and $\tilde{A}_{\mu\nu}$

$$\begin{aligned} \tilde{A}_{\mu\nu} &\equiv \partial_\mu A_\nu - \partial_\nu A_\mu - ig[A_\mu, A_\nu] \\ \tilde{B}_{\mu\nu} &\equiv \partial_\mu B_\nu - \partial_\nu B_\mu \end{aligned} \tag{2.15}$$

The $\tilde{B}_{\mu\nu}$ is gauge invariant as such and we can add aterm $\propto \tilde{B}_{\mu\nu}\tilde{B}^{\mu\nu}$ into the Lagrangian. Although $\tilde{A}_{\mu\nu}$ is not invariant,

$$\tilde{A}_{\mu\nu} \to \tilde{A}'_{\mu\nu} = V\tilde{A}_{\mu\nu}V^\dagger,$$

it is easy to see that the trace of the product $\tilde{A}_{\mu\nu}\tilde{A}^{\mu\nu}$ is:

$$\mathrm{Tr}\left(\tilde{A}'_{\mu\nu}\tilde{A}'^{\mu\nu}\right) = \mathrm{Tr}\left(V\tilde{A}_{\mu\nu}V^{\dagger}V\tilde{A}^{\mu\nu}V^{\dagger}\right) = \mathrm{Tr}\left(\tilde{A}_{\mu\nu}\tilde{A}^{\mu\nu}\right). \tag{2.16}$$

The trace can be evaluated using the $SU(2)$ algebra (2.2) giving

$$\mathrm{Tr}\left(\tilde{A}_{\mu\nu}\tilde{A}^{\mu\nu}\right) \propto \tilde{A}^{i}_{\mu\nu}\tilde{A}^{\mu\nu,\,i}. \tag{2.17}$$

Thus, the properly normalized gauge invariant terms we add to the Lagrangian are

$$-\frac{1}{4}\tilde{B}_{\mu\nu}\tilde{B}^{\mu\nu} - \frac{1}{4}\tilde{A}^{i}_{\mu\nu}\tilde{A}^{\mu\nu,\,i}. \tag{2.18}$$

2.4 Particle content

The interactions between fermions and gauge fields are fixed by the covariant derivative in (2.13) and as the $W^{\pm}$ bosons should couple only to the left-handed fermions, we should treat left- and right-handed fermions in a different manner.

The left- and right-handed components of the Dirac spinor Ψ are most conveniently obtained using the projection operators:

$$\text{Left handed spinor}: \quad \Psi_L = P_L\Psi = \left(\frac{1-\gamma^5}{2}\right)\Psi \tag{2.19}$$

$$\text{Right handed spinor}: \quad \Psi_R = P_R\Psi = \left(\frac{1+\gamma^5}{2}\right)\Psi, \tag{2.20}$$

with $\gamma^5 \equiv i\gamma^0\gamma^1\gamma^2\gamma^3$. Using these it is easy to see that the kinetic term for fermions splits in two pieces

$$i\overline{\Psi}\gamma^{\mu}\partial_{\mu}\Psi = i\overline{\Psi}_L\gamma^{\mu}\partial_{\mu}\Psi_L + i\overline{\Psi}_R\gamma^{\mu}\partial_{\mu}\Psi_R, \tag{2.21}$$

and we are fully allowed to assign Ψ_L and Ψ_R in different representations of the gauge group and still maintain the gauge invariance.

In the GWS-theory, the left-handed fermions are assigned to doublets whereas the right-handed fermions are assigned to singlets:

$$\begin{pmatrix}\nu_e\\ e^-\end{pmatrix}_L \quad \begin{pmatrix}u\\ d\end{pmatrix}_L \quad (e^-)_R \quad (u)_R \quad (d)_R$$

$$\begin{pmatrix}\nu_\mu\\ \mu^-\end{pmatrix}_L \quad \begin{pmatrix}c\\ s\end{pmatrix}_L \quad (\mu^-)_R \quad (c)_R \quad (s)_R$$

$$\begin{pmatrix}\nu_\tau\\ \tau^-\end{pmatrix}_L \quad \begin{pmatrix}t\\ b\end{pmatrix}_L \quad (\tau^-)_R \quad (t)_R \quad (b)_R$$

In the Standard Model there is no right-handed neutrinos and hence they are not included to the chart above.

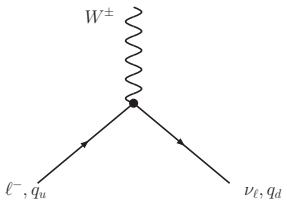

Figure 2.1: Charged-current interaction vertex where charged lepton ℓ^- and corresponding neutrino ν_ℓ interact. 'Upper quarks' u, c and t are denoted collectively by q_u and 'lower quarks' d, s and b by q_d.

2.5 Charged-current interactions

Charged current interactions are mediated by charged $W^{\pm}$ boson and hence the corresponding vector field should be complex. Indeed, as left-handed particles are assigned to doublets the corresponding generators T are just Pauli matrices $T^i = \sigma^i/2$ and then

$$\begin{aligned} A_\mu \equiv A_\mu^i \frac{\sigma^i}{2} &= \frac{1}{2}\begin{pmatrix} A_\mu^3 & A_\mu^1 - iA_\mu^2 \\ A_\mu^1 + iA_\mu^2 & -A_\mu^3 \end{pmatrix} \\ &= \frac{1}{\sqrt{2}}\begin{pmatrix} A_\mu^3/\sqrt{2} & W_\mu^\dagger \\ W_\mu & -A_\mu^3/\sqrt{2} \end{pmatrix}, \end{aligned} \tag{2.22}$$

where we defined a complex vector field $W_\mu \equiv \left(A_\mu^1 + iA_\mu^2\right)/\sqrt{2}$. To see that W_μ is really involved in CC interactions consider the interaction term for left-handed fermions

$$g\overline{\Psi}_L \gamma^\mu A_\mu \Psi_L. \tag{2.23}$$

Writing out terms containing W_μ and $W_\mu^\dagger$ for a single family of quarks and leptons produces interaction terms

$$\begin{aligned} \mathcal{L}_{CC} &= \frac{g}{\sqrt{2}}\left\{W_\mu^\dagger\left[\overline{u}_L\gamma^\mu d_L + \overline{\nu}_{eL}\gamma^\mu e_L\right] + \text{h.c.}\right\} \\ &= \frac{g}{2\sqrt{2}}\left\{W_\mu^\dagger\left[\overline{u}\gamma^\mu(1-\gamma^5)d + \overline{\nu}_e\gamma^\mu(1-\gamma^5)e\right] + \text{h.c.}\right\}, \end{aligned} \tag{2.24}$$

where *h.c.* stands for hermitian conjugation.

2.6 Neutral-current interactions

There are still two neutral fields A_μ^3 and B_μ from which we would like to identify Z and γ (photon) bosons. However, we cannot identify either of these alone as a photon field: A_μ^3 does not couple to right-handed fermions and if B_μ was to correspond photon field, fermions within the same doublet would have similar strength of interaction, i.e. the same electric charge. This is not true. The solution is to try an arbitrary linear combination of them

$$\begin{pmatrix} A_\mu^3 \\ B_\mu \end{pmatrix} = \begin{pmatrix} \cos\theta_{\text{W}} & \sin\theta_{\text{W}} \\ -\sin\theta_{\text{W}} & \cos\theta_{\text{W}} \end{pmatrix}\begin{pmatrix} Z_\mu^0 \\ A_\mu \end{pmatrix}, \tag{2.25}$$

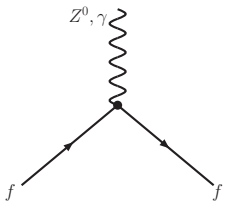

Figure 2.2: Neutral current and QED interaction vertex. In the case of Z interaction f can be any fermion but when the intermediate boson is photon, the fermion f must be a charged one.

where parameter θ_{W} is the *Weinberg weak-mixing angle* and A_μ and Z^0_μ are the fields corresponding to the real observed photon and Z-boson. Writing out the remaining interaction terms yields

$$\overline{\Psi}\gamma^\mu \left[A_\mu \left(\frac{\sigma^3}{2} g \sin\theta_{\mathrm{W}} + Y g' \cos\theta_{\mathrm{W}} \right) + Z^0_\mu \left(\frac{\sigma^3}{2} g \cos\theta_{\mathrm{W}} - Y g' \sin\theta_{\mathrm{W}} \right) \right] \Psi.$$

In order to have A_μ describing the photon field the following conditions must be satisfied:

$$g \sin\theta_{\mathrm{W}} = g' \cos\theta_{\mathrm{W}} = e \qquad \frac{\sigma^3}{2} + Y = Q, \tag{2.26}$$

where e is unit charge and Q is electric charge operator. Thus, the Lagrangian for electromagnetic interactions becomes

$$\mathcal{L}_{\mathrm{QED}} = e A_\mu \overline{\Psi}\gamma^\mu Q \Psi. \tag{2.27}$$

The conditions (2.26) also fix the Lagrangian for neutral current interactions:

$$\begin{aligned} \mathcal{L}_{NC} &= \frac{e}{2\sin\theta_{\mathrm{W}}\cos\theta_{\mathrm{W}}} Z^0_\mu \overline{\Psi}\gamma^\mu \left(\sigma^3 - 2Qe\sin^2\theta_{\mathrm{W}}\right)\Psi \\ &= \frac{e}{2\sin\theta_{\mathrm{W}}\cos\theta_{\mathrm{W}}} Z^0_\mu \\ &\quad \left[\overline{\Psi}_L\gamma^\mu \left(\sigma^3 - 2Qe\sin^2\theta_{\mathrm{W}}\right)\Psi_L + \overline{\Psi}_R\gamma^\mu \left(-2Qe\sin^2\theta_{\mathrm{W}}\right)\Psi_R\right]. \end{aligned} \tag{2.28}$$

Since σ^3 and Q are diagonal this can be written separately for each fermion type in terms of usual Dirac spinors f as

$$\mathcal{L}_{NC} = g_Z \overline{f}\gamma^\mu \left[L_f(1-\gamma^5) + R_f(1+\gamma^5)\right] f, \tag{2.29}$$

where

$$\begin{aligned} g_Z &= \frac{e}{4\sin\theta_{\mathrm{W}}\cos\theta_{\mathrm{W}}} \\ L_f &= T^3_f - 2Q_f \sin^2\theta_{\mathrm{W}} \\ R_f &= -2Q_f \sin^2\theta_{\mathrm{W}}. \end{aligned} \tag{2.30}$$

Here $T^3_f \equiv \sigma^3$ and Q_f are the quantum numbers of the corresponding operators. The values of L_f and R_f for fermions are summarized in Table (2.1).

Table 2.1: Neutral-current couplings of fermions

coupling	ν_e, ν_μ, ν_τ	e, μ, τ	u, c, t	d, s, b
L_f	1	$-1+2\sin\theta_{\rm W}$	$1-\frac{4}{3}\sin\theta_{\rm W}$	$-1+\frac{2}{3}\sin\theta_{\rm W}$
R_f	0	$2\sin\theta_{\rm W}$	$-\frac{4}{3}\sin\theta_{\rm W}$	$\frac{2}{3}\sin\theta_{\rm W}$

2.7 Gauge boson self-interactions

Due to the non-Abelian nature of $SU(2)$, eq. (2.18) includes, apart from the kinetic terms, interactions between gauge bosons. There are cubic and quartic terms:

$$\begin{aligned}
\mathcal{L}_3 &= -ie\cot\theta_{\rm W}\left\{\left(\partial^\mu W^\nu-\partial^\nu W^\mu\right)W^\dagger_\mu Z_\nu-\left(\partial^\mu W^{\nu\dagger}-\partial^\nu W^{\mu\dagger}\right)W_\mu Z_\nu\right.\\
&\quad\left.+\left(\partial^\mu Z^\nu-\partial^\nu Z^\mu\right)W_\mu W^\dagger_\nu\right\}\\
&\quad -ie\left\{\left(\partial^\mu W^\nu-\partial^\nu W^\mu\right)W^\dagger_\mu A_\nu-\left(\partial^\mu W^{\nu\dagger}-\partial^\nu W^{\mu\dagger}\right)W_\mu A_\nu\right.\\
&\quad\left.+\left(\partial^\mu A^\nu-\partial^\nu A^\mu\right)W_\mu W^\dagger_\nu\right\}\\
\mathcal{L}_4 &= -\frac{e^2}{2\sin\theta_{\rm W}}\left\{(W^\dagger_\mu W^\mu)^2-W^\dagger_\mu W^{\mu\dagger}W_\nu W^\nu\right\}\\
&\quad -e^2\cot^2\theta_{\rm W}\left\{W^\dagger_\mu W^\mu Z_\nu Z^\nu+W^\dagger_\mu W^\nu Z_\nu Z^\mu\right\}\\
&\quad -e^2\left\{W^\dagger_\mu W^\mu A_\nu A^\nu+W^\dagger_\mu W^\nu A_\nu A^\mu\right\}\\
&\quad -e^2\cot\theta_{\rm W}\left\{2W^\dagger_\mu W^\mu A_\nu Z_\nu-W^\dagger_\mu W^\nu\left[A_\nu Z^\mu+Z_\nu A^\mu\right]\right\}.
\end{aligned}\tag{2.31}$$

The generated vertices are shown in fig. 2.3.

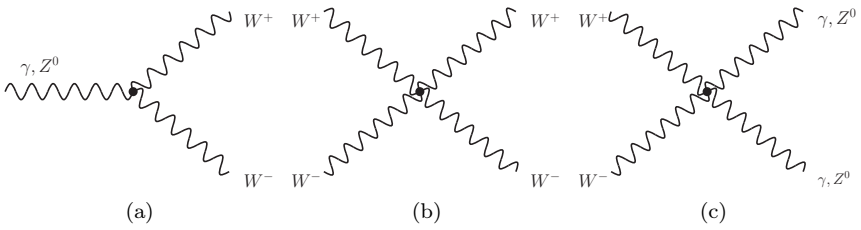

Figure 2.3: Gauge interactions

2.8 The Higgs mechanism

At this stage all particles, fermions and gauge bosons, are still massless: had we included the mass terms $-m\overline{\Psi}\Psi=-m\left(\overline{\Psi}_L\Psi_R+\overline{\Psi}_R\Psi_L\right)$ for fermions and/or $M_W^2W^\dagger_\mu W^\mu+\frac{1}{2}M_Z^2Z_\mu Z^\mu$ for gauge bosons, the gauge invariance would not be respected. However, we know that fermions and gauge bosons are massive and a possible way to introduce mass terms is via the Higgs mechanism.

Let us introduce a doublet of complex scalar fields

$$\phi(x) \equiv \begin{pmatrix} \phi^{(+)}(x) \\ \phi^{(0)}(x) \end{pmatrix} = \frac{1}{\sqrt{2}} \begin{pmatrix} \phi_1(x) + i\phi_2(x) \\ \phi_3(x) + i\phi_4(x) \end{pmatrix}, \tag{2.32}$$

where + and 0 refer to the electric charges, with a Lagrangian

$$\mathcal{L}_{\text{Higgs}} = (D_\mu \phi)^\dagger (D^\mu \phi) - V(\phi, \phi^\dagger), \tag{2.33}$$

where the potential V is

$$V = \mu^2 \phi^\dagger \phi + \lambda (\phi^\dagger \phi)^2 \tag{2.34}$$

with $\lambda > 0$ and $\mu^2 < 0$. Due to the covariant derivative, this is explicitly invariant under local $SU(2) \times U(1)$ gauge transformation. The Y quantum number of the doublet is fixed to be $Y_\phi = 1/2$ by the requirement that fields in the doublet have correct QED interactions.

Since $\mu^2 < 0$, the potential $V = \mu^2 \phi^\dagger \phi + \lambda (\phi^\dagger \phi)$ has a minimum that satisfies

$$\phi^\dagger \phi = \frac{1}{2}(\phi_1^2 + \phi_2^2 + \phi_3^2 + \phi_4^2) = \frac{-\mu^2}{2\lambda}. \tag{2.35}$$

There is of course an infinite amount of solutions for this equation and choosing one of them corresponds to the *spontaneous symmetry breaking* (SSB). Since the vacuum should be electrically neutral, only $Q = 0$ field can acquire vacuum expectation value and we choose $\phi_1 = \phi_2 = \phi_4 = 0$, whence

$$\phi_3^2 = \frac{-\mu^2}{\lambda} \equiv v^2, \tag{2.36}$$

and the field ϕ acquires a vacuum expectation value

$$< \phi > \equiv \phi_0 = \frac{1}{\sqrt{2}} \begin{pmatrix} 0 \\ v \end{pmatrix}. \tag{2.37}$$

Without loss of generality we can parametrize ϕ around the vacuum as

$$\phi(x) = \exp\left(i \frac{\sigma_i}{2} \chi_i(x) \right) \frac{1}{\sqrt{2}} \begin{pmatrix} 0 \\ v + H(x) \end{pmatrix}. \tag{2.38}$$

The three fields $\chi^i(x)$ correspond to the so called *Goldstone bosons* but due to the invariance of the Lagrangian under $SU(2)$ transformation we can always rotate away any χ dependence with a proper gauge transformation. This property makes these three fields unphysical and only one physical field $H(x)$ corresponding to the Higgs boson remains in the Lagrangian as we choose physical (unitary) gauge $\chi_i = 0$.

2.9 Gauge boson masses

In the unitary gauge the Lagrangian (2.33) becomes

$$\begin{aligned} \mathcal{L}_{\text{Higgs}} &= \frac{1}{2}\partial_\mu H \partial^\mu H + \frac{1}{4}\lambda v^4 - v^2 \lambda H^2 - \lambda v H^3 - \frac{1}{4} H^4 \\ &+ (v + H)^2 \left\{ \frac{g^2}{4} W_\mu^\dagger W^\mu + \frac{g^2}{8 \cos^2 \theta_{\text{W}}} Z_\mu Z^\mu \right\} \end{aligned} \tag{2.39}$$

which includes gauge boson and Higgs mass terms

$$M_W^2 W_\mu^\dagger W^\mu + \frac{1}{2} M_Z^2 Z_\mu Z^\mu - \frac{1}{2} M_H^2 H^2 \tag{2.40}$$

where

$$M_Z \cos\theta_{\rm W} = M_W = \frac{1}{2} v g, \qquad M_H = \sqrt{-2\mu^2} = \sqrt{2\lambda} v. \tag{2.41}$$

Thus, we can rewrite (2.39) as

$$\begin{aligned} \mathcal{L}_{\rm Higgs} &= \frac{1}{2}\partial_\mu H \partial^\mu H + \frac{1}{4}\lambda v^4 - \frac{1}{2} M_H^2 H^2 - \frac{M_H^2}{2v} H^3 - \frac{M_H^2}{8v^2} H^4 \\ &+ (1 + \frac{H}{v})^2 \left\{ M_W^2 W_\mu^\dagger W^\mu + \frac{1}{2} M_Z^2 Z_\mu Z^\mu \right\}, \end{aligned} \tag{2.42}$$

where also interaction terms appear. Interactions between Higgs and gauge bosons are shown in fig. 2.4 and Higgs self-interactions in fig. 2.5.

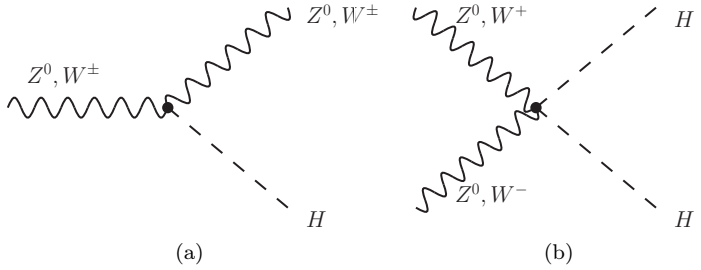

Figure 2.4: Gauge-Higgs interaction vertices

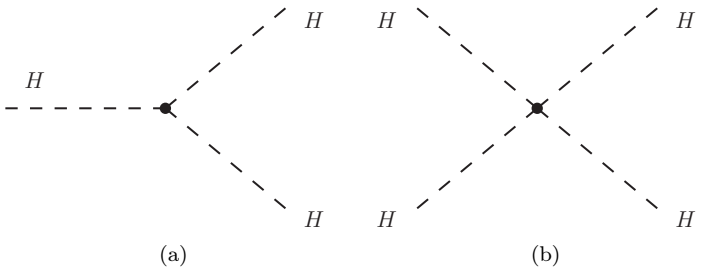

Figure 2.5: Higgs self-interaction vertices

2.10 Fermion masses

Let us couple the scalar doublet $\phi(x)$ and fermions in a gauge invariant way:

$$\begin{aligned} \mathcal{L}_{\rm Yukawa} &= f^e (\overline{\nu_e}\ \overline{e})_L \begin{pmatrix} \phi^{(+)} \\ \phi^{(0)} \end{pmatrix} e_R + f^d (\overline{u}\ \overline{d})_L \begin{pmatrix} \phi^{(+)} \\ \phi^{(0)} \end{pmatrix} d_R \\ &+ f^u (\overline{u}\ \overline{d})_L \begin{pmatrix} \phi*^{(0)} \\ -\phi^{(-)} \end{pmatrix} d_R + h.c. \end{aligned} \tag{2.43}$$

and similarly for other generations. Here f^e, f^u and f^d are arbitrary constants that are to be fixed by experiment, and the last term includes charge conjugate of the scalar field $\phi^c = i\sigma_2\phi^*$. After SSB and going to unitary gauge this reduces to

$$\mathcal{L}_{\text{Yukawa}} = \tfrac{1}{\sqrt{2}}(v+H)\left\{f^e\,\overline{e}e + f^d\,\overline{d}d + f^u\,\overline{u}u\right\}, \tag{2.44}$$

which contains fermion masses

$$m_i = -\frac{v}{\sqrt{2}}f^i, \tag{2.45}$$

and we can write

$$\mathcal{L}_{\text{Yakawa}} = -(1+\tfrac{H}{v})\left\{m_e\,\overline{e}e + m_d\,\overline{d}d + m_u\,\overline{u}u\right\}. \tag{2.46}$$

Thus, the fermions become massive and we get an additional coupling between Higgs boson and fermions where the coupling strength is proportional to fermion masses.

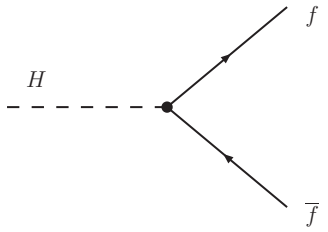

Figure 2.6: Higgs coupling to fermions

For convenience, the whole GWS-Lagrangian in the unitary gauge is given below:

$$\begin{aligned}
\mathcal{L}_{\text{GWS}} &= i\overline{f}\gamma^\mu D_\mu f - \frac{1}{4}\left(\partial_\mu Z_\nu - \partial_\nu Z_\mu\right)^2 \\
&+ \underbrace{-\frac{1}{4}\left(\partial_\mu A_\nu - \partial_\nu A_\mu\right)^2 - \frac{1}{2}\left(\partial_\mu W_\nu^\dagger - \partial_\nu W_\mu^\dagger\right)\left(\partial^\mu W^\nu - \partial^\nu W^\mu\right)}_{\text{kinetic terms for massless fermions and gauge bosons}} \\
&+ \underbrace{\frac{g}{2\sqrt{2}}\left\{W_\mu^\dagger\left[\overline{u}\gamma^\mu(1-\gamma^5)d + \overline{\nu}_e\gamma^\mu(1-\gamma^5)e\right] + \text{h.c.}\right\} + \text{other families}}_{\text{charged}-\text{current interactions}} \\
&+ \underbrace{g_Z\overline{f}\gamma^\mu\left[L_f(1-\gamma^5) + R_f(1+\gamma^5)\right]f}_{\text{neutral}-\text{current interactions}} + \underbrace{eA_\mu\overline{f}\gamma^\mu Qf}_{\text{QED interactions}} \\
&+ \underbrace{(1+\frac{H}{v})\left\{-m_f\,\overline{f}f + M_W^2 W_\mu^\dagger W^\mu + \frac{1}{2}M_Z^2 Z_\mu Z^\mu\right\}}_{\text{fermion and gauge boson mass terms and interactions with Higgs}} \\
&+ \underbrace{\frac{1}{2}\partial_\mu H\partial^\mu H + \frac{1}{4}\lambda v^4 - \frac{1}{2}M_H^2 H^2 - \frac{M_H^2}{2v}H^3 - \frac{M_H^2}{8v^2}H^4}_{\text{Higgs mass term and self}-\text{interactions}} \\
&+ \underbrace{\mathcal{L}_3 + \mathcal{L}_4.}_{\text{gauge boson self}-\text{interactions}}
\end{aligned}$$

Chapter 3

Tree-level quantization

In this chapter we perform the tree level quantization for the GWS theory, that is, we work out the Feynman rules for computing diagrams that do not contain loops. What we will ultimately need are the gauge boson and fermion propagators and the vertex factors for the interactions. As we proceed we will make use of some general results of quantum field theory that can be found, for example, from the excellent book of Peskin and Schroeder [19].

3.1 Correlation functions in path integral formalism

The path integral formalism is an efficient way to quantize gauge theories. It is straightforwardly based on the classical action $\int \mathcal{L}$ and has a certain advantage that is absent in the canonical formalism, namely, gauge freedom.

Suppose we have a Lagrangian $\mathcal{L}$ and let us label the independent fields it contains with Ψ_i. With this notation the correlation functions in a path integral formalism are obtained from

$$\langle \Omega \left| T\{\mathcal{O}(\Psi_H)\} \right| \Omega \rangle = \lim_{T\to\infty(1-i\epsilon)} \frac{1}{N} \int \mathcal{D}\Psi \mathcal{O}(\Psi) \exp\left\{ i \int_{-T}^{T} d^4x \mathcal{L} \right\}, \qquad (3.1)$$

where the limit $\epsilon \to 0$ should be taken at the end.

The structure of the equation above is the following: On the left-hand side $|\Omega\rangle$ is the ground state (vacuum) of the theory and $T\{\mathcal{O}(\Psi_H)\}$ is the time-ordered product of Heisenberg picture field operators. This is replaced on the right-hand side with a similar term $\mathcal{O}(\Psi)$ where the Ψ's are no longer operators but fields appearing in the Lagrangian. The integration is performed over all field configurations. This is usually defined by discretizing the space-time whence the integration measure $\mathcal{D}\Psi$ is, up to possible constant

$$\mathcal{D}\Psi := \prod_{i,j} d\Psi_j(x_i). \qquad (3.2)$$

The whole thing is divided by the normalization factor N which is nothing but the same integral without $\mathcal{O}(\Psi)$, and thus the possible constant in front of the integration measure is irrelevant.

The correlation function can be seen as an expectation value of the operator $\mathcal{O}(\Psi)$ — a quantum amplitude for the process described by $\mathcal{O}(\Psi)$ to happen.

3.2 Change of representation

Under an infinitesimal transformation the complex scalar doublet ϕ transforms as

$$\phi(x) \to \left(1 + i\alpha^a \frac{\sigma^a}{2} + i\frac{\beta}{2}\right)\phi(x).$$

This doublet is now the one where our Higgs and Goldstone bosons reside. Rather than dealing with two complex quantities it will be easier to write them as four real-valued fields. Then, the transformation above can be expressed as

$$\phi_i(x) \to \phi_i(x) - \alpha^a T^a_{ij}\phi_j \tag{3.3}$$

where summation runs over $a = 1, 2, 3, Y$ and *representation matrices* T are real and antisymmetric

$$T^1 = \frac{1}{2}\begin{pmatrix} 0 & 0 & 0 & 1 \\ 0 & 0 & -1 & 0 \\ 0 & 1 & 0 & 0 \\ -1 & 0 & 0 & 0 \end{pmatrix} \quad T^2 = \frac{1}{2}\begin{pmatrix} 0 & 0 & -1 & 0 \\ 0 & 0 & 0 & -1 \\ 1 & 0 & 0 & 0 \\ 0 & 1 & 0 & 0 \end{pmatrix}$$

$$T^3 = \frac{1}{2}\begin{pmatrix} 0 & 1 & 0 & 0 \\ -1 & 0 & 0 & 0 \\ 0 & 0 & 0 & -1 \\ 0 & 0 & 1 & 0 \end{pmatrix} \quad T^Y = \frac{1}{2}\begin{pmatrix} 0 & 1 & 0 & 0 \\ -1 & 0 & 0 & 0 \\ 0 & 0 & 0 & 1 \\ 0 & 0 & -1 & 0 \end{pmatrix}$$

Within this representation the Lagrangian (2.33) becomes

$$L = \frac{1}{2}(D_\mu\phi_i)(D^\mu\phi_i) - \frac{1}{2}\mu^2\phi_i^2 - \frac{\lambda}{4}(\phi_i^2)^2, \tag{3.4}$$

where the covariant derivative is

$$D_\mu\phi_i = \partial_\mu\phi_i + g^a A^a_\mu T^a_{ij}\phi_j. \tag{3.5}$$

We have here made our notation slightly faster by obvious definitions: $g^a = g$ for $a = 1, 2, 3$ and $g^Y \equiv g'$ and $A^Y_\mu \equiv B_\mu$.

As the SSB happens ϕ_i acquires vacuum expectation value

$$\langle\phi\rangle_i = (0, 0, v, 0), \tag{3.6}$$

and we can expand the scalar multiplet around the vacuum as

$$\phi_i = \langle\phi\rangle_i + (\chi_1, \chi_2, H, \chi_3), \tag{3.7}$$

where we have distinguished the Higgs $H \equiv H(x)$ from the Goldstone bosons $\chi_i \equiv \chi_i(x)$.

Terms involving χ_is in the Lagrangian (3.4) are

$$\mathcal{L}_{\text{Goldstone}} = \frac{1}{2}(\partial_\mu\chi_i)(\partial^\mu\chi_i) + g^a(\partial_\mu\chi_i)A^a_\mu F^a_i + \text{interaction terms} \tag{3.8}$$

where we have defined a matrix

$$F_i^a \equiv T_{ij}^a \langle\phi\rangle_j = \frac{v}{2}\begin{pmatrix} 0 & -1 & 0 \\ -1 & 0 & 0 \\ 0 & 0 & 1 \\ 0 & 0 & -1 \end{pmatrix}. \tag{3.9}$$

The terms in (3.8) are those that contribute to the Goldstone propagators and, as we shall see, the peculiar 'mixed' term linear in $\partial_\mu\chi_i$ and A_μ^a can be wiped out with a suitable choice of gauge condition. There are no terms quadratic in χ_i which means that the Goldstone bosons remain massless at this stage.

3.3 Choice of gauge

Let us forget the fermion content of the GWS-theory for a moment and consider the path integral

$$Z = \int \mathcal{D}A\mathcal{D}\chi\mathcal{D}H e^{iS[A,\chi,H]}. \tag{3.10}$$

The integral is troublesome: due to our freedom to make an action-preserving gauge transformation

$$A_\mu^a \to (A^\alpha)_\mu^a = A_\mu^a + \frac{1}{g^a}\partial_\mu\alpha^a + \epsilon^{abc}A_\mu^b\alpha^c, \tag{3.11}$$

there is an infinite number of physically equivalent field configurations which are inevitably counted repeadetly. As such, the integral above is infinite and meaningless. However, there is a way to isolate the physically interesting part from the formal infinity.

This is accomplished by imposing a set of gauge conditions $G(A^a) = 0$ so that only one representative of each inequivalent field configurations contributes to the integral. To do so without affecting the value of integral we follow Faddeev and Popov and use the identity

$$1 = \Delta_{FP}^a \int \mathcal{D}\alpha^a(x)\,\delta\left(G(A^\alpha)_\mu^a\right) \tag{3.12}$$

where

$$\Delta_{FP}^a \equiv \det\left(\frac{\delta(G(A^\alpha)_\mu^a)}{\delta\alpha^a}\right) \tag{3.13}$$

is the *Faddeev-Popov determinant*. It involves a functional derivative with respect to the gauge transformation parameter and it is gauge invariant if $G^a(A^a)$ is linear in A^a (and this will be the case).

Since the action and the integration measure are both invariant under gauge transformation we have

$$Z = \prod_a \int \mathcal{D}\alpha^a \int \mathcal{D}A\mathcal{D}\chi\mathcal{D}H\, e^{iS}\delta\left(G(A)^a\right)\Delta_{FP}^a. \tag{3.14}$$

The path integral is now restricted to the physically inequivalent field configurations and the formal infinity is pushed to multiplicative integral $\int \mathcal{D}\alpha^a$.

To proceed, we have to specify the gauge condition. A specially suitable choice is

$$G(A^a) = \frac{1}{\sqrt{\xi}}\left(\partial^\mu A^a_\mu - \xi g^a F^a_i \chi_i\right) - \omega^a(x) \tag{3.15}$$

where ξ is any constant and $\omega^a(x)$ is an arbitrary scalar function. We can as well write Z as combination of different $\omega^a(x)$'s weighted by a function $\exp\left[-i\int d^4x \frac{(\omega^a)^2}{2}\right]$. Translating this to the path integral language we get

$$Z = \prod_a N' \int \mathcal{D}\omega^a \exp\left[-i\int d^4x \frac{(\omega^a)^2}{2}\right] \int \mathcal{D}\alpha \int \mathcal{D}A\mathcal{D}\chi\mathcal{D}H\, e^{iS}\delta\left(G(A)^a\right)\Delta^a_{FP},$$

where N' is an unimportant normalization factor. Doing the $\omega(x)$ integrals gives

$$Z = \tilde{N}\int \mathcal{D}A\mathcal{D}\chi\mathcal{D}H \exp\left\{i\int d^4x\left[\mathcal{L} - \frac{\sum_a\left(\partial^\mu A^a_\mu - \xi g^a F^a_i\chi_i\right)^2}{2\xi}\right]\right\}\prod_a \Delta^a_{FP}. \tag{3.16}$$

This is the normalization factor appearing in (3.1) and provided that the operator $\mathcal{O}(A,H,\chi)$ is gauge invariant, similar manipulations can be done in the numerator. Thus, the awkward constants $\tilde{N}$ cancel and we are left with

$$\langle\Omega\,|T\{\mathcal{O}\}|\,\Omega\rangle = \lim_{T\to\infty(1-i\epsilon)}\frac{1}{N}\int \mathcal{D}A\mathcal{D}\chi\mathcal{D}H\,\mathcal{O}\exp\left\{i\int_{-T}^{T} d^4x\mathcal{L}'\right\}\prod_a\Delta^a_{FP}, \tag{3.17}$$

where

$$\begin{aligned}\mathcal{L}' &= \mathcal{L}_{\text{old}} - \frac{1}{2\xi}(\partial^\mu A^a_\mu)^2 - \frac{1}{2}\xi(g^a)^2(F^a_i\chi_i)^2 + g^a(\partial^\mu A^\mu_a)F^a_i\chi_i \\ &= \mathcal{L}_{\text{old}} + \frac{1}{2}A^a_\mu\left(\frac{1}{\xi}\partial^\mu\partial^\nu\right)A^a_\nu - g^a(\partial^\mu\chi_i)A^a_\mu F^a_i - \frac{1}{2}\xi(g^a)^2(F^a_i\chi_i)^2\end{aligned} \tag{3.18}$$

Notice that the term linear in A^a_μ exactly cancels the one in (3.8) and that the Goldstone bosons acquire a mass term $-\frac{1}{2}m^2_{ij}\chi_i\chi_j$ where the mass matrix m_{ij} is

$$m^2_{ij} \equiv \xi(g^a)^2F^a_iF^a_j = \xi\frac{v^2}{4}\begin{pmatrix} g^2 & 0 & 0 \\ 0 & g^2 & 0 \\ 0 & 0 & g^2+g'^2\end{pmatrix} = \begin{pmatrix}\xi m_W^2 & 0 & 0 \\ 0 & \xi m_W^2 & 0 \\ 0 & 0 & \xi m_Z^2\end{pmatrix}. \tag{3.19}$$

We have now successfully made the path integral well-defined effectively adding few extra terms to the Lagrangian. However, the Faddeev-Popov determinants Δ^a_{FP} are completely new ingredient. They can be expressed as a Gaussian Grassman integral (see eq. 3.50) and included into the Lagrangian. This gives rise to so called *ghosts* that appear in the loop-level computations and processes involving gauge boson self-couplings. Since our interest is only in the simple tree-level calculations without gauge boson self-couplings we shall forget the ghost terms hereafter.

3.4 Heavy boson propagator

A specially important class of correlation functions are the two-point correlation functions for a non-interacting Lagrangian. These are the *propagators* that appear in the Feynman rules.

Let us now compute the propagator for massive gauge boson Z^0 in a rigorous manner. This will illustrate the general way how the propagators can be read off from the action. The Z-propagator is given by the following two-point correlation function

$$\langle 0\,|T\{Z_\mu(x)Z_\nu(y)\}|\,0\rangle = \lim_{T\to\infty(1-i\epsilon)} \frac{\int \mathcal{D}Z\, Z_\mu(x)Z_\nu(y)e^{iS_0^Z}}{\int \mathcal{D}Z e^{iS_0^Z}}, \tag{3.20}$$

where, after the Faddeev-Popov procedure, the non-interacting part of the action is

$$\begin{aligned} S_0^Z &= \int d^4x \left[-\frac{1}{4}(\partial_\mu Z_\nu - \partial_\nu Z_\mu)(\partial^\mu Z^\nu - \partial^\nu Z^\mu) - \frac{1}{2\xi}(\partial^\mu Z_\mu)^2 + \frac{1}{2}M_Z^2 Z_\mu Z^\mu\right] \\ &= \frac{1}{2}\int d^4x \left[Z_\mu(x)\left(g^{\mu\nu}(\partial^2 + M_Z^2) - \left(1-\frac{1}{\xi}\right)\partial^\mu\partial^\nu\right)Z_\nu(x)\right]. \end{aligned} \tag{3.21}$$

To compute the path integral we discretize the space-time with a periodic square lattice with volume $V = L^4$ and lattice spacing ϵ. The integration measure is

$$\mathcal{D}Z \equiv \prod_{i,j} dZ_j(x_i), \tag{3.22}$$

where a possible constant factor is suppressed as it would cancel in (3.20). The fields $Z_\mu(x_i)$ can be expanded as a discrete Fourier series of momentum space functions

$$Z_\mu(x_i) = \frac{1}{V}\sum_n e^{-ik_n\cdot x_i}\, Z_\mu(k_n), \tag{3.23}$$

where $k_n^\mu = \frac{2\pi n^\mu}{L}$, with n^μ an integer.

Although the vector field $Z_\mu(x_i)$ is real the coefficients $Z_\mu(k_n)$ appearing in the Fourier series are, in general, complex. This implies that the coefficients obey $Z_\mu^*(k_n) = Z_\mu(-k_n)$ and

$$\begin{aligned} \mathrm{Re}Z_\mu(k_n) &= \mathrm{Re}Z_\mu(-k_n) \\ \mathrm{Im}Z_\mu(k_n) &= -\mathrm{Im}Z_\mu(-k_n). \end{aligned} \tag{3.24}$$

This means that we can consider real and imaginary parts of $Z_\mu(k_n)$ with $k_n^0 > 0$ as independent variables. The unitarity of Fourier transformation guarantees the unity of Jacobian and the integration measure is simply

$$\mathcal{D}Z = \prod_j \prod_{k_n^0>0} d\,\mathrm{Re}Z_j(k_n)\, d\,\mathrm{Im}Z_j(k_n). \tag{3.25}$$

The action $S_0(k)$ becomes

$$\begin{aligned} S_0(k) &= \frac{1}{2V}\sum_n Z_\mu(k_n)\left[g^{\mu\nu}\left(M_Z^2 - k_n^2\right) + \left(1-\frac{1}{\xi}\right)k_n^\mu k_n^\nu\right]Z_\nu(-k_n) \\ &= -\frac{1}{2V}\sum_n Z_\mu(k_n)\Delta^{\mu\nu}Z_\nu^*(k_n) \\ &= -\frac{1}{2V}\sum_n \Delta^{\mu\nu}\left[\mathrm{Re}Z_\mu(k_n)\mathrm{Re}Z_\nu(k_n) + \mathrm{Im}Z_\mu(k_n)\mathrm{Im}Z_\nu(k_n)\right] \\ &= -\frac{1}{V}\sum_{k_n^0>0}\left[\mathrm{Re}Z_\mu(k_n)\Delta^{\mu\nu}\mathrm{Re}Z_\nu(k_n) + \mathrm{Im}Z_\mu(k_n)\Delta^{\mu\nu}\mathrm{Im}Z_\nu(k_n)\right], \end{aligned} \tag{3.26}$$

where we have defined

$$\Delta^{\mu\nu}_{k_n} = \Delta^{\nu\mu}_{k_n} = -g^{\mu\nu}\left(M_Z^2 - k_n^2\right) - \left(1 - \frac{1}{\xi}\right) k_n^\mu k_n^\nu \tag{3.27}$$

to speed up our notation. Note that since the time integral is tilted slightly in the imaginary direction $t \to t(1 - i\epsilon)$ we should change $k^0 \to k^0(1 + i\epsilon)$ in the above. We will keep this implicit in what follows.

After this change of variables the denominator of (3.20) is

$$\begin{aligned} N &= \left(\prod_j \prod_{k_n^0>0} \int d\,\mathrm{Re}Z_j(k_n)\, d\,\mathrm{Im}Z_j(k_n)\right) \\ &\quad \exp\left(-\frac{i}{V}\sum_{k_m^0>0} \Delta^{\mu\nu}\left[\mathrm{Re}Z_\mu(k_m)\mathrm{Re}Z_\nu(k_m) + \mathrm{Im}Z_\mu(k_m)\mathrm{Im}Z_\nu(k_m)\right]\right) \\ &= \prod_{k_n^0>0}\left[\int \prod_j d\,\mathrm{Re}Z_j(k_n) \exp\left(-\frac{i}{V}\,\mathrm{Re}Z_\mu(k_n)\Delta^{\mu\nu}\mathrm{Re}Z_\nu(k_n)\right)\right. \\ &\quad \left.\int \prod_j d\,\mathrm{Im}Z_j(k_n) \exp\left(-\frac{i}{V}\,\mathrm{Im}Z_\mu(k_n)\Delta^{\mu\nu}\mathrm{Im}Z_\nu(k_n)\right)\right]. \end{aligned} \tag{3.28}$$

To proceed we use the general identity for Gaussian integrals

$$\int \prod_n d\xi_n \exp\left(-\xi_i B_{ij}\xi_j\right) = \sqrt{\frac{\pi^n}{\det B}}, \tag{3.29}$$

which works if B is a symmetric matrix and by analytic continuation it goes also for imaginary matrices. We get

$$N = \prod_{k_n^0>0} \sqrt{\frac{\pi^4}{\det\left(\frac{i}{V}\Delta_{k_n}\right)}} \sqrt{\frac{\pi^4}{\det\left(\frac{i}{V}\Delta_{k_n}\right)}} \tag{3.30}$$

The numerator of (3.20) is somewhat more complicated due to the additional factor

$$Z_\mu(x)Z_\nu(y) = \frac{1}{V^2}\sum_{m,\ell} e^{-i(k_m\cdot x + k_\ell\cdot y)} Z_\mu(k_m)Z_\nu(k_\ell)e^{iS_0}$$

in the integral. The Fourier coefficients can be splitted in to a real and imaginary parts as

$$\begin{aligned} Z_\mu(k_m)Z_\nu(k_\ell) &= \mathrm{Re}Z_\mu(k_m)\mathrm{Re}Z_\nu(k_\ell) - \mathrm{Im}Z_\mu(k_m)\mathrm{Im}Z_\nu(k_\ell) \\ &+ i\mathrm{Re}Z_\mu(k_m)\mathrm{Im}Z_\nu(k_\ell) + i\mathrm{Im}Z_\mu(k_m)\mathrm{Re}Z_\nu(k_\ell), \end{aligned} \tag{3.31}$$

and the whole integral becomes then

$$\begin{aligned} &\frac{1}{V^2}\sum_{m,\ell} e^{-i(k_m\cdot x + k_\ell\cdot y)} \prod_{k_n^0>0}\left[\left(\int \prod_j d\,\mathrm{Re}Z_j(k_n)\, d\,\mathrm{Im}Z_j(k_n)\right)\right. \\ &\left(\begin{array}{c} \mathrm{Re}Z_\mu(k_m)\mathrm{Re}Z_\nu(k_\ell) - \mathrm{Im}Z_\mu(k_m)\mathrm{Im}Z_\nu(k_\ell) \\ +i\mathrm{Re}Z_\mu(k_m)\mathrm{Im}Z_\nu(k_\ell) + i\mathrm{Im}Z_\mu(k_m)\mathrm{Re}Z_\nu(k_\ell) \end{array}\right) \\ &\left.\exp\left(-\frac{i}{V}\Delta^{\eta\rho}\left[\mathrm{Re}Z_\eta(k_n)\mathrm{Re}Z_\rho(k_n) + \mathrm{Im}Z_\eta(k_n)\mathrm{Im}Z_\rho(k_n)\right]\right)\right]. \end{aligned} \tag{3.32}$$

At first sight this looks quite nasty but can, in fact, be evaluated with two additional Gaussian identities:

$$\int \prod_n d\xi_n \xi_a \exp\left(-\xi_i B_{ij} \xi_j\right) = 0 \tag{3.33}$$

$$\int \prod_n d\xi_n \xi_a \xi_b \exp\left(-\xi_i B_{ij} \xi_j\right) = \frac{1}{2}\sqrt{\frac{\pi^n}{\det B}} (B^{-1})_{ab}. \tag{3.34}$$

Terms that contain the product $\mathrm{Re}Z_\mu \mathrm{Im}Z_\nu$ or $\mathrm{Im}Z_\mu \mathrm{Re}Z_\nu$ are odd and vanish due to the identity (3.33) for all k_m and k_ℓ. Similarly, if $k_m \neq \pm k_\ell$ the product $\prod_{k_n^0>0}$ contains odd integrals that cause the expression go to zero. If $k_m = k_\ell$ the part with $\mathrm{Re}Z_\mu \mathrm{Re}Z_\nu$ gives

$$\begin{aligned} &\prod_{k_n^0>0} \left(\int \prod_j d\,\mathrm{Re}Z_j(k_n) \right) \mathrm{Re}Z_\mu(k_m) \mathrm{Re}Z_\nu(k_m) \exp\left(-\frac{i}{V} \mathrm{Re}Z_\eta(k_n) \Delta^{\eta\rho} \mathrm{Re}Z_\rho(k_n) \right) \\ = &\prod_{k_n^0>0} \frac{1}{2} \sqrt{\frac{\pi^4}{\det\left(\frac{i}{V}\Delta_{k_n}\right)}} (\Delta^{-1}_{k_m})_{\mu\nu}, \end{aligned}$$

but there is a similar term from $\mathrm{Im}Z_\mu \mathrm{Im}Z_\nu$ part with minus sign and these terms cancel. However, if $k_m = -k_\ell$ the relation (3.24) gives an additional minus sign to $\mathrm{Im}A_\mu \mathrm{Im}A_\nu$ term and the two terms add giving

$$-\frac{i}{V} \sum_m e^{-ik_m\cdot(x-y)} \prod_{k_n^0>0} \sqrt{\frac{\pi^4}{\det\left(\frac{i}{V}\Delta_{k_n}\right)}} \sqrt{\frac{\pi^4}{\det\left(\frac{i}{V}\Delta_{k_n}\right)}} (\Delta^{-1}_{k_m})_{\mu\nu}.$$

Quite remarkably, the normalization factor N in (3.30) occurs also in the numerator and they will eventually cancel!

Going back to the continuum limit means

$$\frac{1}{V}\sum_m \to \int \frac{d^4k_m}{(2\pi)^4}, \tag{3.35}$$

and we find

$$\langle 0\,|T\{Z_\mu(x)Z_\nu(y)\}|\,0\rangle = \int \frac{d^4k}{(2\pi)^4} e^{-ik\cdot(x-y)} \left[-i(\Delta^{-1})_{\mu\nu}\right]. \tag{3.36}$$

This is nothing but a Fourier transform of a momentum space propagator $D_F^{\mu\nu}(k) = -i(\Delta^{-1})^{\mu\nu}$ that can be worked out from equation

$$\left[-g_{\mu\rho}\left(M_Z^2 - k^2\right) - \left(1 - \frac{1}{\xi}\right) k_\mu k_\rho\right] D_F^{\mu\nu}(k) = -i\delta^\nu_\rho.$$

This has the solution

$$D_F^{\mu\nu}(k) = \frac{-i}{k^2 - M_Z^2 + i\epsilon} \left(g^{\mu\nu} - \frac{k^\mu k^\nu}{k^2 - \xi M_Z^2}(1-\xi) \right), \tag{3.37}$$

where we have now explicitly restored the $i\epsilon$ prescription mentioned earlier.

In order to get other gauge boson propagators we just replace the M_Z above with a appropriate mass, namely M_W for $W^\pm$ or 0 for photon. The parameter ξ is, in principle, a free parameter to choose. But as we choose it once, the same parameter must be used consistently when calculating the S-matrix. The other sector where the parameter ξ appears is in the propagators for Goldstone bosons. We deal with these next.

3.5 Goldstone propagator

The non-interacting action for each three Goldstone bosons is given by

$$S_i^G = \int d^4x \left[\frac{1}{2}(\partial_\mu \chi_i)(\partial^\mu \chi_i) - \frac{1}{2}\xi m_i^2 \chi_i^2 \right], \tag{3.38}$$

where the squared masses are $m_1^2 = m_2^2 = m_W^2$ and $m_3^2 = m_Z^2$. Doing the Fourier expansion as earlier we get

$$S_i(k) \quad = \quad -\frac{1}{2V} \sum_n \chi_i(k_n) \left[m_i^2 - k_n^2 \right] \chi_i(-k_n), \tag{3.39}$$

and we can immediately write down the equation for momentum space Goldstone propagator $D_F^{\mathrm{G}_i}(k)$:

$$\left(m_i^2 - k_n^2 \right) D_F^{\mathrm{G}_i}(k) = -i. \tag{3.40}$$

This implies

$$D_F^{\mathrm{G}_i}(k) = \frac{i}{k^2 - \xi m_i^2 + i\epsilon}, \tag{3.41}$$

$$D_F^{\mathrm{G}_i}(x-y) = \int \frac{d^4k}{(2\pi)^4} e^{-ik\cdot(x-y)} \frac{i}{k^2 - \xi m_i^2 + i\epsilon}. \tag{3.42}$$

where we have again restored the $i\epsilon$ prescription. From this we see that the limit $\xi \to \infty$ makes the Goldstone propagators vanish — it is the quantum realization of the unitary gauge that was used during construction of the classical Lagrangian. If we choose some other value of ξ, the Goldstone bosons must be included in the Feynman rules!

There is of course a Higgs particle that has a propagator that comes independently of ξ-parameter:

$$D_F^{\mathrm{Higgs}}(k) = \frac{i}{k^2 - m_H^2 + i\epsilon}, \tag{3.43}$$

3.6 Fermion propagator

The expression that gives the Fermion propagator is given by the correlation function

$$\left\langle 0 \left| T\{\Psi(x)\overline{\Psi}(y)\} \right| 0 \right\rangle = \lim_{T\to\infty(1-i\epsilon)} \frac{\int \mathcal{D}\overline{\Psi}\mathcal{D}\Psi\, \Psi(x)\overline{\Psi}(y) e^{iS_0^F}}{\int \mathcal{D}\overline{\Psi}\mathcal{D}\Psi\, e^{iS_0^F}}, \tag{3.44}$$

where S_0^F is the action for free massive fermion

$$S_0^F = \int d^4x \overline{\Psi}(x) \left(i\gamma^\mu \partial_\mu - m\right) \Psi(x). \tag{3.45}$$

The fermionic field operators on the left-hand side of (3.44) obey the canonical anticommutation relations and the Ψ's appearing in the right-hand side of (3.44) are Grassmann variables. Since Ψ's are four-component objects we can express the fields as

$$\begin{aligned} \Psi(x) &= \sum_i \eta^i(x)\psi_i, \\ \overline{\Psi}(x) &= \sum_i \overline{\eta}^i(x)\psi_i^T, \end{aligned} \tag{3.46}$$

where each $\eta^i(x)$ is a Grassmann number and ψ_i is a some four component basis. The simplest choice for the basis is of course

$$\psi_1 = \begin{pmatrix} 1 \\ 0 \\ 0 \\ 0 \end{pmatrix} \quad \psi_2 = \begin{pmatrix} 0 \\ 1 \\ 0 \\ 0 \end{pmatrix} \quad \psi_3 = \begin{pmatrix} 0 \\ 0 \\ 1 \\ 0 \end{pmatrix} \quad \psi_4 = \begin{pmatrix} 0 \\ 0 \\ 0 \\ 1 \end{pmatrix}. \tag{3.47}$$

To proceed, we do as earlier and expand $\Psi(x)$ as a discrete Fourier series

$$\Psi(x) = \frac{1}{V} \sum_{i,n} \eta^i(k_n) e^{-ik_n \cdot x} \psi_i, \tag{3.48}$$

and the action becomes then

$$\begin{aligned} S_0^F &= \frac{1}{V^2} \int d^4x \sum_{i,n} \psi_i^T \overline{\eta}^i(k_n) e^{ik_n \cdot x} \left(i\gamma^\mu \partial_\mu - m\right) \sum_{j,\ell} \eta^j(k_\ell) e^{-ik_\ell \cdot x} \psi_j \\ &= \frac{1}{V^2} \sum_{i,j,n,\ell} \int d^4x \psi_i^T \overline{\eta}^i(k_n) e^{ik_n \cdot x} \left(\not{k}_\ell - m\right) \eta^j(k_\ell) e^{-ik_\ell \cdot x} \psi_j \\ &= \frac{1}{V^2} \sum_{i,j,n,\ell} \int d^4x \, e^{-ix \cdot (k_\ell - k_n)} \psi_i^T \overline{\eta}^i(k_n) \left(\not{k}_\ell - m\right) \eta^j(k_\ell) \psi_j \\ &= \frac{1}{V} \sum_{i,j,n} \overline{\eta}^i(k_n) \left(\not{k}_n - m\right)_{ij} \eta^j(k_n). \end{aligned} \tag{3.49}$$

The denominator of (3.44) can then be written as

$$\begin{aligned} \int \mathcal{D}\overline{\Psi}\mathcal{D}\Psi \, e^{iS_0^F} &= \int \prod_\ell d\overline{\eta}^i(k_\ell) d\eta^i(k_\ell) \exp\left\{ \frac{i}{V} \sum_{i,j,n} \overline{\eta}^i(k_n) \left(\not{k}_n - m\right)_{ij} \eta^j(k_n) \right\} \\ &= \prod_n \int d\overline{\eta}^i(k_n) d\eta^i(k_n) \exp\left\{ \frac{i}{V} \sum_{i,j} \overline{\eta}^i(k_n) \left(\not{k}_n - m\right)_{ij} \eta^j(k_n) \right\}, \end{aligned}$$

and using the Grassmann identity

$$\int \prod_i d\overline{\theta}_i d\theta_i e^{-\overline{\theta}_i B_{ij} \theta_j} = \det B \tag{3.50}$$

we finally get

$$\int \mathcal{D}\overline{\Psi}\mathcal{D}\Psi\, e^{iS_0^F} \;=\; \prod_n \det\left[\frac{-i}{V}\left(\not{k}_n - m\right)\right]. \tag{3.51}$$

The numerator includes an additional factor

$$\begin{aligned}\Psi(x)\overline{\Psi}(y) &= \frac{1}{V^2}\sum_{i,j,q,r}\psi_i\eta^i(k_q)e^{-ix\cdot k_q}\psi_j^T\overline{\eta}^j(k_r)e^{iy\cdot k_r}\\ &= \frac{1}{V^2}\sum_{i,j,q,r}e^{i(y\cdot k_r - x\cdot k_q)}\,\psi_i\psi_j^T\,\eta^i(k_q)\overline{\eta}^j(k_r),\end{aligned} \tag{3.52}$$

and we have to compute the following expression

$$\begin{aligned}&\frac{1}{V^2}\sum_{i,j,q,r}e^{i(y\cdot k_r - x\cdot k_q)}\,\psi_i\psi_j^T\prod_n\int\prod_s d\overline{\eta}^s(k_n)d\eta^s(k_n)\\ &\left(\eta^i(k_q)\overline{\eta}^j(k_r)\exp\left\{\frac{i}{V}\sum_{i,j}\overline{\eta}^i(k_n)\left(\not{k}_n - m\right)_{ij}\eta^j(k_n)\right\}\right)\\ =\;&\frac{1}{V^2}\sum_{i,j,q}e^{-ik_q\cdot(x-y)}\,\psi_i\psi_j^T\prod_n\int\prod_s d\overline{\eta}^s(k_n)d\eta^s(k_n)\\ &\left(\eta^i(k_q)\overline{\eta}^j(k_q)\exp\left\{\frac{i}{V}\sum_{i,j}\overline{\eta}^i(k_n)\left(\not{k}_n - m\right)_{ij}\eta^j(k_n)\right\}\right)\end{aligned} \tag{3.53}$$

Using here another Grassmann identity

$$\left(\int\prod_i d\overline{\theta}_i d\theta_i\right)\theta_k\overline{\theta}_\ell e^{-\overline{\theta}_i B_{ij}\theta_j} = \det B(B^{-1})_{k\ell} \tag{3.54}$$

we get

$$\begin{aligned}&\frac{1}{V^2}\sum_{i,j,q}e^{-ik_q\cdot(x-y)}\,\psi_i\psi_j^T\prod_n\det\left[\frac{-i}{V}\left(\not{k}_n - m\right)\right]\left(\left[\frac{-i}{V}\left(\not{k}_q - m\right)\right]^{-1}\right)_{ij}\\ =\;&\frac{i}{V}\sum_{i,j,q}e^{-ik_q\cdot(x-y)}\,\psi_i\psi_j^T\prod_n\det\left[\frac{-i}{V}\left(\not{k}_n - m\right)\right]\left[\left(\not{k}_q - m\right)^{-1}\right]_{ij}\\ =\;&\frac{i}{V}\sum_{q}e^{-ik_q\cdot(x-y)}\prod_n\det\left[-\frac{i}{V}\left(\not{k}_n - m\right)\right]\left[\left(\not{k}_q - m\right)^{-1}\right]\\ \to\;&\int\frac{d^4q}{(2\pi)^4}e^{-iq\cdot(x-y)}\prod_n\det\left[-\frac{i}{V}\left(\not{k}_n - m\right)\right]i\left[\left(\not{q} - m\right)^{-1}\right],\end{aligned}$$

where the last line is achieved by going back to the continuum as in (3.35). Again, the normalization factor occurs in the numerator and we finally get

$$\left\langle 0\left|T\{\Psi(x)\overline{\Psi}(y)\}\right|0\right\rangle = \int\frac{d^4q}{(2\pi)^4}\frac{ie^{-iq\cdot(x-y)}}{\not{q} - m + i\epsilon}, \tag{3.55}$$

which is a Fourier transform of the momentum space propagator

$$S_F(q) = \frac{i}{\not{q} - m + i\epsilon} = \frac{i(\not{q} + m)}{q^2 - m^2 + i\epsilon}, \tag{3.56}$$

where the $i\epsilon$ prescription has again been explicitly restored.

3.7 Interacting theory

To calculate correlation functions within the full interacting theory we must include all the interaction terms into the Lagrangian appearing in (3.1). Performing a small calculation it is easy to see that everything reduces essentially to the correlation functions of the non-interacting theory:

$$\begin{aligned}
\langle \Omega \,|T\{\mathcal{O}(\Psi_H)\}|\, \Omega\rangle &= \lim_{T\to\infty(1-i\epsilon)} \frac{\int \mathcal{D}\Psi \mathcal{O}(\Psi) \exp\left\{i\int d^4x \mathcal{L}\right\}}{\int \mathcal{D}\Psi(\Psi) \exp\left\{i\int d^4x \mathcal{L}\right\}} \\
&= \lim_{T\to\infty(1-i\epsilon)} \frac{\frac{1}{N_0}\int \mathcal{D}\Psi \mathcal{O}(\Psi) \exp\left\{i\int d^4x \mathcal{L}_0\right\} \exp\left\{i\int d^4x \mathcal{L}_{\rm int}\right\}}{\frac{1}{N_0}\int \mathcal{D}\Psi(\Psi) \exp\left\{i\int d^4x \mathcal{L}_0\right\} \exp\left\{i\int d^4x \mathcal{L}_{\rm int}\right\}} \\
&= \frac{\langle 0 \,|T\{\mathcal{O}(\Psi_H) \exp\{iS_{\rm int}\}\}|\, 0\rangle}{\langle 0 \,|T\{\exp\{iS_{\rm int}\}\}|\, 0\rangle}.
\end{aligned}$$

Now, the denominator contains expression that is independent of $\mathcal{O}(\Psi_H)$ and thus it acts as a normalization factor that is common for *all* correlation functions. This notion already implies that this factor should be rather irrelevant since all important information is contained in the numerator.

Indeed, in analogy with the cancellation of the normalization factors in expressions for the free propagators, it can be shown that similar miracle happens here! This result is known as a *vacuum bubble exponentiation* and it states that

$$\langle \Omega \,|T\{\mathcal{O}(\Psi_H)\}|\, \Omega\rangle = \langle 0 \,|T\{\mathcal{O}(\Psi_H) \exp\{iS_{\rm int}\}\}|\, 0\rangle_{\text{connected graphs}}\,, \tag{3.57}$$

where *connected graphs* means that as the factor $\exp\{iS_{\rm int}\}$ is expanded, only those terms that can be represented as Feynman graphs that can be drawn without lifting a pen from the paper are taken into account.

To see how the vertex factors for the GWS-theory can be read off from the Lagrangian let us consider a 4-point correlation function

$$\left\langle \Omega \left|T\{e(x_1)\,\overline{\nu}(x_2)\,u(x_3)\,\overline{d}(x_4)\}\right|\, \Omega\right\rangle, \tag{3.58}$$

where $e(x_1)$ represents an electron in a space-time point x_1, and similarly $\overline{\nu}(x_2)$, $u(x_3)$ and $\overline{d}(x_4)$ represent neutrino, up and down quark respectively. The first non-zero term in the expansion of $\exp\{iS_{\rm int}\}$ is given by (see eq. (2.25))

$$\begin{aligned}
\frac{1}{2!}\cdot 2\int d^4x\, d^4y \quad &\left(\tfrac{ig}{2\sqrt{2}}\right) W^\dagger_\mu(x) \left[\overline{u}(x)\gamma^\mu\left(1-\gamma^5\right) d(x)\right] \\
&\left(\tfrac{ig}{2\sqrt{2}}\right) W_\nu(y) \left[\overline{e}(y)\gamma^\nu\left(1-\gamma^5\right) \nu(y)\right] \quad ,
\end{aligned} \tag{3.59}$$

where the factor $\frac{1}{2!}$ comes from Taylor expansion and the subsequent factor 2 is due to the fact that there is a second similar term with x and y interchanged.

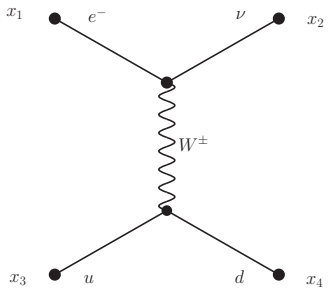

Figure 3.1: Feynman graph for the first non-zero term in 4-point correlation function $\left\langle \Omega \left| T\{e(x_1)\,\overline{\nu}(x_2)\,u(x_3)\,\overline{d}(x_4)\} \right| \Omega \right\rangle$.

The Feynman graph for this expression is illustrated in fig. 3.1. The quantum amplitude for this graph is then

$$\begin{aligned}
&\int d^4x\, d^4y \frac{1}{N_0} \int \mathcal{D}(e,\overline{e},\nu,\overline{\nu},u,\overline{u},d,\overline{d},W,W^\dagger) \exp\{iS_0\} \\
&\left\{ e(x_1)\overline{e}(y) \left(\frac{ig}{2\sqrt{2}}\right) \gamma^\mu \left(1-\gamma^5\right) \nu(y)\overline{\nu}(x_2) W^\dagger_\mu(x) W_\nu(y) \right. \\
&\left. u(x_3)\overline{u}(x) \left(\frac{ig}{2\sqrt{2}}\right) \gamma^\nu \left(1-\gamma^5\right) d(x)\overline{d}(x_4) \right\} \\
= \quad &\int d^4x\, d^4y \quad \left\{ \left[S_F(x_1-y) \left(\frac{ig}{2\sqrt{2}}\right) \gamma^\mu \left(1-\gamma^5\right) S_F(y-x_2) \right] \right. \qquad (3.60) \\
&\left. D_{F,\mu\nu}(x-y) \left[S_F(x_3-x) \left(\frac{ig}{2\sqrt{2}}\right) \gamma^\nu \left(1-\gamma^5\right) S_F(x-x_4) \right] \right\},
\end{aligned}$$

where the S_F's are fermion propagators given by eq. (3.55) and $D_F^{\mu\nu}$ is the heavy boson propagator given by eq. (3.36). The integration $\int d^4x\, d^4y$ tells us, in the spirit of Feynman, that the quantum amplitude gets contribution from all different spatial configurations of the interaction vertices.

As we calculate quantum amplitudes for real scattering processes the incoming and the outgoing (external) particles must be treated in a special manner. The question how to do this, is a deep one since the interactions are not only involved in the scattering, but affect also the single particle-states themselves. At the end, however, the result is simple: By the *LSZ reduction theorem* [20] the propagators corresponding these particles are just replaced by the free particle plane waves. If the external fermion with momentum k and spin-state s is attached to a vertex x, the correct way to do the reduction is

$$\begin{aligned}
\text{Incoming fermion :} \quad & S_F(x-y) \to u(k,s)e^{-ik\cdot x} \\
\text{Outgoing fermion :} \quad & S_F(y-x) \to \overline{u}(k,s)e^{+ik\cdot x} \\
\text{Incoming antifermion :} \quad & S_F(x-y) \to \overline{v}(k,s)e^{+ik\cdot x} \\
\text{Outgoing antifermion :} \quad & S_F(x-y) \to v(k,s)e^{-ik\cdot x}
\end{aligned}$$

where $u(k,s)$ and $\overline{u}(k,s)$ are Dirac spinors.

To continue our example, let us implement these in (3.60) to describe the

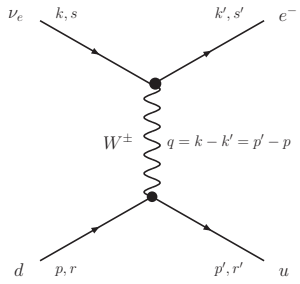

Figure 3.2: Leading order graph in $\nu_e + d \to e^- + u$ scattering.

lowest order contribution to neutrino-quark scattering shown in fig. 3.2.

$$\langle \Omega \left| T\{e(x_1)\,\overline{\nu}(x_2)\,u(x_3)\,\overline{d}(x_4)\} \right| \Omega \rangle \to$$

$$\int d^4x\, d^4y \quad \left\{ \left[\overline{u}(k',s') e^{+ik'\cdot y} \left(\frac{ig}{2\sqrt{2}} \right) \gamma^\mu \left(1-\gamma^5\right) u(k,s) e^{-ik\cdot y} \right] \right.$$
$$\left. \int \frac{d^4q}{(2\pi)^4} e^{-iq\cdot(x-y)} D_{F,\mu\nu}(q) \left[\overline{u}(p',r') e^{+ip'\cdot x} \left(\frac{ig}{2\sqrt{2}} \right) \gamma^\nu \left(1-\gamma^5\right) u(p,r) e^{-ip\cdot x} \right] \right\},$$
$$= (2\pi)^4 \delta^{(4)}(p - p' + k - k')$$
$$\overline{u}(k',s') \left(\frac{ig}{2\sqrt{2}} \right) \gamma^\mu \left(1-\gamma^5\right) u(k,s) D_{F,\,\mu\nu}(q) \overline{u}(p',r') \gamma^\nu \left(\frac{ig}{2\sqrt{2}} \right) \left(1-\gamma^5\right) u(p,r).$$

The factor $(2\pi)^4\delta^{(4)}(p-p'+k-k')$ ensures just the energy-momentum conservation and it is usually implemented into phase-space element in the expression for the corresponding cross-section. Thus the true quantum amplitude for the $\nu_e + d \to e^- + u$ scattering would be

$$\begin{aligned} i\mathfrak{M}(\nu d \to e^- u) \quad \equiv \quad & \left[\overline{u}(k',s') \left(\frac{ig}{2\sqrt{2}} \right) \gamma^\mu \left(1-\gamma^5\right) u(k,s) \right] D_{F,\,\mu\nu}(q) \\ & \left[\overline{u}(p',r') \left(\frac{ig}{2\sqrt{2}} \right) \gamma^\nu \left(1-\gamma^5\right) u(p,r) \right]. \end{aligned}$$

From the expression above we can now straightforwardly read off the charged current vertex factor

$$\text{Charged current vertex factor} = \left(\frac{ig}{2\sqrt{2}} \right) \gamma^\mu \left(1-\gamma^5\right)$$

that enters into the Feynman rules. Similarly, one obtains the QED and neutral current vertex factors

$$\begin{aligned} \text{Neutral current vertex factor} &= ig_Z \gamma^\mu \left[L_f \left(1-\gamma^5\right) + R_f \left(1+\gamma^5\right) \right] \\ \text{QED vertex factor} &= ieQ\gamma^\mu \end{aligned}$$

This example illustrates the general way how the expressions for the Feynman graphs are constructed from the Dirac spinors, free propagators and the vertex factors, all in the momentum-space representation. For convenience, we summarize the relevant vertex factors and propagators in the following page.

- Vertex factors

$$\begin{aligned} \text{QED vertex factor} &= ieQ\gamma^\mu \\ \text{Charged current vertex factor} &= \left(\frac{ig}{2\sqrt{2}}\right)\gamma^\mu\left(1-\gamma^5\right) \\ \text{Neutral current vertex factor} &= ig_Z\gamma^\mu\left[L_f\left(1-\gamma^5\right)+R_f\left(1+\gamma^5\right)\right] \end{aligned}$$

$$\begin{aligned} g_Z &= \frac{e}{4\sin\theta_{\rm W}\cos\theta_{\rm W}} \\ L_f &= T_f^3 - 2Q_f\sin^2\theta_{\rm W} \\ R_f &= -2Q_f\sin^2\theta_{\rm W}. \end{aligned} \tag{3.61}$$

	ν_e, ν_μ, ν_τ	e, μ, τ	u, c, t	d, s, b
L_f	1	$-1+2\sin\theta_{\rm W}$	$1-\frac{4}{3}\sin\theta_{\rm W}$	$-1+\frac{2}{3}\sin\theta_{\rm W}$
R_f	0	$2\sin\theta_{\rm W}$	$-\frac{4}{3}\sin\theta_{\rm W}$	$\frac{2}{3}\sin\theta_{\rm W}$

- Propagators

For each internal particles with momentum q there is a factor

$$\begin{aligned} \text{Intermediate boson propagator} &= \frac{-i}{q^2-M^2+i\epsilon}\left(g^{\mu\nu}-\frac{q^\mu q^\nu}{q^2-\xi M^2}(1-\xi)\right) \\ \text{Goldstone propagator} &= \frac{i}{q^2-\xi M^2+i\epsilon} \\ \text{Higgs propagator} &= \frac{i}{q^2-M_H^2+i\epsilon}, \end{aligned} \tag{3.62}$$

where $M = M_{W^\pm}, M_Z$. For internal fermions

$$\text{Fermion propagator} = \frac{i(\not{q}+m)}{q^2-m^2+i\epsilon}. \tag{3.63}$$

- External particles

For each external fermion with momentum k and spin s there is factor

$$\begin{aligned} \text{Incoming fermion :} &\quad u(k,s) \\ \text{Outgoing fermion :} &\quad \overline{u}(k,s) \\ \text{Incoming antifermion :} &\quad \overline{v}(k,s) \\ \text{Outgoing antifermion :} &\quad v(k,s) \end{aligned}$$

Chapter 4

Deep inelastic scattering

4.1 Deep inelastic scattering in a nutshell

Deep inelastic scattering (DIS) is an invaluable tool for studying the fundamental structure of nuclear matter. When a lepton projectile scatters off a target nucleon some of its initial energy and momentum is lost in the collision. The energy-momentum transfer $q = (\nu, \vec{q})$ is carried to the nucleon by exchange of a photon or heavy $W^{\pm}$ or Z^0 boson. The exchanged boson probes the structure of the nucleon, and in order to resolve individual quarks within the nucleon, momentum transfer, virtuality, $|q^2|$ must be large enough so that the corresponding de Broglie wavelength is small compared to the size of the nucleon. This requires momentum transfer $|q^2| > \text{GeV}^2$.

As the scattering with momentum transfer $|q^2| \gg M^2$ (M is the mass of the nucleon) occurs from an individual quark, the quark acquires high momentum and is therefore virtually "knocked out" from the parent nucleon. However, in nature there is no such thing as free quark and consequently the struck quark and the remnants of the nucleon will fragment to a collection of hadrons allowed by conservation laws. Such scattering is said to be *deep inelastic*: a high energy projectile breaks up the target nucleon and completely wipes out its original identity.

The deep inelastic reactions we are going to consider here are the electromagnetic

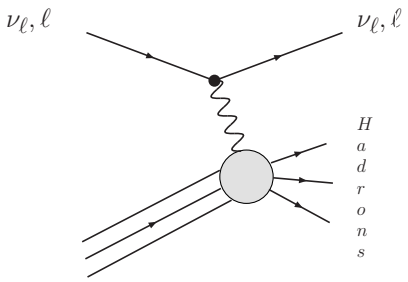

Figure 4.1: Deep inelastic scattering

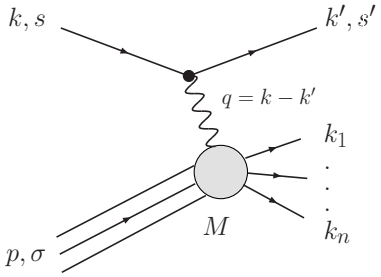

Figure 4.2: Kinematic quantities in DIS. The four-momenta of the incoming and the outgoing leptons with spin states s and s' are denoted by k and k', respectively. Similarly, p and σ are the four-momenta and spin state of initial nucleon with mass M. Momenta of the final state hadrons are denoted with $k_1 ... k_n$.

reactions

$$\text{QED}: \qquad \ell^- + h \to \ell^- + X$$

and the weak interaction neutrino (antineutrino) reactions

$$\text{CC}: \qquad \nu_\ell(\overline{\nu}_\ell) + h \to \ell^{-(+)} + X$$

$$\text{NC}: \qquad \nu_\ell(\overline{\nu}_\ell) + h \to \nu_\ell(\overline{\nu}_\ell) + X$$

where h denotes the initial hadron and X is any set of hadrons allowed by conservation laws. These reactions occur dominantly via one γ, $W^\pm$ or Z^0 boson exchange as shown in fig. 4.1, and in this thesis we will not discuss higher order terms arising from multiple boson exchanges or radiative corrections.

4.1.1 Kinematics

Throughout this thesis, the following conventional Lorentz invariant variables will be used to describe DIS

$$\begin{aligned} Q^2 &\equiv -q^2 \\ x &\equiv \frac{Q^2}{2p \cdot q} \\ y &\equiv \frac{p \cdot q}{p \cdot k}. \end{aligned} \tag{4.1}$$

In the target rest frame (LAB) the the four-momenta of particles can be written as

$$\begin{aligned} k &= (E, \vec{k}) = (E, 0, 0, E) \\ k' &= (E', \vec{k'}) = (E', E' \sin\theta, 0, E' \cos\theta) \\ p &= (p^0, \vec{p}) = (M, 0, 0, 0) \\ q &= (\nu, \vec{q}) = (E - E', \vec{k} - \vec{k'}), \end{aligned} \tag{4.2}$$

where the axes have been chosen so that the motion of the incident lepton is along the z-axis and the final-state lepton lies in the xz-plane. In our discussion the leptons involved are highly relativistic and they will always be treated as massless particles. In LAB frame the invariants (4.1) become

$$\begin{aligned} Q^2 &= 4EE'\sin^2\left(\frac{\theta}{2}\right) \\ x &= \frac{Q^2}{2M\nu} \\ y &= \frac{\nu}{E}. \end{aligned} \tag{4.3}$$

The last two of these variables are in a range $0 \leq x, y \leq 1$, which follows from the requirement $p_X^2 \geq M^2$ where p_X^2 is the invariant mass of the produced hadrons.

4.1.2 General cross-section formula

The differential cross-section for the process shown in fig. 4.2 can be written as

$$d\sigma = \frac{\overline{|\mathfrak{M}|^2}}{F}\, dQ \tag{4.4}$$

where dQ is the Lorentz invariant element of the $n+1$ particle phase space

$$dQ = (2\pi)^4\delta^{(4)}(k+p-k'-\sum_{j=1}^{n} k_j)\frac{d^3\mathbf{k}'}{(2\pi)^3 2E'}\prod_{i=1}^{n}\frac{d^3\mathbf{k}_i}{(2\pi)^3 2k_i^0}\,, \tag{4.5}$$

and F is the incident flux

$$F = 4\big[(k\cdot p)^2 - m^2M^2\big]^{1/2},. \tag{4.6}$$

where m is mass of the projectile lepton. The spin-averaged square of the invariant amplitude is denoted by $\overline{|\mathfrak{M}|^2}$.

4.2 Charged current neutrino DIS

In this and in the following section we shall construct the appropriate DIS cross-section formulas for charged current, neutral current, and QED deep inelastic processes. The conventions we are going to use are adopted from ref. [21]. This reference contains definitions and almost all usual properties of Dirac spinors and gamma matrices we shall need. We also make use of some methods of Ref. [22] as we manipulate matrix elements of the scattering processes.

4.2.1 General charged current matrix element

We are now dealing with weak interaction that violates the parity conservation. This emerges in the matrix element as a V-A (vector–axial vector) structure: The vector part $\propto \gamma^\mu$ is similar to the electromagnetic current while the axial part $\propto -\gamma^\mu\gamma^5$ causes the parity violation.

Using the Feynman rules we just derived, the CC νh-matrix element corresponding n hadrons in the final state X is

$$\mathfrak{M}_n = \overline{u}(k',s')\left(\frac{ig}{2\sqrt{2}}\right)\gamma^\mu(1-\gamma^5)u(k,s)\left(-i\frac{g_{\mu\nu}-\frac{q_\mu q_\nu}{M_W^2}}{q^2-M_W^2}\right) < n, out|\frac{ig}{2\sqrt{2}}\hat{J}^\nu|h, in >, \tag{4.7}$$

where we have adopted the unitary gauge $\xi \to \infty$ for the propagator. The hadronic part of the matrix element is written in a very general way with $\hat{J}^\nu$ representing hadronic part of the charged-current operator.

The matrix element $\mathfrak{M}_n$ above can be immediately simplified: in the term proportional to $q_\mu q_\nu = \left(k_\mu - k'_\mu\right) q_\nu$ we have

$$\overline{u}(k',s')\not{k}(1-\gamma^5)u(k,s) - \overline{u}(k',s')\not{k}'(1-\gamma^5)u(k,s). \tag{4.8}$$

With anticommutator $\left\{\gamma^\mu, \gamma^5\right\} = 0$ and Dirac equations,

$$\begin{aligned}\left(\not{p} - m\right) u\left(p\right) &= 0\\ \overline{u}\left(p\right)\left(\not{p} - m\right) &= 0,\end{aligned}$$

this can be turned to

$$m\overline{u}(k',s')(1+\gamma^5)u(k,s) - m'\overline{u}(k',s')(1-\gamma^5)u(k,s), \tag{4.9}$$

and as we are considering high energy scattering, neglecting lepton masses makes these terms vanish and we are left just with

$$\mathfrak{M}_n = \frac{i}{64}\left(\frac{g_W^2}{q^2 - M_W^2}\right)\overline{u}(k',s')\gamma^\mu(1-\gamma^5)u(k,s) \; < n, out|\hat{J}_\mu|h, in> . \tag{4.10}$$

In the unpolarized situation we do not have *a priori* knowledge of the initial spin-state of the struck hadron and our detector is blind for spin orientations. Then we must account for scattering in all possible spin configurations. The corresponding square of the matrix element $\mathfrak{M}_n$ is constructed by squaring $\mathfrak{M}_n$, summing over the spin states s and s' of the leptons and averaging over the two spin states σ of the initial nucleon.

Now, here is one subtlety: why do we sum over spin states of the initial neutrino although the present belief is that only left-handed neutrinos exist? Notice that the matrix element includes the projection operator $\propto \frac{1}{2}(1-\gamma^5)$ that projects out only the left-handed component of the neutrino spinor $u(k,s)$, and although we formally sum over spin states s of the initial neutrino, the right-handed component does not contribute.

$$\begin{aligned}\overline{|\mathfrak{M}_n|^2} &= \frac{1}{2}\sum_{s,s',\sigma}\mathfrak{M}_{\mathfrak{n}}{\mathfrak{M}_{\mathfrak{n}}}^* \qquad (4.11)\\ &= \frac{g^4}{64\left(q^2 - M_W^2\right)^2}\\ &\quad \sum_{s,s'}\overline{u}(k',s')\gamma^\mu\left(1-\gamma^5\right)u(k,s)\overline{u}(k,s)\gamma^\nu\left(1-\gamma^5\right)u(k',s')\\ &\quad \frac{1}{2}\sum_\sigma < n, out|\hat{J}_\mu|h, in >< h, in|\hat{J}_\nu^\dagger|n, out >\\ &= \frac{G_F^2 M_W^4}{2\left(Q^2 + M_W^2\right)^2}L^{\mu\nu}\frac{1}{2}\sum_\sigma < n, out|\hat{J}_\mu|h, in >< h, in|\hat{J}_\nu^\dagger|n, out >,\end{aligned}$$

where $L^{\mu\nu}$ is a leptonic tensor

$$L^{\mu\nu} \equiv \sum_{s,s'}\overline{u}(k',s')\gamma^\mu\left(1-\gamma^5\right)u(k,s)\overline{u}(k,s)\gamma^\nu\left(1-\gamma^5\right)u(k',s'), \tag{4.12}$$

and we used the definition of the Fermi coupling constant G_F

$$\frac{g^2}{M_W^2} \equiv 4\sqrt{2}G_F, \tag{4.13}$$

which is an effective coupling constant for low Q^2 and the current numerical value is $G_F/(\hbar c)^3 = 1.6637 \times 10^{-5}\,\mathrm{GeV}^{-2}$ [23].

Summing over the contributions of all n-particle final states and setting $m_\nu = 0$ in the flux factor (4.6), we have

$$\begin{aligned} d\sigma &= \frac{1}{4|k\cdot p|}\frac{G_F^2 M_W^4}{2\left(Q^2+M_W^2\right)^2}\frac{d^3\mathbf{k}'}{(2\pi)^3 2E'}L^{\mu\nu} \\ &\quad \frac{1}{2}\sum_n\sum_\sigma\prod_{i=1}^n\frac{d^3\mathbf{k}_i}{(2\pi)^3 2k_i^0}(2\pi)^4\delta^{(4)}(p+q-k'-\sum_{j=1}^n k_j) \\ &\quad < n,out|\hat{J}_\mu|h,in >< h,in|\hat{J}_\nu^\dagger|n,out> . \end{aligned} \tag{4.14}$$

We define the hadronic tensor $W_{\mu\nu}$ as follows

$$\begin{aligned} 4\pi M W_{\mu\nu} &\equiv \frac{1}{2}\sum_n\sum_\sigma\prod_{i=1}^n\frac{d^3\mathbf{k}_i}{(2\pi)^3 2k_i^0}(2\pi)^4\delta^{(4)}(p+q-k'-\sum_{j=1}^n k_j) \\ &\quad < n,out|\hat{J}_\mu|h,in >< h,in|\hat{J}_\nu^\dagger|n,out>, \end{aligned} \tag{4.15}$$

which enables us to write the differential cross-section $d\sigma$ in a simple form involving contraction between leptonic and hadronic tensors

$$d\sigma = \frac{\pi}{2}\frac{G_F^2 M_W^4}{\left(Q^2+M_W^2\right)^2}\frac{M}{|k\cdot p|}\frac{d^3\mathbf{k}'}{(2\pi)^3 2E'}L^{\mu\nu}W_{\mu\nu}. \tag{4.16}$$

All information about the interaction resides now in these tensors $L^{\mu\nu}$ and $W_{\mu\nu}$ — other factors are purely kinematic origin.

4.2.2 Leptonic tensor

The leptonic tensor is now

$$L^{\mu\nu} = \sum_{s,s'}\overline{u}(k',s')\gamma^\mu\left(1-\gamma^5\right)u(k,s)\overline{u}(k,s)\gamma^\nu\left(1-\gamma^5\right)u(k',s')$$

Let us write this explicitly as a sum of spinor and gamma matrix elements labeled c,d,e and f:

$$\begin{aligned} L^{\mu\nu} &= \sum_{s,s'}\overline{u}_c(k',s')\big(\gamma^\mu(1-\gamma^5)\big)_{cd}u_d(k,s) \\ &\quad \overline{u}_e(k,s)\big(\gamma^\nu(1-\gamma^5)\big)_{ef}u_f(k',s'), \end{aligned} \tag{4.17}$$

which can be rearranged to

$$\begin{aligned} L^{\mu\nu} &= \sum_{s'}u_f(k',s')\overline{u}_c(k',s')\big(\gamma^\mu(1-\gamma^5)\big)_{cd} \\ &\quad \sum_s u_d(k,s)\overline{u}_e(k,s)\big(\gamma^\nu(1-\gamma^5)\big)_{ef}. \end{aligned} \tag{4.18}$$

We can now make use of the completeness relation of spinors

$$\sum_s u(p,s)\overline{u}(p,s) = \not{p} + m, \tag{4.19}$$

and neglecting the lepton masses we have

$$\begin{aligned} L^{\mu\nu} &= (\not{k}')_{fc}\left(\gamma^\mu(1-\gamma^5)\right)_{cd}(\not{k})_{de}\left(\gamma^\nu(1-\gamma^5)\right)_{ef} \\ &= \mathrm{Tr}\left[(\not{k}')\left(\gamma^\mu(1-\gamma^5)\right)(\not{k})\left(\gamma^\nu(1-\gamma^5)\right)\right] \\ &= 2\cdot\left[\mathrm{Tr}\left(\not{k}'\gamma^\mu\not{k}\gamma^\nu\right) - Tr\left(\gamma^5\not{k}'\gamma^\mu\not{k}\gamma^\nu\right)\right], \end{aligned}$$

where we have used Dirac algebra

$$\left(\gamma^5\right)^2 = 1 \qquad \gamma^5\gamma^\mu = -\gamma^\mu\gamma^5$$

in reaching the last line. Furthermore, with "Dirac-traceology"

$$\begin{aligned} \mathrm{Tr}\left(\gamma^e\gamma^f\gamma^g\gamma^h\right) &= 4\left(g^{gh}g^{ef} + g^{eh}g^{fg} - g^{fh}g^{eg}\right) \\ \mathrm{Tr}\left(\gamma^5\gamma^a\gamma^b\gamma^c\gamma^d\right) &= -4i\epsilon^{abcd} \end{aligned}$$

where ϵ^{abcd} is the completely antisymmetric Levi-Civita tensor defined as

$$\epsilon^{abcd} = \begin{cases} +1 & \text{if } abcd \text{ is even permutation of 0123,} \\ -1 & \text{if } abcd \text{ is odd permutation of 0123,} \\ 0 & \text{otherwise,} \end{cases} \tag{4.20}$$

we obtain

$$L^{\mu\nu} = 8\left(k'^\mu k^\nu + k'^\nu k^\mu - g^{\mu\nu}k\cdot k' + i\epsilon^{\alpha\mu\beta\nu}k'_\alpha k_\beta\right). \tag{4.21}$$

It turns out to be useful to express this as a sum of terms which are symmetric and antisymmetric under interchange of indices μ and ν:

$$L^{\mu\nu} = L_S^{\mu\nu} + L_A^{\mu\nu}, \tag{4.22}$$

where

$$L_S^{\mu\nu} \equiv 8\left(k'^\mu k^\nu + k'^\nu k^\mu - g^{\mu\nu}k\cdot k'\right) \tag{4.23}$$

$$L_A^{\mu\nu} \equiv 8i\epsilon^{\alpha\mu\beta\nu}k'_\alpha k_\beta. \tag{4.24}$$

4.2.3 Hadronic tensor

The hadronic tensor $W_{\mu\nu}$, *a priori* unknown, contains all information about the structure of the hadron and the coupling of weak current to the hadron. The general form of the hadronic tensor can, however, be determined without further input. Using the initial state momentum p and momentum transfer q as independent variables, the most general hadronic tensor is a sum of all possible rank-two tensors multiplied with arbitrary coefficients. Like the leptonic tensor, it is convenient to express the hadronic tensor as a sum of symmetric and antisymmetric parts:

$$W_{\mu\nu} = W_{\mu\nu}^S + W_{\mu\nu}^A, \tag{4.25}$$

where

$$\begin{aligned} W^S_{\mu\nu} &\equiv V_1 g_{\mu\nu} + V_2 p_\mu p_\nu + V_3(p_\mu q_\nu + p_\nu q_\mu) + V_5 q_\mu q_\nu \\ W^A_{\mu\nu} &\equiv V_4(p_\mu q_\nu - p_\nu q_\mu) + iV_6\epsilon_{\mu\nu\eta\gamma}p^\eta q^\gamma. \end{aligned} \tag{4.26}$$

The symmetric part $W^S_{\mu\nu}$ represents the vector current while the antisymmetric part $W^A_{\mu\nu}$ represents the axial current.

For the parity conserving symmetric part we have, in analogy with the conservation of the electromagnetic current

$$q^\mu W^S_{\mu\nu} = 0, \tag{4.27}$$

and imposing this requirement on $W^S_{\mu\nu}$ we have

$$V_1 q_\nu + V_2(p\cdot q)p_\nu + V_3\left[(p\cdot q)q_\nu + q^2 p_\nu\right] + V_5 q^2 q_\nu = 0. \tag{4.28}$$

Because q and p are linearly independent of each other, the coefficients of p_ν and q_ν must vanish separately:

$$\begin{cases} V_1 + V_3(p\cdot q) + V_5 q^2 &= 0 \\ V_2(p\cdot q) + V_3 q^2 &= 0 \end{cases}$$

Eliminating V_3 and V_5 we find that

$$W^S_{\mu\nu} = V_1\left(g_{\mu\nu} - \frac{q_\mu q_\nu}{q^2}\right) + V_2\left(p_\mu - \frac{p\cdot q}{q^2}q_\mu\right)\left(p_\nu - \frac{p\cdot q}{q^2}q_\nu\right). \tag{4.29}$$

It is conventional to define coefficients W_1, W_2 and W_3 through

$$V_1 \equiv -W_1 \quad V_2 \equiv \tfrac{W_2}{M^2} \quad V_6 \equiv \tfrac{W_3}{2M^2},$$

in terms of which we can rewrite the hadronic tensor as

$$\begin{aligned} W^S_{\mu\nu} &= -W_1\left(g_{\mu\nu} - \frac{q_\mu q_\nu}{q^2}\right) + \frac{W_2}{M^2}\left(p_\mu - \frac{p\cdot q}{q^2}q_\mu\right)\left(p_\nu - \frac{p\cdot q}{q^2}q_\nu\right) \\ W^A_{\mu\nu} &= V_4(p_\mu q_\nu - p_\nu q_\mu) + i\frac{W_3}{2M^2}\epsilon_{\mu\nu\eta\gamma}p^\eta q^\gamma. \end{aligned} \tag{4.30}$$

The term proportional to V_4 will vanish under contraction with leptonic tensor (as we shall shortly see), and it has not therefore been redefined.

4.2.4 Contraction $L^{\mu\nu}W_{\mu\nu}$

Having now determined the exact form of leptonic tensor and the general structure of the hadronic tensor we can now proceed and make the contraction.

$$\begin{aligned} L^{\mu\nu}W_{\mu\nu} &= \left(L^{\mu\nu}_S + L^{\mu\nu}_A\right)\left(W^S_{\mu\nu} + W^A_{\mu\nu}\right) \\ &= L^{\mu\nu}_S W^S_{\mu\nu} + L^{\mu\nu}_A W^A_{\mu\nu} + \underbrace{L^{\mu\nu}_A W^S_{\mu\nu} + L^{\mu\nu}_S W^A_{\mu\nu}}_{=0} \end{aligned} \tag{4.31}$$

Using equations (4.23) and (4.30), and neglecting lepton masses

$$L^{\mu\nu}_S W^S_{\mu\nu} = 16W_1(k'\cdot k) + \frac{4W_2}{M^2}\left[4(k'\cdot p)(k\cdot p) + p^2q^2\right]. \tag{4.32}$$

For the antisymmetric tensors we have, using (4.24) and (4.30)

$$L_A^{\mu\nu} W_{\mu\nu}^A = 8iV_4 \epsilon^{\alpha\mu\beta\nu} k'_\alpha k_\beta (p_\mu q_\nu - p_\nu q_\mu) - 4\frac{W_3}{M^2} \epsilon^{\alpha\mu\beta\nu} \epsilon_{\mu\nu\eta\gamma} k'_\alpha k_\beta p^\eta q^\gamma \quad (4.33)$$

Because

$$\begin{aligned} \epsilon^{\alpha\mu\beta\nu} k'_\alpha k_\beta (p_\mu q_\nu - p_\nu q_\mu) &= 2\epsilon^{\alpha\mu\beta\nu} k'_\alpha p_\mu k_\beta q_\nu \\ &= 2 \det(k', p, k, q) \\ &= 2 \det(k', p, k, k - k') \\ &= 2 \det(k', p, k, k) = 0, \end{aligned} \quad (4.34)$$

we can set $V_4 = 0$ in (4.30). Using identity (in Minkowski space-time)

$$\epsilon^{abcd} \epsilon_{abef} = -2 \left(\delta_{ce} \delta_{df} - \delta_{cf} \delta_{de} \right),$$

we have

$$\epsilon^{\alpha\mu\beta\nu} \epsilon_{\mu\nu\eta\gamma} k'_\alpha k_\beta p^\eta q^\gamma = 2 \left[(k' \cdot p)(k \cdot q) - (k' \cdot q)(k \cdot p) \right], \quad (4.35)$$

and consequently

$$L_A^{\mu\nu} W_{\mu\nu}^A = -8\frac{W_3}{M^2} \left[(k' \cdot p)(k \cdot q) - (k' \cdot q)(k \cdot p) \right]. \quad (4.36)$$

Neglecting the lepton masses

$$k' \cdot q = -k \cdot q = k' \cdot k = -\frac{1}{2} q^2,$$

and hence

$$L_A^{\mu\nu} W_{\mu\nu}^A = -4\frac{W_3}{M^2} q^2 \left[(k' \cdot p) + (k \cdot p) \right]. \quad (4.37)$$

Transforming to the the LAB frame where

$$(p \cdot k) = ME \quad (p \cdot k') = ME' \quad p^2 = M^2,$$

we have

$$L_S^{\mu\nu} W_{\mu\nu}^S = 16EE' \left[2W_1 \sin^2 \left(\frac{\theta}{2} \right) + W_2 \cos^2 \left(\frac{\theta}{2} \right) \right] \quad (4.38)$$

$$L_A^{\mu\nu} W_{\mu\nu}^A = 16EE' \left[\frac{W_3}{M} (E' + E) \sin^2 \left(\frac{\theta}{2} \right) \right]. \quad (4.39)$$

Neglecting the mass of the final state lepton

$$d^3\mathbf{k}' = |k'|^2 d|k'| d\Omega = E'^2 dE' d\Omega, \quad (4.40)$$

the differential cross-section (4.16) can be written in LAB as

$$d\sigma = \frac{G_F^2 M_W^4}{\left(Q^2 + M_W^2 \right)^2} \frac{1}{32\pi^2} \frac{E'}{E} dE' d\Omega \cdot L^{\mu\nu} W_{\mu\nu}, \quad (4.41)$$

and hence the cross-section for charged-current νh DIS in LAB is

$$\frac{d\sigma}{dE'd\Omega} = \frac{G_F^2 M_W^4}{\left(Q^2+M_W^2\right)^2}\frac{E'^2}{2\pi^2}\left[2W_1\sin^2\left(\frac{\theta}{2}\right)+W_2\cos^2\left(\frac{\theta}{2}\right) + W_3\frac{(E'+E)}{M}\sin^2\left(\frac{\theta}{2}\right)\right]. \quad (4.42)$$

It is conventional to define the following dimensionless structure functions

$$\begin{cases} F_1(x,Q^2) \equiv MW_1 \\ F_2(x,Q^2) \equiv \nu W_2 \\ F_3(x,Q^2) \equiv \nu W_3. \end{cases} \quad (4.43)$$

In terms of these the cross-section becomes

$$\frac{d\sigma}{dE'd\Omega} = \frac{G_F^2 M_W^4}{\left(Q^2+M_W^2\right)^2}\frac{E'^2}{2\pi^2}\left[\frac{2}{M}F_1\sin^2\left(\frac{\theta}{2}\right)+\frac{F_2}{\nu}\cos^2\left(\frac{\theta}{2}\right). + \frac{(E'+E)}{\nu M}F_3\sin^2\left(\frac{\theta}{2}\right)\right] \quad (4.44)$$

The cross-sections are usually expressed in an invariant form. With the relation

$$\frac{d^2\sigma}{dxdy} = \frac{2\pi M\nu}{E'}\frac{d^2\sigma}{dE'd\Omega} = x(s-M^2)\frac{d^2\sigma}{dxdQ^2} \quad (4.45)$$

between the invariant variables x, y, Q^2 and LAB coordinates, we obtain the charged-current νh cross-section:

$$\frac{d\sigma^{CC}(\nu h)}{dxdy} = \frac{G_F^2 M_W^4}{\left(Q^2+M_W^2\right)^2}\frac{ME}{\pi}\left[F_1\cdot xy^2+F_2\left(1-y-\frac{xyM^2}{2ME}\right) + F_3\cdot xy\left(1-\frac{y}{2}\right)\right], \quad (4.46)$$

or

$$\frac{d\sigma^{CC}(\nu h)}{dxdQ^2} = \frac{G_F^2 M_W^4}{\left(Q^2+M_W^2\right)^2}\frac{1}{2\pi x}\left[F_1\cdot xy^2+F_2\left(1-y-\frac{xyM^2}{2ME}\right) + F_3\cdot xy\left(1-\frac{y}{2}\right)\right], \quad (4.47)$$

where $2ME$ can also be written as $s-M^2$ which is clearly Lorentz invariant.

4.2.5 Antineutrino scattering

In order to obtain the corresponding cross-section for antineutrino scattering (fig. 4.3), we must make the following replacement in matrix element (4.10):

$$\overline{u}(k',s')\gamma^\mu(1-\gamma^5)u(k,s) \to \overline{v}(k,s)\gamma^\mu(1-\gamma^5)v(k',s'), \quad (4.48)$$

in which $\overline{v}(k,s)$ and $v(k',s')$ are the antifermion spinors of the initial and the final state antileptons respectively. The calculation then proceeds similarly as

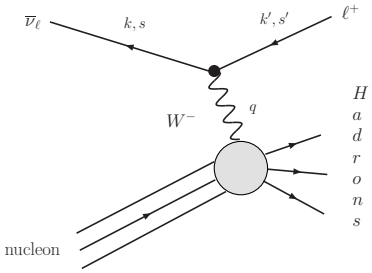

Figure 4.3: Charged-current $\overline{\nu}h$ scattering where k and k' are the four-momenta of leptons and s and s' denotes their spins. Note that the direction of the fermion particle-number flow is reversed compared to fig. 4.1.

in the case of neutrinos. The only difference is in the leptonic tensor (4.21) where the sign of the antisymmetric term reverses:

$$L^{\mu\nu} = 8\left(k'^{\mu}k^{\nu} + k'^{\nu}k^{\mu} - g^{\mu\nu}k\cdot k' - i\epsilon^{\alpha\mu\beta\nu}k'_{\alpha}k_{\beta}\right), \tag{4.49}$$

and this causes also a change of sign in the coefficient of structure functions W_3 and F_3. Consequently, the general CC cross-section for antineutrino-hadron ($\overline{\nu}h$) scattering is

$$\frac{d\sigma^{CC}(\overline{\nu}h)}{dxdQ^2} = \frac{G_F^2 M_W^4}{\left(Q^2+M_W^2\right)^2}\frac{1}{2\pi x} \left[F_1\cdot xy^2 + F_2\left(1-y-\frac{xyM^2}{2ME}\right) - F_3\cdot xy\left(1-\frac{y}{2}\right)\right]. \tag{4.50}$$

We can now sum up the results for general CC cross-sections in νh and $\overline{\nu}h$ scatterings as

$$\frac{d\sigma^{CC}(\nu h,\overline{\nu}h)}{dxdQ^2} = \frac{G_F^2 M_W^4}{\left(Q^2+M_W^2\right)^2}\frac{1}{2\pi x} \left[{}^{CC}F_1\cdot xy^2 + {}^{CC}F_2\left(1-y-\frac{xyM^2}{2ME}\right) \pm {}^{CC}F_3\cdot xy\left(1-\frac{y}{2}\right)\right]. \tag{4.51}$$

The + sign in front of ${}^{CC}F_3$ corresponds to the neutrino scattering and − sign to the antineutrino scattering. We have also explicitly expressed that the structure functions involved are those for CC interaction.

4.2.6 DIS in the parton model

Next we work out the neutrino-nucleon cross-section assuming that the hadron consists of individual spin-$\frac{1}{2}$ partons (quarks) from which the scattering occurs. First, the intermediate boson interacts with one of the constituent quarks and then a complicated fragmentation process converts the recoiled quark and remains of the nucleon into hadrons (fig. 4.4).

In order to establish the connection between the structure functions F_1, F_2, F_3 and the parton model we must be able to construct an equation for parton model cross-section similar to (4.16) where $L^{\mu\nu}$ is defined as in (4.21). Then we

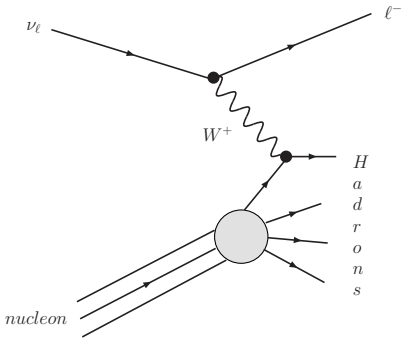

Figure 4.4: Neutrino scattering off an individual parton of a nucleon.

can compare the obtained hadronic tensor with the general form of (4.30) and deduce what the structure functions are.

One way to achieve this is to work in the "infinite momentum frame" in which the momentum of the target hadron is extremely large. In this frame, taking the z-axis parallel with the hadron's momentum, we can write

$$p = (|\mathbf{p}|, 0, 0, -|\mathbf{p}|),$$

and the motion of the constituent quarks will be mainly collinear with the hadron's momentum. Assuming the quark masses to be insignificant, the four-momentum of each quark within the parent hadron is then simply

$$\hat{p_i} = \xi_i p, \tag{4.52}$$

where ξ_i is the fraction of the hadron's momentum carried by the individual quark.

We will also assume that interactions between quarks may be neglected, so that the total cross-section is just a sum over contributions of all quarks. This assumption is justified with the notion that in this frame the quarks are highly relativistic, and time dilatation slows down the rate at which the quarks interact with one another. Hence, quarks may be treated as free particles during the short time that they interact with the intermediate W^+-boson. We will make use of this *incoherence assumption* [24] later.

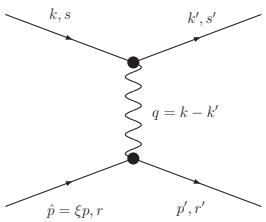

Figure 4.5: Subprocess of νh-scattering where k, s and k', s' are (four-momentum, spin) for incoming neutrino and outgoing lepton respectively. Similarly $\hat{p}, r$ and p', r' for incoming and outgoing quarks.

The subcross-section for scattering of a neutrino off an individual quark within the nucleon can now be written as

$$d\hat{\sigma}^q = \frac{1}{4|k\cdot\hat{p}|}\frac{d^3\mathbf{k}'}{(2\pi)^3 2E'}\frac{d^3\mathbf{p}'}{(2\pi)^3 2p'^0}(2\pi)^4\delta(q+\hat{p}-p')\overline{|\mathfrak{M}_q|^2}, \tag{4.53}$$

where the variables are as explained in fig. 4.5. The corresponding matrix element is now

$$\begin{aligned}\mathfrak{M}_q &= \overline{u}(k',s')\left(\frac{ig}{2\sqrt{2}}\right)\gamma^\mu(1-\gamma^5)u(k,s)\left(-i\frac{g_{\mu\nu}-\frac{q_\mu q_\nu}{M_W^2}}{q^2-M_W^2}\right)\\ &\quad \overline{u}(p',r')\left(\frac{ig}{2\sqrt{2}}\right)\gamma^\nu(1-\gamma^5)u(\hat{p},r)\end{aligned} \tag{4.54}$$

Construction of spin-averaged square of the matrix element (4.54) proceeds as in Eq. (4.11), and the result is

$$\overline{|\mathfrak{M}_q|^2} = \frac{G_F^2 M_W^4}{2\left(Q^2+M_W^2\right)^2}L^{\mu\nu}Q_{\mu\nu}, \tag{4.55}$$

where the neutrino tensor $L^{\mu\nu}$ is identical with (4.21) and quark tensor $Q_{\mu\nu}$ has a similar structure:

$$\begin{aligned}L^{\mu\nu} &= 8\left(k'^\mu k^\nu + k'^\nu k^\mu - g^{\mu\nu}k\cdot k' + i\epsilon^{\alpha\mu\beta\nu}k'_\alpha k_\beta\right)\\ Q_{\mu\nu} &= 4\left(p'_\mu\hat{p}_\nu + p'_\nu\hat{p}_\mu - g_{\mu\nu}\,\hat{p}\cdot p' + i\epsilon_{\phi\mu\eta\nu}\cdot p'^\phi\hat{p}^\eta\right).\end{aligned} \tag{4.56}$$

It will turn out to be useful to rewrite the quark tensor as

$$Q_{\mu\nu} = 4\left[2(p\cdot q)\xi\,\Phi + i\xi\epsilon_{\mu\nu\phi\eta}p^\phi q^\eta\right] \tag{4.57}$$

$$\Phi = -\frac{1}{2}\left(g_{\mu\nu}-\frac{q_\mu q_\nu}{q^2}\right)+\frac{\xi}{p\cdot q}\left(p_\mu-\frac{p\cdot q}{q^2}q_\mu\right)\left(p_\nu-\frac{p\cdot q}{q^2}q_\nu\right). \tag{4.58}$$

It might not be obvious that these two descriptions are equivalent and it indeed requires a bit of work to establish. The cross-section (4.53) may now be integrated over $\mathbf{p}'$ and rearranged,

$$\begin{aligned}d\hat{\sigma}^q &= \frac{1}{4\xi|k\cdot p|}\frac{G_F^2M_W^4}{2(Q^2+M_W^2)^2}\frac{d^3\mathbf{k}'}{(2\pi)^3 2E'}L^{\mu\nu}\overbrace{\int\frac{d^3\mathbf{p}'}{(2\pi)^3 2p'^{(0)}}(2\pi)^4\delta^{(4)}(q+\hat{p}-p')Q_{\mu\nu}}^{4\pi M\cdot W^q_{\mu\nu}}\\ &= \frac{\pi}{2}\frac{G_F^2M_W^4}{(Q^2+M_W^2)^2}\frac{M}{\xi|k\cdot p|}\frac{d^3\mathbf{k}'}{(2\pi)^3 2E'}L^{\mu\nu}W^q_{\mu\nu},\end{aligned} \tag{4.59}$$

where we have defined

$$4\pi M W^q_{\mu\nu} \equiv \int\frac{d^3\mathbf{p}'}{(2\pi)^3 2p'^{(0)}}(2\pi)^4\delta^{(4)}(q+\hat{p}-p')Q_{\mu\nu}. \tag{4.60}$$

Inserting unit operator

$$\int dp'^0 2p'^0\theta\left(p'^0\right)\delta\left(p'^2\right)=1 \tag{4.61}$$

in to the (4.60) we obtain

$$\begin{aligned} 4\pi M W^q_{\mu\nu} &= 2\pi \int d^4p' \underbrace{\delta\left(p'^2\right)\theta\left(p'^{(0)}\right)}_{\delta_+(p'^2)} \delta^{(4)}(q+\hat{p}-p')Q_{\mu\nu} \\ &= 2\pi\delta_+\left(q^2+\hat{p}^2+2q\cdot\hat{p}\right)Q_{\mu\nu} \\ &\approx 2\pi\delta\left(q^2+2\xi p\cdot q\right)Q_{\mu\nu} \\ &= \frac{\pi}{p\cdot q}\delta\left(\frac{q^2}{2p\cdot q}+\xi\right)Q_{\mu\nu} \\ &= \frac{\pi}{p\cdot q}\delta\left(\xi-x\right)Q_{\mu\nu}, \end{aligned} \tag{4.62}$$

where we have neglected the term $\hat{p}^2 = (\xi p)^2 = \xi^2 M^2$, which is safe as we assume $Q^2 \gg M^2$. Thus we find

$$W^q_{\mu\nu} = \frac{\delta\left(\xi-x\right)}{4M(p\cdot q)}Q_{\mu\nu} = \frac{\xi}{M}\delta\left(\xi-x\right)\left[2\Phi + \frac{i}{p\cdot q}\epsilon_{\mu\nu\phi\eta}p^\phi q^\eta\right]. \tag{4.63}$$

The delta-function in the expression suggests that x — also known as Bjorken-x — can be interpreted as the fraction of hadron's momentum carried by the struck quark.

Introducing the momentum distribution $q(\xi)$ of each quark flavor, so that

$$\int_0^1 d\xi\, q(\xi)$$

is the total number of quarks of flavor q in the hadron h, the total cross-section — according to incoherence assumption mentioned earlier — is now obtained as an incoherent sum over all quark flavors:

$$\begin{aligned} d\sigma &= \sum_q \int_0^1 d\xi\, q(\xi) d\hat{\sigma}^q \\ &= \frac{\pi}{2}\frac{G_F^2 M_W^4}{\left(Q^2+M_W^2\right)^2}\frac{M}{|k\cdot p|}\frac{d^3\mathbf{k}'}{(2\pi)^3 2E'}L^{\mu\nu}\underbrace{\sum_q \int_0^1 d\xi\, q(\xi)\frac{1}{\xi}W^q_{\mu\nu}}_{W_{\mu\nu}} \\ &= \frac{\pi}{2}\frac{G_F^2 M_W^4}{\left(Q^2+M_W^2\right)^2}\frac{M}{|k\cdot p|}\frac{d^3\mathbf{k}'}{(2\pi)^3 2E'}L^{\mu\nu}W_{\mu\nu}, \end{aligned} \tag{4.64}$$

where we have defined *hadronic tensor* $W_{\mu\nu}$ as

$$W_{\mu\nu} \equiv \sum_q \int_0^1 d\xi\, q(\xi)\frac{1}{\xi}W^q_{\mu\nu} \tag{4.65}$$

Thus, we see that with a proper definition of hadronic tensor $W_{\mu\nu}$ the cross-

section becomes formally same as in Eq. (4.16). Now, using (4.63) we have

$$\begin{aligned}
W_{\mu\nu} &= \sum_q \int_0^1 d\xi\, q(\xi) \frac{1}{\xi} W^q_{\mu\nu} \\
&= \sum_q \int_0^1 d\xi\, q(\xi) \frac{1}{M} \delta(\xi - x) \left[2\Phi(\xi) + \frac{i}{p\cdot q} \epsilon_{\mu\nu\phi\eta} p^\phi q^\eta \right] \\
&= \sum_q q(x) \frac{1}{M} \left[2\Phi(x) + \frac{i}{p\cdot q} \epsilon_{\mu\nu\phi\eta} p^\phi q^\eta \right] \\
&= -\sum_q \frac{q(x)}{M} \left(g_{\mu\nu} - \frac{q_\mu q_\nu}{q^2} \right) \\
&\quad + \sum_q \frac{2xq(x)}{M(p\cdot q)} \left(p_\mu - \frac{p\cdot q}{q^2} q_\mu \right) \left(p_\nu - \frac{p\cdot q}{q^2} q_\nu \right) \\
&\quad + i \sum_q \frac{q(x)}{M(p\cdot q)} \epsilon_{\mu\nu\phi\eta} p^\phi q^\eta .
\end{aligned} \tag{4.66}$$

Comparing this result with the general hadronic tensor (4.30) we can identify the coefficients W_1, W_2, W_3 as:

$$\begin{aligned}
W_1 &= \sum_q \frac{q(x)}{M} \\
W_2 &= \sum_q \frac{2xq(x)}{M(p\cdot q)} \\
W_3 &= \sum_q \frac{q(x)}{M(p\cdot q)}
\end{aligned}$$

Using definitions (4.43) with $M\nu = p\cdot q$, the dimensionless structure functions for CC interaction become

$$\begin{aligned}
{}^{CC}F_1(x,Q^2) &= \sum_q q(x,Q^2) \\
{}^{CC}F_2(x,Q^2) &= \sum_q 2xq(x,Q^2) \\
{}^{CC}F_3(x,Q^2) &= \sum_q 2q(x,Q^2).
\end{aligned} \tag{4.67}$$

We have now incorporated also Q^2 dependence in the momentum distributions and hence in the structure functions although the origin of this dependence can not be seen from our current discussion. The Q^2 dependence follows from the strong interactions (QCD) between quarks and gluons, and we shall return to this issue later on.

4.2.7 Accommodating antiquarks

The contribution of antiquarks (fig. 4.6) can be obtained by performing the following replacement in (4.54):

$$\overline{u}(p',r')\gamma^\nu(1-\gamma^5)u(\hat{p},r) \to \overline{v}(\hat{p},r)\gamma^\nu(1-\gamma^5)v(p',r').$$

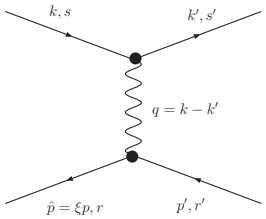

Figure 4.6: Subprocess of νh scattering involving antiquarks.

This replacement causes the sign of antisymmetric part in the quark tensor (4.56) to reverse:

$$\overline{Q}_{\mu\nu} = 4\left(p'_\mu \hat{p}_\nu + p'_\nu \hat{p}_\mu - g_{\mu\nu}\,\hat{p}\cdot p' - i\epsilon_{\phi\mu\eta\nu} p'^{\phi}\hat{p}^{\eta}\right). \tag{4.68}$$

Consequently, the sign of the structure function F_3 also changes:

$$\begin{aligned} {}^{CC}F_1^{\overline{q}}(x,Q^2) &= \sum_q \overline{q}(x,Q^2) \\ {}^{CC}F_2^{\overline{q}}(x,Q^2) &= \sum_q 2x\overline{q}(x,Q^2) \\ {}^{CC}F_3^{\overline{q}}(x,Q^2) &= -\sum_q 2\overline{q}(x,Q^2). \end{aligned} \tag{4.69}$$

The intermediate W^+ boson can interact only with negatively charged quarks and antiquarks. Hence, using (4.67) and (4.69) charged-current νh scattering structure functions can be summarized as

$$\begin{aligned} {}^{CC}F_2^{\nu}(x,Q^2) &= 2x\cdot {}^{CC}F_1^{\nu}(x,Q^2) = 2x\left[d+s+b+\overline{u}+\overline{c}+\overline{t}\right] \\ {}^{CC}F_3^{\nu}(x,Q^2) &= 2\left[d+s+b-\overline{u}-\overline{c}-\overline{t}\right] \end{aligned} \tag{4.70}$$

where $q \equiv q(x,Q^2)$ for each quark flavor. They, supplemented with the gluon distributions, are usually what is referred to as *parton distribution functions* (PDFs).

4.2.8 $\overline{\nu}h$ DIS in the parton model

Having already worked out the general cross-section for $\overline{\nu}h$ scattering (4.50) and structure functions F_1, F_2, F_3 for quarks and antiquarks, the extension to antineutrino scattering is rather easy. The quark and antiquark contributions for $\overline{\nu}h$ CC cross-section are obtained using results (4.67) and (4.69) with cross-section (4.50).

The intermediate W^- boson can interact only with positively charged quarks and antiquarks and so we have

$$\begin{aligned} {}^{CC}F_2^{\overline{\nu}}(x,Q^2) &= 2x\cdot F_1^{\overline{\nu}}(x,Q^2) = 2x\left[u+c+t+\overline{d}+\overline{s}+\overline{b}\right] \\ {}^{CC}F_3^{\overline{\nu}}(x,Q^2) &= 2\left[u+c+t-\overline{d}-\overline{s}-\overline{b}\right] \end{aligned} \tag{4.71}$$

We have seen that the the structure functions do not depend explicitly on E. Thus, looking back to eq. (4.46), we would expect that in the limit $E \gg M$

$$\sigma_{\text{total}}(\nu N, \overline{\nu}N \to \ell^{\pm} + \text{anything}) \propto E.$$

Indeed, the experimental results shown in fig. 4.7 reveal this to be true to an excellent approximation!

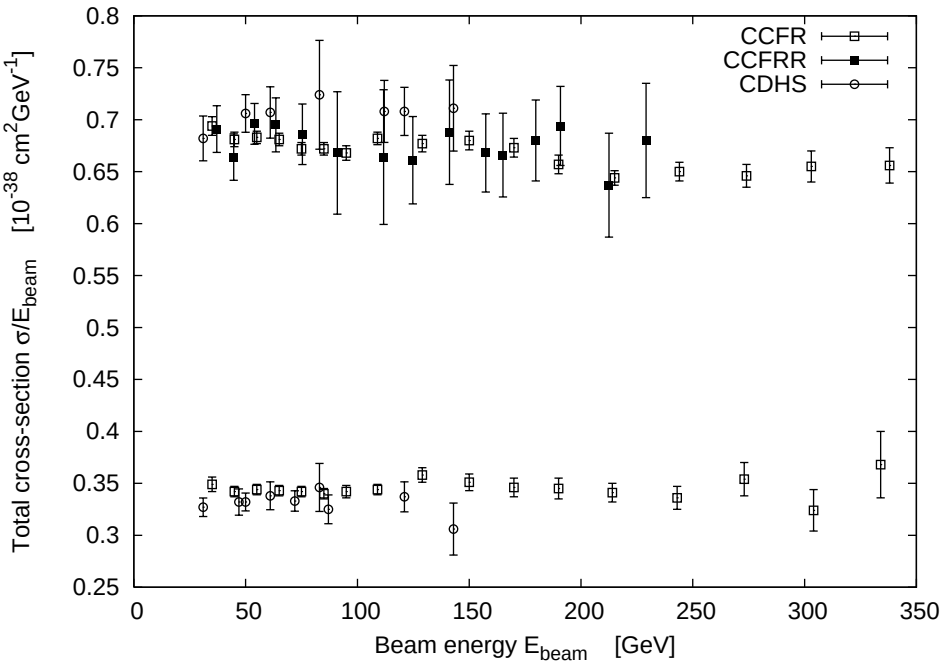

Figure 4.7: The total cross-section for CC neutrino and antineutrino scattering off iron target divided by the neutrino beam energy. Data is from **CCFR** [25], **CCFR** [26] and **CDHS** [27] experiments.

4.3 Neutral current DIS

4.3.1 General neutral current cross-section

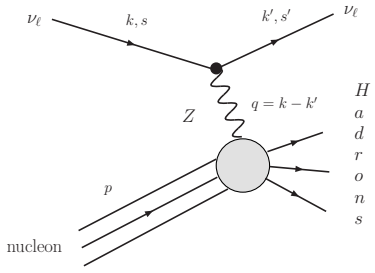

Figure 4.8: Neutral current νh-scattering

Construction of general neutrino-hadron neutral current (NC) DIS cross-section proceeds similarly to the case of charged-current process. The scattering

matrix-element related to an n hadron final-state is

$$\begin{aligned}\mathfrak{M}_n &= \overline{u}(k',s')\left(ig_Z\gamma^\mu(1-\gamma^5)\right)u(k,s)\left(-i\frac{g_{\mu\nu}-\frac{q_\mu q_\nu}{M_Z^2}}{q^2-M_Z^2}\right)\\ &\quad < n,out|ig_Z\,\hat{J}^\nu|h,in > \end{aligned} \tag{4.72}$$

where $\hat{J}^\nu$ denotes the neutral weak-current operator. Formally, this is rather similar to the charged current matrix element (4.10) and the calculation proceeds exactly in the same way. The result is

$$d\sigma = \frac{\pi}{8}\frac{G_F^2M_Z^4}{\left(Q^2+M_Z^2\right)^2}\frac{M}{|k\cdot p|}\frac{d^3\mathbf{k}'}{(2\pi)^3 2E'}L^{\mu\nu}W_{\mu\nu}, \tag{4.73}$$

where the tensors are defined as in (4.21) and (4.30):

$$\begin{aligned}L^{\mu\nu} &= 8\left(k'^\mu k^\nu + k'^\nu k^\mu - g^{\mu\nu}k\cdot k' + i\epsilon^{\alpha\mu\beta\nu}k'_\alpha k_\beta\right)\\ W_{\mu\nu} &= -W_1\left(g_{\mu\nu}-\frac{q_\mu q_\nu}{q^2}\right)+\frac{W_2}{M^2}\left(p_\mu-\frac{p\cdot q}{q^2}q_\mu\right)\left(p_\nu-\frac{p\cdot q}{q^2}q_\nu\right)\\ &\quad +i\frac{W_3}{2M^2}\epsilon_{\mu\nu\eta\gamma}p^\eta q^\gamma,\end{aligned}$$

and we have used the relation

$$\frac{16g_Z^2}{M_Z^2} = 4\sqrt{2}G_F \tag{4.74}$$

where G_F is again the low-energy Fermi coupling constant. Consequently, the cross-sections for neutral current DIS are obtained straightforwardly from (4.51):

$$\begin{aligned}&\frac{d^2\sigma^{NC}(\nu h,\overline{\nu}h)}{dxdQ^2} = \frac{G_F^2M_Z^4}{\left(Q^2+M_Z^2\right)^2}\frac{1}{2\pi x}\\ &\left[{}^{NC}F_1\cdot xy^2 + {}^{NC}F_2\left(1-y-\frac{xyM^2}{2ME}\right)\pm {}^{NC}F_3\cdot xy\left(1-\frac{y}{2}\right)\right].\end{aligned} \tag{4.75}$$

The + sign corresponds to neutrinos and − sign to antineutrinos in the initial state.

4.3.2 Connection to the parton model

While charged current interaction couples only left-handed quarks and right-handed antiquarks, neutral current interaction couples both helicity-states of quarks and antiquarks (left and right handed) and the matrix element therefore includes an additional term proportional to $+\gamma_\mu\gamma^5$:

$$\begin{aligned}\mathfrak{M}_q^{NC} &= \overline{u}(k',s')\left[ig_Z\gamma^\mu(1-\gamma^5)\right]u(k,s)\left(-i\frac{g_{\mu\nu}-\frac{q_\mu q_\nu}{M_Z^2}}{q^2-M_Z^2}\right)\\ &\quad \overline{u}(p',r')\left[ig_Z\gamma^\nu\left(R_q(1+\gamma^5)+L_q(1-\gamma^5)\right)\right]u(\hat{p},r).\end{aligned} \tag{4.76}$$

The coefficients L_q and R_q are defined in eq. (3.61)

$$\begin{aligned}L_q &= \tau_3 - 2e_q\sin^2\theta_W,\\ R_q &= -2e_q\sin^2\theta_W.\end{aligned} \tag{4.77}$$

The spin-averaged square of the matrix element (4.76) can be again expressed as a contraction of rank-two tensors

$$\overline{|\mathfrak{M}_q^{NC}|^2} = \frac{G_F^2 M_Z^4}{8\left(Q^2+M_Z^2\right)^2} L_{NC}^{\mu\nu} Q_{\mu\nu}^{NC}, \tag{4.78}$$

where the neutrino tensor $L^{\mu\nu}$ is identical with that in Eq. (4.21) but the quark tensor $Q_{\mu\nu}$ has now more complicated structure:

$$\begin{aligned} L_{NC}^{\mu\nu} &= 8\left(k'^{\mu}k^{\nu}+k'^{\nu}k^{\mu}-g^{\mu\nu}k\cdot k'+i\epsilon^{\alpha\mu\beta\nu}k'_{\alpha}k_{\beta}\right) \\ Q_{\mu\nu}^{NC} &= 4\left(L_q^2+R_q^2\right)\left(p'_{\mu}\hat{p}_{\nu}+p'_{\nu}\hat{p}_{\mu}-g_{\mu\nu}\,\hat{p}\cdot p'\right)+ \qquad (4.79) \\ &\quad 4i\left(L_q^2-R_q^2\right)\epsilon_{\phi\mu\eta\nu}p'^{\phi}\hat{p}^{\eta}. \qquad (4.80) \end{aligned}$$

The quark mass has again been neglected. From here on the calculation proceeds as in the case of CC (sections 4.2.6–4.2.7) but keeping the coefficients $\left(L_q^2+R_q^2\right)$ and $\left(L_q^2-R_q^2\right)$ in front of symmetric and antisymmetric term respectively. The equations for structure functions F_1, F_2, and F_3 are therefore easy to track. For quarks we obtain:

$$\begin{aligned} {}^{NC}F_1^q(x,Q^2) &= \sum_q \left(L_q^2+R_q^2\right) q(x,Q^2) \\ {}^{NC}F_2^q(x,Q^2) &= \sum_q 2\left(L_q^2+R_q^2\right) xq(x,Q^2) \qquad (4.81) \\ {}^{NC}F_3^q(x,Q^2) &= \sum_q 2\left(L_q^2-R_q^2\right) q(x,Q^2), \end{aligned}$$

and for antiquarks:

$$\begin{aligned} {}^{NC}F_1^{\overline{q}}(x,Q^2) &= \sum_q \left(L_q^2+R_q^2\right) \overline{q}(x,Q^2) \\ {}^{NC}F_2^{\overline{q}}(x,Q^2) &= \sum_q 2\left(L_q^2+R_q^2\right) x\overline{q}(x,Q^2) \qquad (4.82) \\ {}^{NC}F_3^{\overline{q}}(x,Q^2) &= \sum_q 2\left(R_q^2-L_q^2\right) \overline{q}(x,Q^2). \end{aligned}$$

Unlike $W^{\pm}$, the intermediate Z^0 can interact with all quarks and antiquarks and hence the sums in equations above must extend over all flavors.

4.4 QED DIS

QED analysis for DIS proceeds as in the case of weak interaction but is simplified by the absence of the axial-vector part.

The QED matrix element corresponding to ℓ + nucleon scattering with n hadrons in the final state X reads now

$$\mathfrak{M}_n = \overline{u}(k',s')\left(-ie\gamma^{\mu}\right)u(k,s)\left(-i\frac{g_{\mu\nu}}{q^2}\right) < n,out|ie\hat{J}_{em}^{\nu}|h,in> . \tag{4.83}$$

where e is the electron charge and $\hat{J}_{em}^{\nu}$ is electromagnetic current operator. The differential cross-section for unpolarized scattering can, again, be expressed in

terms of leptonic and hadronic tensors as

$$d\sigma = \pi \frac{e^4}{q^4} \frac{M}{|k \cdot p|} \frac{d^3\mathbf{k}'}{(2\pi)^3 2E'} L^{\mu\nu} W_{\mu\nu}, \tag{4.84}$$

where

$$\begin{aligned} L^{\mu\nu} &= \frac{1}{2} \sum_{s,s'} \overline{u}(k',s') \gamma^\mu u(k,s) \overline{u}(k,s) \gamma^\nu u(k',s') \\ &= 2\left(k'^\mu k^\nu + k'^\nu k^\mu - g^{\mu\nu} k \cdot k'\right) \qquad (4.85) \\ W_{\mu\nu} &= -W_1 \left(g_{\mu\nu} - \frac{q_\mu q_\nu}{q^2}\right) + \frac{W_2}{M^2} \left(p_\mu - \frac{p \cdot q}{q^2} q_\mu\right) \left(p_\nu - \frac{p \cdot q}{q^2} q_\nu\right). \end{aligned}$$

We have now explicitly included a factor of $1/2$ in the leptonic tensor $L^{\mu\nu}$ which is due to averaging over two spin states of a charged lepton. Note that $W_{\mu\nu}$ is now fully symmetric as all antisymmetric terms would vanish under contraction with $L^{\mu\nu}$. This means that we eventually get just two structure functions F_1, F_2 instead of three as in the ν-scattering. Doing the same analysis as earlier but omitting all antisymmetric terms we end up with a differential cross-section for QED DIS

$$\frac{d\sigma^{EM}}{dx dQ^2} = \frac{4\pi\alpha^2}{Q^4} \frac{1}{x} \left[{}^{EM}F_1 \cdot xy^2 + {}^{EM}F_2 \left(1 - y - \frac{xyM^2}{2ME}\right)\right], \tag{4.86}$$

where $\alpha \equiv e^2/4\pi$ is the Sommerfeld fine structure constant. We have also explicitly written ${}^{EM}F_1$ and ${}^{EM}F_2$ to distinguish them for structure functions in ν-scatterings.

4.4.1 Parton model DIS in QED

As earlier, we want to know the explicit form of the structure functions in terms of parton distribution functions. Thus, we begin with the matrix element for QED scattering of a charged lepton off an individual quark

$$\mathfrak{M}_q = \overline{u}(k',s') \left(-ie\gamma^\mu\right) u(k,s) \left(-i\frac{g_{\mu\nu}}{q^2}\right) \overline{u}(p',r') \left(iee_q\gamma^\mu\right) u(\hat{p},r), \tag{4.87}$$

where e_q is the electric charge of a struck quark. The spin-averaged square is then

$$\overline{|\mathfrak{M}_q|^2} = \frac{e^4 e_q^2}{q^4} L^{\mu\nu} Q_{\mu\nu} \tag{4.88}$$

where

$$\begin{aligned} L^{\mu\nu} &= 2\left(k'^\mu k^\nu + k'^\nu k^\mu - g^{\mu\nu} k \cdot k'\right) \qquad (4.89) \\ Q_{\mu\nu} &= 2\left(p'_\mu \hat{p}_\nu + p'_\nu \hat{p}_\mu - g_{\mu\nu} \hat{p} \cdot p'\right). \end{aligned}$$

The quark tensor $Q_{\mu\nu}$ differs from (4.56), aside from lacking the antisymmetric part, with the factor of 2 and hence we can simply read the outcome for our parton model result for hadronic tensor $W_{\mu\nu}$ appearing in 4.84 from eqn. (4.66)

to be

$$\begin{aligned} W_{\mu\nu} &= -\sum_q e_q^2 \frac{q(x)}{2M}\left(g_{\mu\nu} - \frac{q_\mu q_\nu}{q^2}\right) \\ &\quad + \sum_q e_q^2 \frac{xq(x)}{M\,(p\cdot q)}\left(p_\mu - \frac{p\cdot q}{q^2}q_\mu\right)\left(p_\nu - \frac{p\cdot q}{q^2}q_\nu\right). \end{aligned}$$

Comparing this with (4.86) we deduce

$$\begin{aligned} W_1 &= \sum_q e_q^2 \frac{q(x)}{2M} \\ W_2 &= \sum_q e_q^2 M \frac{xq(x)}{(p\cdot q)}, \end{aligned}$$

and with the definitions of (4.43) we obtain

$$^{EM}F_2^q(x,Q^2) = 2x\,{}^{EM}F_1^q(x,Q^2) = \sum_q e_q^2 xq(x,Q^2), \tag{4.90}$$

where the superscript q reminds us that only quarks are considered. The sums above extend of course over all flavors since all quarks are charged particles and can interact exchanging a photon. Furthermore, it is easy to see that a similar result holds for scattering off an antiquark and we can finally write the complete QED structure functions:

$$^{EM}F_2(x,Q^2) = 2x\,{}^{EM}F_1(x,Q^2) = \sum_q e_q^2 x\left[q(x,Q^2) + \overline{q}(x,Q^2)\right], \tag{4.91}$$

the sum ranging over all quark flavors q.

4.5 Drell-Yan process

One other process that is closely related to DIS and which we will discuss shortly is the Drell-Yan (DY) process.

$$\text{hadron} + \text{hadron} \to \mu^+ + \mu^- + \text{anything}$$

This process was initially proposed to explain the observed fall of the cross-section with increasing invariant mass M of the dimuon pair (fig. 4.9). Drell and Yan suggested [28] that this happened mainly through a channel shown in fig. (4.10) in which an antiquark from one hadron annihilates with a quark from the other hadron to produce a virtual photon which subsequently splits to a pair of opposite-sign leptons. The remainder of the hadrons fragment to produce a background of various hadrons allowed by conservation laws.

4.5.1 The quark sub-process

The cross-section for DY-process is most easily constructed by computing first the total cross-section for the sub-process

$$q + \overline{q} \to \mu^+ + \mu^-.$$

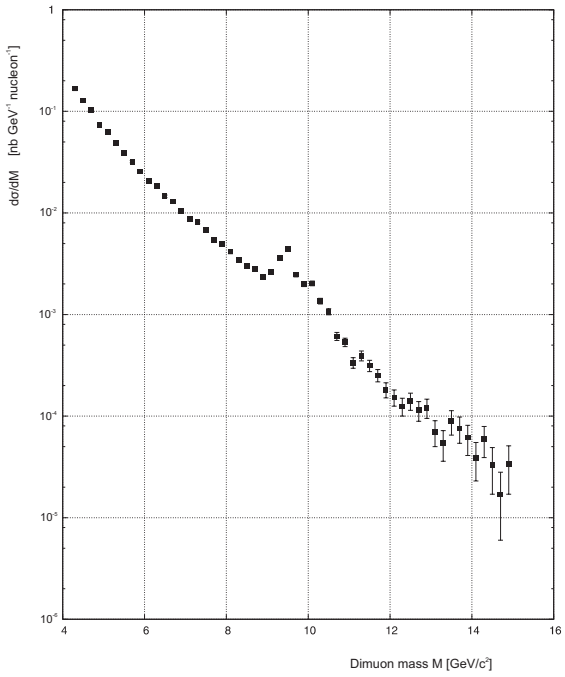

Figure 4.9: Dimuon spectra for 800 GeV/c protons. Enhancements around $M \approx 9.5\,\text{GeV}$ and $M \approx 11\,\text{GeV}$ are due to Υ ($b\overline{b}$ meson) resonances. Data is from the Fermilab experiment [29].

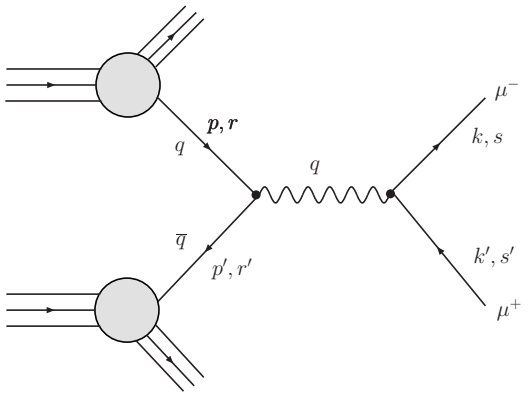

Figure 4.10: The Drell-Yan process with associated kinematic quantities. The momentum and spin for quark and antiquark emerging from the initial state hadrons are denoted by (p, r) and (p', r'). Similarly (k, s) and (k', s') are the momentum and spin for outgoing muon and antimuon. The momentum of the virtual photon is $q = p + p'$.

The matrix element for this process is

$$i\mathfrak{M}_q = \overline{u}(k,s)\left(-ie\gamma^\mu\right)v(k',s')\left(-i\frac{g_{\mu\nu}}{q^2}\right)\overline{v}(p',r')\left(iee_q\gamma^\nu\right)u(p,r), \tag{4.92}$$

where the kinematic quantities are given in fig. 4.10. As in DIS, we are not interested in any particular spin configuration and thus, after squaring $\mathfrak{M}_q$ we sum over the lepton pair spin states and average over the annihilating quark's spin states. The result can be written as

$$\overline{|\mathfrak{M}_q|^2} = \frac{1}{4}\sum_{\text{spins}}|\mathfrak{M}_q|^2 = \frac{e_q^2e^4}{q^4}L_\ell^{\mu\nu}L^q_{\mu\nu}, \tag{4.93}$$

where

$$L_\ell^{\mu\nu} = \frac{1}{2}\sum_{s,s'}\overline{u}(k,s)\gamma^\mu v(k',s')\overline{v}(k',s')\gamma^\nu u(k,s) \tag{4.94}$$

$$L^q_{\mu\nu} = \frac{1}{2}\sum_{r,r'}\overline{v}(p',r')\gamma_\mu u(p,r)\overline{u}(p,r)\gamma_\nu v(p',r'). \tag{4.95}$$

Using the methods of section 4.2.2 and neglecting all masses involved we get

$$L_\ell^{\mu\nu} = 4\left[k^\mu k'^\nu + k^\nu k'^\mu - g^{\mu\nu}(k\cdot k')\right] \tag{4.96}$$

$$L^q_{\mu\nu} = 4\left[p^\mu p'^\nu + p^\nu p'^\mu - g^{\mu\nu}(p\cdot p')\right], \tag{4.97}$$

which under contraction yield

$$L_\ell^{\mu\nu}L^q_{\mu\nu} = 32\left[(k\cdot p)(k'\cdot p') + (k\cdot p')(k'\cdot p)\right]. \tag{4.98}$$

Thus, the unpolarized matrix element reads

$$\overline{|\mathfrak{M}_q|^2} = 8\frac{e_q^2e^4}{q^4}\left[(k\cdot p)(k'\cdot p') + (k\cdot p')(k'\cdot p)\right]. \tag{4.99}$$

The kinematics is most easily done in the CMS frame of the colliding quarks. The total cross-section at the parton level is now

$$\hat{\sigma} = \frac{(2\pi)^4}{4\sqrt{(p\cdot p')^2 - m_q^2m_{\overline{q}}^2}}\int\frac{d^3\mathbf{k}}{(2\pi)^3 2E_k}\frac{d^3\mathbf{k}'}{(2\pi)^3 2E_{k'}}\delta^{(4)}\left(p+p'-k-k'\right)\overline{|\mathfrak{M}_q|^2} \tag{4.100}$$

Integrating over $\mathbf{k}'$ fixes the condition $\mathbf{k}' = \mathbf{p}+\mathbf{p}'-\mathbf{k}$, and transforming to the spherical coordinates we get

$$\hat{\sigma} = \frac{(2\pi)^4}{2\hat{s}}\int\frac{|\mathbf{k}|^2 d|\mathbf{k}|d\Omega}{4(2\pi)^6E_kE_{k'}}\delta\left(\sqrt{\hat{s}}-k^0-k'^0\right)\overline{|\mathfrak{M}_q|^2}, \tag{4.101}$$

where we also neglected all quark masses and used

$$\hat{s} \equiv (p+p')^2 = \left(p^0+p'^0\right)^2 \approx 2p\cdot p'.$$

The δ-function can be written as

$$\delta\left(\sqrt{\hat{s}}-2|\mathbf{k}|\right) = \frac{1}{2}\delta\left(|\mathbf{k}|-\frac{1}{2}\sqrt{\hat{s}}\right). \tag{4.102}$$

Hence we get

$$\hat{\sigma} = \frac{(2\pi)^4}{2\hat{s}} \int \frac{\hat{s}\, d\Omega}{32(2\pi)^6 E_k E_{k'}} \overline{|\mathfrak{M}_q|^2} \tag{4.103}$$

$$= \frac{(2\pi)^4}{2\hat{s}} \int \frac{\hat{s}\, d\Omega}{8(2\pi)^6 \hat{s}} \overline{|\mathfrak{M}_q|^2} \tag{4.104}$$

$$= \frac{1}{64\pi^2 \hat{s}} \int d\Omega \overline{|\mathfrak{M}_q|^2}, \tag{4.105}$$

where we used CMS-frame result $\hat{s} = 4E_k E_{k'}$. In this frame the matrix element 4.99 takes a simple form

$$\overline{|\mathfrak{M}_q|^2} = e_q^2 e^4 \left(1 + \cos^2\theta\right), \tag{4.106}$$

and inserting this in to the cross-section formula we can perform the angular integration

$$\hat{\sigma} = \int \frac{e_q^2 e^4}{64\pi\hat{s}} \left(1 + \cos^2\theta\right) d\Omega = \frac{4\pi\alpha^2}{3\hat{s}} e_q^2. \tag{4.107}$$

Note that the quark colour effects have not been considered yet — these will be discussed below.

4.5.2 Embedding to hadronic level

Now we are ready to consider the process at the hadronic level. We are interested in the differential cross-section for particular invariant mass M of the final state lepton pair and we first rewrite (4.107) as

$$\frac{d\hat{\sigma}}{dM^2} = \frac{4\pi\alpha^2}{3M^2} e_q^2 \delta\left(M^2 - \hat{s}\right) \tag{4.108}$$

This expression has now to be multiplied by a factor $q_1(x_1)$ that gives the number of quarks of flavor q with momentum fraction x_1 in the first hadron and by a factor $\overline{q}_2(x_2)$ that gives the number of antiquarks of the same flavor in the second hadron. For the total cross-sections the integration $\int_0^1 dx_1 \int_0^1 dx_2$ should the be performed. It is also possible that the origins of the quark and the antiquark are reversed. This gives an an additional term where $q_1(x_1)dx_1\overline{q}_2(x_2)dx_2$ is replaced with $\overline{q}_1(x_1)dx_1 q_2(x_2)dx_2$.

Because each quark flavor can contribute we must sum over all flavors. Furthermore, the colors of the annihilating quark and antiquark must match which reduces the cross-section by a factor of 3. Putting these together we arrive at

$$\frac{d\sigma}{dM^2} = \frac{4\pi\alpha^2}{9M^2} \sum_q e_q^2 \int \left[q_1(x_1)\overline{q}_2(x_2) + \overline{q}_1(x_1)q_2(x_2)\right] dx_1 dx_2\, \delta\left(M^2 - x_1 x_2 s\right),$$

where s is the squared total CMS-energy of the colliding hadrons. The integration over x_1 can be performed, yielding

$$\frac{d\sigma}{dM^2} = \frac{4\pi\alpha^2}{9M^2 s} \sum_q e_q^2 \int \left[q_1(x_1)\overline{q}_2(x_2) + \overline{q}_1(x_1)q_2(x_2)\right] \frac{1}{x_2} dx_2, \tag{4.109}$$

where it is implicitly understood that $x_1 = \frac{M^2}{sx_2}$. Although the remaining x_2 integration can not be done analytically eq. (4.109) suggests that the cross-section should go as

$$\frac{d\sigma}{dM^2} \propto \frac{1}{M^2}, \tag{4.110}$$

explaining the observed decrease in the cross-section with increasing dilepton mass.

For our later purposes, we will need the double differential cross-section

$$\frac{d^2\sigma}{dM^2 dx_2} = \frac{4\pi\alpha^2}{9M^4} \sum_q e_q^2 \left[q_1(x_1, Q^2)\overline{q}_2(x_2, Q^2) + \overline{q}_1(x_1, Q^2) q_2(x_2, Q^2) \right] x_1 dx_2, \tag{4.111}$$

where the QCD scale in the PDFs is $Q^2 \sim M^2$.

4.6 Phenomenology: from free proton to the bound nucleus

In this section, we will discuss the phenomenology of DIS. We will restrict our discussion to the QED structure function

$$^{EM}F_2(x, Q^2) = \sum_q e_q^2 x \left[q(x, Q^2) + \overline{q}(x, Q^2) \right],$$

since it reflects the behavior of the PDFs most explicitly.

4.6.1 Structure function $^{EM}F_2$ for free proton

Neglecting the transverse momentum of the partons in the infinite-momentum frame and assuming $Q^2 \gg M^2$ led us to the conclusion that the structure functions of DIS seem to come independent of Q^2 and depend only on a single variable, the Bjorken-x. In fact, this so called *Bjorken-scaling*, derived originally by Bjorken [30], is one of the most striking predictions of the parton model.

The structure functions are measurable quantities, and whether the theoretical predictions are correct is always up to experiments to verify. Indeed, the early experiments at SLAC for QED structure function $^{EM}F_2$ seemed to confirm the Bjorken-scaling and were the first clear experimental evidence about the existence of the quarks!

That the Bjorken-scaling was really seen in the SLAC experiment was, however, somewhat accidental. This is because the further experiments that probed a larger area with respect to the (Q^2, x)-plane revealed that the Bjorken-scaling is *not* an exact result. This is evident from fig. 4.11 that shows a set of representative data from measurements of $^{EM}F_2$ for the free proton. It just happened, that the pioneering SLAC experiments probed a region of the (Q^2, x)-plane where the Bjorken-scaling happens to hold, i.e. the Q^2-evolution is slow.

At low x, the structure function increases with increasing Q^2 whilst at larger x there is a fall with increasing Q^2. The reason behind this apparent contradiction between experimental evidence and the naive parton model prediction is

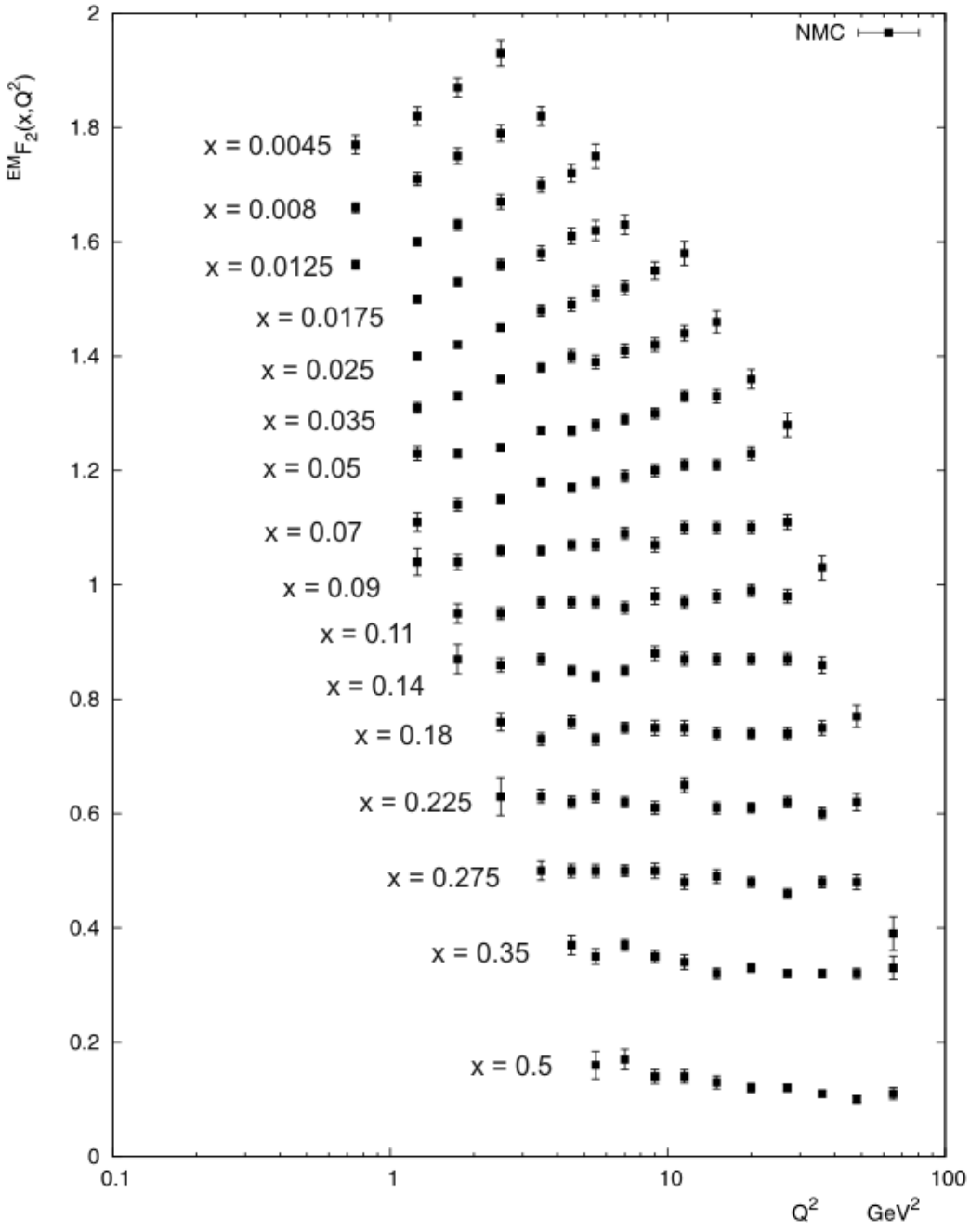

Figure 4.11: Structure function $^{EM}F_2$ for the free proton as a function of Q^2. To make the plot readable each $^{EM}F_2$ has been scaled by adding constant i ranging from 0 to 0.15 in 0.1 steps for $x = 0.5$ to $x = 0.0045$. The data shown is from **NMC** [37] experiment.

that the effects of QCD were completely ignored. Within the framework of per-

turbative QCD, this Q^2 evolution is described by so called DGLAP equations [31, 32, 33]. Here we will not give an exact QCD explanation of the Q^2 dependence but merely a qualitative picture about the physics behind this apparent scaling violation.

According to QCD the quarks within the proton interact via emission and absorption of coloured massless bosons, gluons. A gluon can split up to create a quark-antiquark pair which in turn can annihilate back to a gluon and this process leads to the picture of a proton in which the three valence quarks are surrounded by a wildly fluctuating sea of gluons and quark-antiquark pairs.

As the proton is probed at a given Q^2 a certain number of quarks, antiquarks and gluons is observed. The duration of interaction goes as $\propto 1/Q^2$ and quantum fluctuations — creation of quark-antiquark pairs via emission of gluons — that happen within a timescale much shorter than $1/Q^2$ remains unobserved. As Q^2 increases the timescale gets shorter and more short-lived virtual quark-antiquark pairs and gluons are resolved. The partons are seen to contain partons, which at larger Q^2 are seen to contain partons and so on. In each successive gluon emission partons lose momentum and consequently their momentum fraction x declines. Thus, the PDFs and ${}^{EM}F_2$ tend to increase at small x and fall at large x as Q^2 increases.

Another feature that follows from QCD is that at the given Q^2 the PDFs should rise towards lower x. This is because the celebrated *asymptotic freedom* of QCD: coupling strength increases as the energy involved in the process falls. Since the energy decreases toward lower x there should be greater tendency of quarks to radiate gluons which can eventually create quark-antiquark pairs. Therefore the PDFs and ${}^{EM}F_2$ should peak as x tends to zero. Such a behavior is very evident in fig. 4.12.

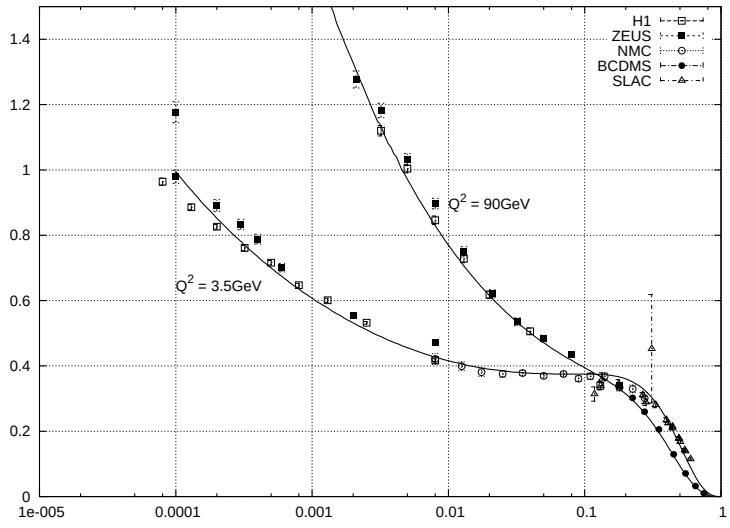

Figure 4.12: Structure functions $F_2(x, Q^2)$ for free proton shown at two values of Q^2. The solid lines are computed form the latest CTEQ6 parton distributions. The data is from **BCDMS** [38], **H1** [39], **NMC** [37], **SLAC** [40], and **ZEUS** [41] experiments. The solid line is computed from **CTEQ6** [35] PDF parametrization.

From the measurements of DIS and other hard-scattering processes like Drell-Yan dimuon production described earlier, the actual PDFs for protons can be unfolded through process that is usually referred as *global analysis*. In this process the PDFs are first parametrized at some initial scale Q_0^2 from which the PDFs at other values of $Q^2 > Q_0^2$ are obtained by DGLAP evolution. Using the PDFs at Q_0^2 as non-perturbative input, structure functions and cross-sections for variety of hard-scattering processes can be computed and eventually compared with experimental results. Adjusting the parametrization in such a way that the experimental results are recovered gives then the correct PDFs. A nice description about the procedure and current state-of-art of PDFs can be found in ref. [34].

Nowadays, several sets of proton PDFs are available. They are distributed as a program-callable functions so that they can readily be used in computer based calculations. In this thesis we will be using exclusively the latest CTEQ [35] distributions of which fig. 4.13 shows an example.

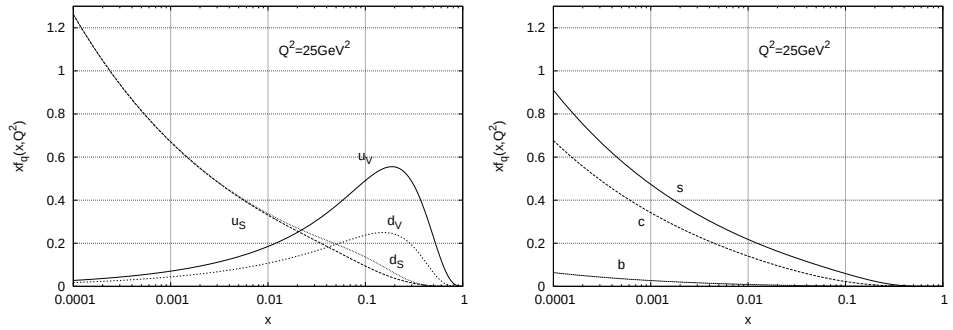

(a) up and down (b) strange, charm and bottom

Figure 4.13: Distributions $xq(x, Q^2)$ in the free proton at $Q^2 = 25\,\mathrm{GeV}^2$ for (a) the valence and sea distributions of up and down quarks and (b) the sea distributions of strange, charm and bottom quarks.

4.6.2 Nuclear effects

The difference between F_2 in heavier nuclei and deuterium is a well known phenomenon. Fig. 4.14 shows an example of measured ratios, $F_2^{\ell^\pm}$ of a heavy nucleus (calsium) to that of deuteron, and it indeed reveals a clear deviation from unity. These *nuclear effects* in the ratios $\frac{1}{A}F_2^A/\frac{1}{2}F_2^D$ are usually divided

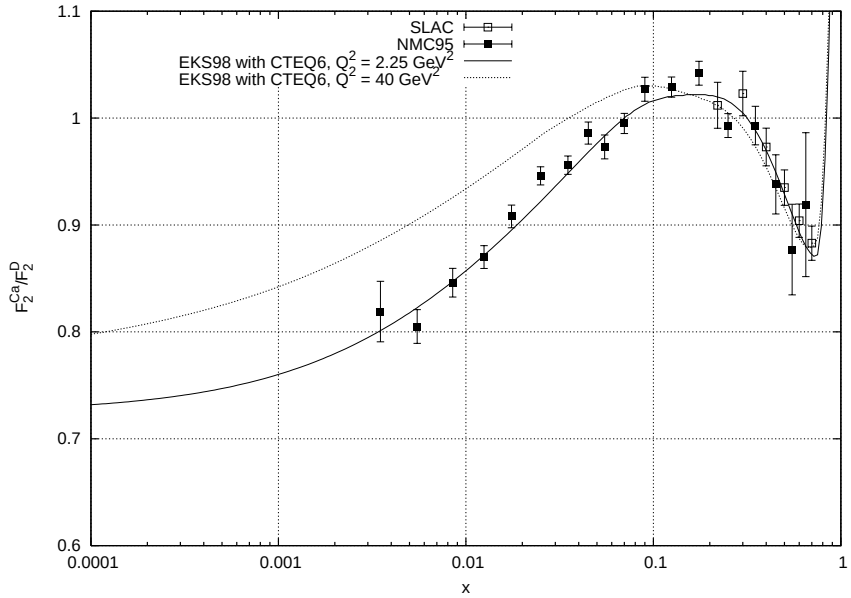

Figure 4.14: Ratio $\frac{1}{A}F_2^{\mathrm{Ca}}/\frac{1}{2}F_2^{\mathrm{D}}$ as a function of x. Data points are at various values of $Q^2 = 0.4...40\,\mathrm{GeV}^2$ but the parametrization shown is at fixed $Q^2 = 2.25\,\mathrm{GeV}^2$ and $Q^2 = 40\,\mathrm{GeV}^2$. Data is from **NMC** [42] experiment and the curves are calculated with EKS98 parametrization [43, 44] supplemented with CTEQ6 parton distributions.

as follows:

- The suppression at low x ($x < 0.1$) is conventionally referred to as *shadowing*.
- Subsequent enhancement at slightly higher x ($0.1 < x < 0.3$) is correspondingly called *anti-shadowing*.
- The depletion at high x ($0.3 < x < 0.7$) is the *EMC effect*.
- The sharp enhancement at very high x ($x > 0.7$) is attributed to *Fermi motion*.

Comparing these regions with fig. 4.13 we can deduce that EMC effect and Fermi motion primarily affects the scattering from the valence quarks, while the shadowing mainly affects the scattering off the sea. Anti-shadowing occurs in the region of x where both sea and valence quarks are active.

4.6.3 EKS98 parametrization

The EKS98 parametrization [43, 44] is a quantitative, perturbative QCD based study of the PDFs of a bound proton in a nucleus with mass number $A > 2$. Basically, the procedure is rather similar than the one in extracting the PDFs of a free proton. The observables that have been compared with the experimental data are the ratios of the QED structure functions F_2 between nucleus A and deuterium D

$$R^A_{F_2}(x,Q^2) \equiv \frac{\frac{1}{A}F_2^A(x,Q^2)}{\frac{1}{2}F_2^D(x,Q^2)}, \tag{4.112}$$

and the ratios of differential Drell-Yan cross-sections between nucleus A and deuterium D

$$R^A_{\mathrm{DY}}(x_2,Q^2) \equiv \frac{\frac{1}{A}d\sigma^{pA}_{\mathrm{DY}}/dx_2dQ^2}{\frac{1}{2}d\sigma^{pD}_{\mathrm{DY}}/dx_2dQ^2}. \tag{4.113}$$

In the EKS98 framework the total nPDFs are expressed in terms of the nPDFs of a bound proton. This is achieved by means of assuming the *isospin symmetry*

$$u_{n/A} = d_{p/A} \qquad d_{n/A} = u_{p/A}, \tag{4.114}$$

where $q_{p/A} \equiv q_{p/A}(x,Q^2)$ is the average quark distribution in a bound proton of a nucleus A and similarly $q_{n/A} \equiv q_{n/A}(x,Q^2)$ for bound neutron, to hold for an arbitrary nucleus A. Similarly for antiquarks. This correspondence can be justified by noting that the strong interactions dominate inside the nucleon and from the point of view of strong interactions up and down quarks are just similar particles. Thus, the normalization of valence quarks

$$\begin{aligned}
\int_0^1 dx\left[u_{p/A} - u^{\mathrm{sea}}_{p/A}\right] &= 2 = \int_0^1 dx\left[d_{n/A} - d^{\mathrm{sea}}_{n/A}\right] \\
\int_0^1 dx\left[d_{p/A} - d^{\mathrm{sea}}_{p/A}\right] &= 1 = \int_0^1 dx\left[u_{n/A} - u^{\mathrm{sea}}_{n/A}\right]
\end{aligned}$$

implies that the isospin symmetry (4.114) should be rather reasonable as a first approximation.

Now the total up quark distribution u_A in a nucleus A with possible neutron excess $\Delta \equiv N - Z$, where $N = A - Z$ is the neutron number, can be expressed as

$$\begin{aligned}
u_A &= Zu_{p/A} + Nu_{n/A} \\
&\approx Zu_{p/A} + Nd_{p/A} \\
&= \frac{A}{2}\left(u_{p/A} + d_{p/A}\right) + \frac{\Delta}{2}\left(d_{p/A} - u_{p/A}\right).
\end{aligned} \tag{4.115}$$

Similarly for down quark

$$\begin{aligned}
d_A &= Zd_{p/A} + Nd_{n/A} \\
&\approx Zd_{p/A} + Nu_{p/A} \\
&= \frac{A}{2}\left(u_{p/A} + d_{p/A}\right) - \frac{\Delta}{2}\left(d_{p/A} - u_{p/A}\right).
\end{aligned} \tag{4.116}$$

For other flavors the distributions in a neutron and a proton are assumed to be equal

$$q_{n/A} = q_{p/A} \quad \text{for} \quad q = c, s, b, t.$$

Since the quarks and antiquarks are always produced in pairs, any differences between the quarks and the antiquarks in a nuclear sea can be neglected

$$q_A^S = \overline{q}_A^S = \overline{q}_A,$$

and the valence quark distributions is just $q_V^A \equiv q_A - \overline{q}_A$.

In this framework, the F_2 ratio becomes

$$\begin{aligned} R_{F_2}^A &= \frac{1}{N_{F_2}} \{5 \left(u_{p/A} + d_{p/A} + \overline{u}_{p/A} + \overline{d}_{p/A}\right) \\ &+ \frac{3\Delta}{A} \left(d_{p/A} - u_{p/A} + \overline{d}_{p/A} - \overline{u}_{p/A}\right) \\ &+ 4s_{p/A}\} \end{aligned} \tag{4.117}$$

where

$$N_{F_2} = 5 \left(u_{p/D} + d_{p/D} + \overline{u}_{p/D} + \overline{d}_{p/D}\right) + 4s_{p/D}.$$

The Drell-Yan ratio can be worked out from eq. (4.111). Denoting the free proton PDFs as $q_1(x_1) \equiv q_p$ and the PDFs of a proton in a heavy target nucleus as $q_2(x_2) \equiv q_{p/A}$ we get

$$\begin{aligned} R_{\mathrm{DY}}^A &= \{4 \left[u_p \left(\overline{u}_{p/A} + \overline{d}_{p/A}\right) + \overline{u}_p \left(u_{p/A} + d_{p/A}\right)\right] \\ &+ \left[d_p \left(\overline{d}_{p/A} + \overline{u}_{p/A}\right) + \overline{d}_p \left(d_{p/A} + u_{p/A}\right)\right] \\ &+ \frac{4\Delta}{A} \left[u_p \left(\overline{d}_{p/A} - \overline{u}_{p/A}\right) + \overline{u}_p \left(d_{p/A} - u_{p/A}\right)\right] \\ &+ \frac{\Delta}{A} \left[d_p \left(\overline{u}_{p/A} - \overline{d}_{p/A}\right) + \overline{d}_p \left(u_{p/A} - d_{p/A}\right)\right] \\ &+ 4s_p s_{p/A}\} \frac{1}{N_{\mathrm{DY}}}, \end{aligned} \tag{4.118}$$

where

$$\begin{aligned} N_{\mathrm{DY}} &= 4 \left[u_p \left(\overline{u}_{p/D} + \overline{d}_{p/D}\right) + \overline{u}_p \left(u_{p/D} + d_{p/D}\right)\right] \\ &+ \left[d_p \left(\overline{d}_{p/D} + \overline{u}_{p/D}\right) + \overline{d}_p \left(d_{p/D} + u_{p/D}\right)\right] + 4s_p s_{p/D} \end{aligned}$$

Instead of absolute nPDFs, the quantities that have been quantified in the EKS98 analysis are the ratios between the parton distributions of a proton in a bound nucleus and those of the free proton

$$R_q^A(x, Q^2) \equiv \frac{q_{p/A}(x, Q^2)}{q_p(x, Q^2)} \tag{4.119}$$

for each flavor of quarks and antiquarks and separately for sea and valence quarks in the case of u and d quarks. Due to the suppressing factor $\frac{\Delta}{A}$ in the non-isoscalar parts of the Drell-Yan and F_2 ratios and partly to the lack of non-isoscalar (meaning $N \neq Z$) experimental F_2^A data the individual ratios $R_{u_V}^A$, $R_{d_V}^A$

for the valence distributions and $R^A_{\overline{u}}, R^A_{\overline{d}}$ for the sea have been impossible to fold out. However, the combined valence and sea modifications, defined as

$$R^A_V(x,Q^2) \equiv \frac{u^V_{p/A}(x,Q^2) + d^V_{p/A}(x,Q^2)}{u^V_p(x,Q^2) + d^V_p(x,Q^2)} \tag{4.120}$$

$$R^A_{\overline{u}+\overline{d}}(x,Q^2) \equiv \frac{\overline{u}_{p/A}(x,Q^2) + \overline{d}_{p/A}(x,Q^2)}{\overline{u}_p(x,Q^2) + \overline{d}_p(x,Q^2)}, \tag{4.121}$$

can be rather well constrained and without a better knowledge, they are also assumed to be equal to the individual modifications

$$\begin{aligned} R^A_V(x,Q^2_0) &= R^A_{u_V}(x,Q^2_0) = R^A_{d_V}(x,Q^2_0) \\ R^A_{\overline{u}+\overline{d}}(x,Q^2_0) &= R^A_{\overline{u}}(x,Q^2_0) = R^A_{\overline{d}}(x,Q^2_0) \end{aligned}$$

at chosen initial scale $Q^2_0 = 2.25\,\mathrm{GeV}^2$ [43, 44]. It has turned out that once this assumption is made it holds also in the higher Q^2 — the DGLAP evolution to arbitrary Q^2 does not generate significant deviations. In fig. 4.15 we show an example of the the nuclear ratios and, not surprisingly, they closely resemble the behavior seen in fig. 4.14.

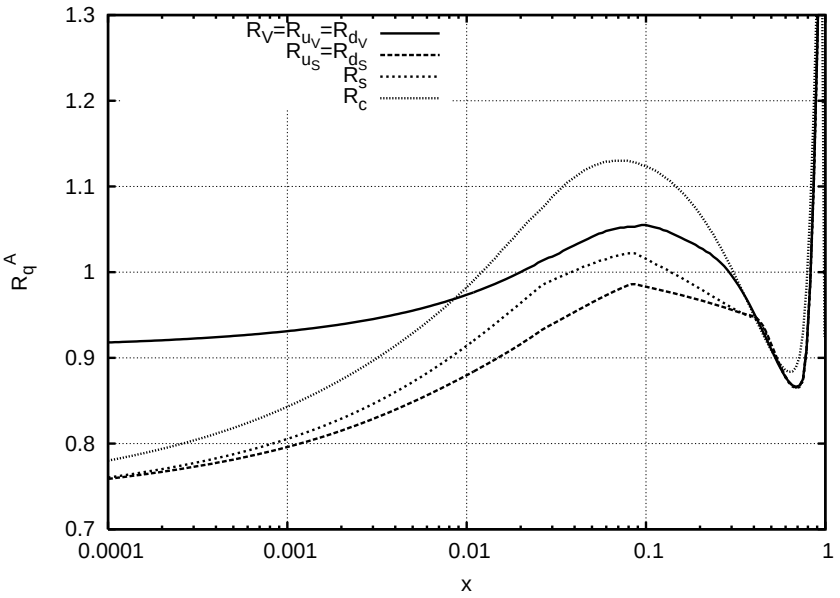

Figure 4.15: Example of nuclear ratios $R^A_q(x,Q^2)$ from EKS98 for $A = 56$ (iron) at $Q^2 = 25\,\mathrm{GeV}^2$. For up and down quarks both the valence and sea ratios are shown and from the heavier quarks strange and charm ratios.

Chapter 5

nPDFs and NuTeV anomaly

5.1 Observables R^{ν}, $R^{\overline{\nu}}$ and R^{-}

In this section we derive some simple formulas that relate the observables in neutrino DIS to the weak mixing angle $\sin^2\theta_{\mathrm{W}}$.

5.1.1 Sophistications to structure functions

So far we have treated all quarks as massless particles. However, under CC-interaction flavor of the struck quark changes and when a heavy quark is produced our zero mass approximation is no longer valid. For heavy quark production we have

$$\begin{aligned} (\xi p + q)^2 &= m_{q'}^2 \\ \underbrace{(\xi p)^2}_{\approx 0} + 2\xi p \cdot q + q^2 &= m_{q'}^2 \end{aligned}$$

$$\xi = \frac{m_{q'}^2 - q^2}{2p\cdot q} = \frac{Q^2}{2p\cdot q} + \frac{m_{q'}^2}{Q^2}\frac{Q^2}{2p\cdot q} = x\left(1 + \frac{m_{q'}^2}{Q^2}\right) \equiv x_{q'}, \qquad (5.1)$$

where $m_{q'}$ is the mass of the produced quark. We notice that Bjorken-x no longer represents the momentum fraction carried by the struck quark but it must be rescaled according to the equation above. Furthermore, because the momentum fraction $x_{q'}$ should not exceed unity we assume that

$$q\left(x_{q'} \geq 1\right) = 0$$

for each flavor q.

There is still one more thing to remember before writing down the structure functions for a nuclear target. The quarks that participate in weak interactions are not pure mass eigenstates but they are mixed according to Cabibbo-Kobayashi-Maskawa (CKM) matrix [23]:

$$\begin{pmatrix} d' \\ s' \\ b' \end{pmatrix} = \begin{pmatrix} V_{ud} & V_{us} & V_{ub} \\ V_{cd} & V_{cs} & V_{cb} \\ V_{td} & V_{ts} & V_{tb} \end{pmatrix} \begin{pmatrix} d \\ s \\ b \end{pmatrix}$$

$$\begin{pmatrix} |V_{ud}| & |V_{us}| & |V_{ub}| \\ |V_{cd}| & |V_{cs}| & |V_{cb}| \\ |V_{td}| & |V_{ts}| & |V_{tb}| \end{pmatrix} = \begin{pmatrix} 0.9739 \cdots 0.9751 & 0.221 \cdots 0.227 & 0.0029 \cdots 0.0045 \\ 0.221 \cdots 0.227 & 0.9730 \cdots 0.9744 & 0.039 \cdots 0.044 \\ 0.0048 \cdots 0.014 & 0.037 \cdots 0.043 & 0.9990 \cdots 0.9992 \end{pmatrix}$$

When the CKM-matrix elements and rescaling due to heavy quark production are taken account the structure functions for CC processes can be written as

$$\begin{aligned} {}^{CC}F_1^{\nu}\left(x,Q^2\right) &= \sum_{q,q'} |V_{qq'}|^2 \left[q\left(x_{q'},Q^2\right) + \overline{q}'\left(x_q,Q^2\right)\right] \\ {}^{CC}F_2^{\nu}\left(x,Q^2\right) &= 2\sum_{q,q'} |V_{qq'}|^2 \left[x_{q'}q\left(x_{q'},Q^2\right) + x_q\overline{q}'\left(x_q,Q^2\right)\right] \\ {}^{CC}F_3^{\nu}\left(x,Q^2\right) &= 2\sum_{q,q'} |V_{qq'}|^2 \left[q\left(x_{q'},Q^2\right) - \overline{q}'\left(x_q,Q^2\right)\right], \end{aligned} \tag{5.2}$$

where $q' = \{u,c,t\}$, $q = \{d,s,b\}$ and $|V_{qq'}|$ denotes the CKM-matrix element between flavors q and q'. Structure functions for antineutrino scattering are easily obtained just interchanging q and q':

$$\begin{aligned} {}^{CC}F_1^{\overline{\nu}}\left(x,Q^2\right) &= \sum_{q,q'} |V_{qq'}|^2 \left[q'\left(x_q,Q^2\right) + \overline{q}\left(x_{q'},Q^2\right)\right] \\ {}^{CC}F_2^{\overline{\nu}}\left(x,Q^2\right) &= 2\sum_{q,q'} |V_{qq'}|^2 \left[x_q q'\left(x_q,Q^2\right) + x_{q'}\overline{q}\left(x_{q'},Q^2\right)\right] \\ {}^{CC}F_3^{\overline{\nu}}\left(x,Q^2\right) &= 2\sum_{q,q'} |V_{qq'}|^2 \left[q'\left(x_q,Q^2\right) - \overline{q}\left(x_{q'},Q^2\right)\right]. \end{aligned} \tag{5.3}$$

In the neutral current processes the flavor of the struck quark does not change and we do not have rescaling in the Bjorken-x variable. Formulas for the structure functions are then

$$\begin{aligned} {}^{NC}F_1\left(x,Q^2\right) &= \sum_{q} \left(L_q^2 + R_q^2\right)\left[q\left(x,Q^2\right) + \overline{q}\left(x,Q^2\right)\right] \\ {}^{NC}F_2\left(x,Q^2\right) &= 2x\sum_{q} \left(L_q^2 + R_q^2\right)\left[q\left(x,Q^2\right) + \overline{q}\left(x,Q^2\right)\right] \\ {}^{NC}F_3\left(x,Q^2\right) &= 2\sum_{q} \left(L_q^2 - R_q^2\right)\left[q\left(x,Q^2\right) - \overline{q}\left(x,Q^2\right)\right], \end{aligned} \tag{5.4}$$

which are same for both ν and $\overline{\nu}$, and in which the sums now extend over all flavors $q = \{d,u,s,c,b,t\}$. In principle, these are now the structure functions that can be used together with general formulas (4.51) and (4.75) to compute cross-sections for scattering off a nuclear target.

5.1.2 Observables R^{ν} and $R^{\overline{\nu}}$ and Llewellyn Smith formula

As we now have the structure functions for nuclear target available we can derive simple expressions for the observables (1.1) and (1.2)

$$R^{\nu} \equiv \frac{\sigma^{NC}\left(\nu N\right)}{\sigma^{CC}\left(\nu N\right)}$$

$$R^{\overline{\nu}} \equiv \frac{\sigma^{NC}\left(\overline{\nu}N\right)}{\sigma^{CC}\left(\overline{\nu}N\right)}$$

for an isoscalar nuclear target in an approximation where just up and down quarks are present and there is no heavy quark production. Due to the negligible current masses of up and down quarks we can replace x_u and x_d in (5.2) and (5.3) with x. Leaving the Q^2 dependence implicit below the structure functions reduce to

$$\begin{aligned}
{}^{CC}F_1^\nu &= \left[d_A(x) + \overline{u}_A(x)\right] & {}^{CC}F_1^{\overline{\nu}} &= \left[u_A(x) + \overline{d}_A(x)\right] \\
{}^{CC}F_2^\nu &= {}^{CC}F_1^\nu \cdot 2x & {}^{CC}F_2^{\overline{\nu}} &= {}^{CC}F_1^{\overline{\nu}} \cdot 2x \\
{}^{CC}F_3^\nu &= 2\left[d_A(x) - \overline{u}_A(x)\right] & {}^{CC}F_3^{\overline{\nu}} &= 2\left[u_A(x) - \overline{d}_A(x)\right]
\end{aligned}$$

$$\begin{aligned}
{}^{NC}F_1 &= \left(L_u^2 + R_u^2\right)\left[u_A(x) + \overline{u}_A(x)\right] + \left(L_d^2 + R_d^2\right)\left[d_A(x) + \overline{d}_A(x)\right] \\
{}^{NC}F_2 &= {}^{NC}F_1 \cdot 2x \\
{}^{NC}F_3 &= 2\left(L_u^2 - R_u^2\right)\left[u_A(x) - \overline{u}_A(x)\right] + 2\left(L_d^2 - R_d^2\right)\left[d_A(x) - \overline{d}_A(x)\right].
\end{aligned}$$

Due to the isospin symmetry $u_{n/A} = d_{p/A}$ and $d_{n/A} = u_{p/A}$ we have, for example

$$\begin{aligned}
{}^{CC}F_1^\nu = d_A(x,Q^2) + \overline{u}_A(x,Q^2) &= \frac{A}{2}\left[d_{p/A} + d_{n/A} + \overline{u}_{p/A} + \overline{u}_{n/A}\right] \\
&= \frac{A}{2}\left[d_{p/A} + u_{p/A} + \overline{u}_{p/A} + \overline{d}_{p/A}\right].
\end{aligned}$$

Decomposing all other structure functions above similarly we get

$$\begin{aligned}
{}^{CC}F_1^\nu &= {}^{CC}F_1^{\overline{\nu}}, \quad {}^{CC}F_2^\nu = {}^{CC}F_2^{\overline{\nu}}, \quad {}^{CC}F_3^\nu = {}^{CC}F_3^{\overline{\nu}} \\
{}^{NC}F_1^\nu &= {}^{CC}F_1^\nu\left[\left(L_u^2 + L_d^2\right) + \left(R_u^2 + R_d^2\right)\right] \\
{}^{NC}F_2^\nu &= {}^{CC}F_2^\nu\left[\left(L_u^2 + L_d^2\right) + \left(R_u^2 + R_d^2\right)\right] \\
{}^{NC}F_3^\nu &= {}^{CC}F_3^\nu\left[\left(L_u^2 + L_d^2\right) - \left(R_u^2 + R_d^2\right)\right].
\end{aligned} \tag{5.5}$$

Plugging these into the differential cross-section formulas (4.51) and (4.75), and taking $Q^2 \ll M_Z^2, M_W^2$, we obtain

$$\begin{aligned}
R^\nu &= \frac{1}{4}\left(L_u^2 + L_d^2\right) + r\frac{1}{4}\left(R_u^2 + R_d^2\right) \\
&= \left(\frac{1}{2} - \sin^2\theta_W + \frac{5}{9}\sin^4\theta_W\right) + r\left(\frac{5}{9}\sin^4\theta_W\right) \\
&= g_L^2 + r\, g_R^2
\end{aligned} \tag{5.6}$$

$$\begin{aligned}
R^{\overline{\nu}} &= \frac{1}{4}\left(L_u^2 + L_d^2\right) + r^{-1}\frac{1}{4}\left(R_u^2 + R_d^2\right) \\
&= \left(\frac{1}{2} - \sin^2\theta_W + \frac{5}{9}\sin^4\theta_W\right) + r^{-1}\left(\frac{5}{9}\sin^4\theta_W\right) \\
&= g_L^2 + r^{-1}\, g_R^2,
\end{aligned} \tag{5.7}$$

where we have used the couplings (4.77) and introduced definitions

$$\begin{aligned} r &\equiv \frac{d^2\sigma^{CC}\left(\overline{\nu}N\right)/(dxdQ^2)}{d^2\sigma^{CC}\left(\nu N\right)/(dxdQ^2)} \\ g_L^2 &\equiv \frac{1}{2} - \sin^2\theta_{\mathrm{W}} + \frac{5}{9}\sin^4\theta_W \\ g_R^2 &\equiv \frac{5}{9}\sin^4\theta_W . \end{aligned} \tag{5.8}$$

The equations (5.7) and (5.6) are the Llewellyn Smith ratios [45].

Although both of these are related to the weak mixing angle $\sin^2\theta_{\mathrm{W}}$ one should still explicitly know the ratio r to extract the value of mixing angle. Furthermore, these relations were derived simply forgetting the sea of heavier quarks and the uncertainties arising from these would make extraction of Weinberg angle more difficult. The solution is to combine these two to a single quantity R^-.

5.1.3 Observable R^- and Paschos-Wolfenstein formula

The observable that we are ultimately interested in is the ratio already introduced in eq. (1.3),

$$R^- = \frac{\sigma^{NC}(\nu N) - \sigma^{NC}(\overline{\nu}N)}{\sigma^{CC}(\nu N) - \sigma^{CC}(\overline{\nu}N)},$$

which was also used in NuTeV the analysis. It is clear from the general formulas (4.51) and (4.75) that we need to compute quantities $F_1^\nu - F_1^{\overline{\nu}}$, $F_2^\nu - F_2^{\overline{\nu}}$ and $F_3^\nu + F_3^{\overline{\nu}}$ for both CC and NC structure functions. Let us start with the CC structure functions (5.3):

$$\begin{aligned} {}^{CC}F_1^\nu - {}^{CC}F_1^{\overline{\nu}} &= \sum_{qq'} |V_{qq'}|^2 \left[q\left(x_{q'}\right) - \overline{q}\left(x_{q'}\right) + \overline{q}'\left(x_q\right) - q'\left(x_q\right)\right] \\ &= \sum_{qq'} |V_{qq'}|^2 \left[q_V\left(x_{q'}\right) - q'_V\left(x_q\right)\right]. \end{aligned}$$

In a nuclear target A only up and down quarks have non-zero valence distributions and we get

$$\begin{aligned} {}^{CC}F_1^\nu - {}^{CC}F_1^{\overline{\nu}} &= |V_{ud}|^2 \left[d_V^A\left(x_u\right) - u_V^A\left(x_d\right)\right] - |V_{us}|^2 u_V^A\left(x_s\right) \\ &\quad - |V_{ub}|^2 u_V^A\left(x_b\right) + |V_{cd}|^2 d_V^A\left(x_c\right), \end{aligned}$$

in which we have already omitted the term corresponding to top quark production because its high mass and small CKM-matrix element $|V_{td}|$. Due to the small mass of u, d and s quarks, we can replace all x_u, x_d and x_s with x and

implementing this simplification we obtain

$$\begin{aligned}
{}^{CC}F_1^{\nu} - {}^{CC}F_1^{\overline{\nu}} &= |V_{ud}|^2 \left[d_V^A(x) - u_V^A(x)\right] - |V_{us}|^2 u_V^A(x) \\
&\quad - |V_{ub}|^2 u_V^A(x_b) + |V_{cd}|^2 d_V^A(x_c) \\
{}^{CC}F_2^{\nu} - {}^{CC}F_2^{\overline{\nu}} &= 2|V_{ud}|^2 x\left[d_V^A(x) - u_V^A(x)\right] - 2|V_{us}|^2 x u_V^A(x) \\
&\quad -2|V_{ub}|^2 x_b u_V^A(x_b) + 2|V_{cd}|^2 x_c d_V^A(x_c) \qquad (5.9) \\
{}^{CC}F_3^{\nu} + {}^{CC}F_3^{\overline{\nu}} &= 2|V_{ud}|^2 \left[d_V^A(x) + u_V^A(x)\right] + 2|V_{us}|^2 u_V^A(x) \\
&\quad +2|V_{ub}|^2 u_V^A(x_b) + 2|V_{cd}|^2 d_V^A(x_c).
\end{aligned}$$

The results for $F_2^{\nu} - F_2^{\overline{\nu}}$ and $F_3^{\nu} + F_3^{\overline{\nu}}$ are also shown above.

It is straightforward to calculate these same quantities for NC structure functions with the same procedure just explained and we now merely quote the results

$$\begin{aligned}
{}^{NC}F_1^{\nu} - {}^{NC}F_1^{\overline{\nu}} &= {}^{NC}F_2^{\nu} - {}^{NC}F_2^{\overline{\nu}} = 0 \qquad (5.10) \\
{}^{NC}F_3^{\nu} + {}^{NC}F_3^{\overline{\nu}} &= 4\left(1 - \frac{8}{3}\sin^2\theta_W\right) u_V^A(x) + 4\left(1 - \frac{4}{3}\sin^2\theta_W\right) d_V^A(x),
\end{aligned}$$

where we have explicitly used the couplings (4.77).

If we consider R^- in the case of an isoscalar target, when mixing between quark generations is neglected, we set the neutron excess $\Delta = 0$ and for CKM-matrix elements $|V_{us}| = |V_{ub}| = |V_{cd}| = 0$, $|V_{ud}| = 1$. The quantities above then reduce to

$$\begin{aligned}
u_V^A = d_V^A &= \frac{A}{2}\left(u_{p/A}^V + d_{p/A}^V\right) \\
{}^{CC}\left(F_3^{\nu} + F_3^{\overline{\nu}}\right) &= 2A\left[u_{p/A}^V + d_{p/A}^V\right] \\
{}^{NC}\left(F_3^{\nu} + F_3^{\overline{\nu}}\right) &= 4A\left(1 - 2\sin^2\theta_W\right)\left[u_{p/A}^V + d_{p/A}^V\right].
\end{aligned}$$

With these simplifications together with an assumption of the range of low momentum transfer $Q^2 \ll M_W^2, M_Z^2$, we get a very neat result

$$R^- = \frac{1}{2} - \sin^2\theta_W. \qquad (5.11)$$

This is known as *Paschos-Wolfenstein relation*, originally derived in [46]. In this quantity the contribution of heavier sea quarks is stripped away and it is thus more reliable to extract the value of $\sin^2\theta_{\mathrm{W}}$ in this way.

5.2 Can $R^A_{d/V} \neq R^A_{u/V}$ cause NuTeV anomaly?

Iron ($A = 56$, $\Delta = 4$) used in the NuTeV experiment is not an isoscalar target and corrections to the simple Paschos-Wolfenstein relationship do arise. To first order in $\frac{\Delta}{A} \sim 0.07$ the corrected version is

$$R^-(x,Q^2,s_{\rm W}) \approx \left(\frac{1}{2}-s_{\rm W}\right)\left[1-\frac{\Delta}{A}h(y,s_{\rm W})\frac{u^V_{p/A}-d^V_{p/A}}{u^V_{p/A}+d^V_{p/A}}\right] \quad (5.12)$$

where

$$h(y,s_{\rm W}) \equiv \frac{1+(1-y)^2}{1-(1-y)^2} - \frac{2s_{\rm W}}{3-6s_{\rm W}} \quad (5.13)$$

and

$$s_{\rm W} \equiv \sin^2\theta_{\rm W}.$$

Interestingly, if the individual nuclear modifications $R^A_{u_V} = R^A_{d_V} = R^A_V$ as in EKS98, the nuclear effects cancel! But are they really equal?

Let us now suppose that $R^A_{dV} \neq R^A_{uV}$, and see what consequences it may bring about. Since R^A_V is constrained by the measurable quantities $R_{\rm DY}$ and R_{F_2}, the condition

$$R^A_V(x,Q^2) = \frac{u^V_{p/A}(x,Q^2)+d^V_{p/A}(x,Q^2)}{u^V_p(x,Q^2)+d^V_p(x,Q^2)} = \frac{R^A_{u_V}\,u^V_p(x,Q^2)+R^A_{d_V}\,d^V_p(x,Q^2)}{u^V_p(x,Q^2)+d^V_p(x,Q^2)}$$

should always be satisfied. This means that in the symmetric combination

$$u^V_{p/A}+d^V_{p/A} = R^A_V\left(u^V_p+d^V_p\right)$$

no change relative to the EKS98 is induced and the conservation of momentum is guaranteed (meaning that valence quarks carry the same fraction of nucleon momentum as before). However, the antisymmetric combination

$$u^V_{p/A}-d^V_{p/A} \neq R^A_V\left(u^V_p-d^V_p\right),$$

and consequently also the value of R^- changes!

In what follows our ambitious intention is to show that instead of suggesting a deviation in $\sin^2\theta_{\rm W}$, the NuTeV anomaly could be as well as consequence of simply having $R^A_{uV} \neq R^A_{dV}$!

5.2.1 The procedure

We want to understand quantitatively how $R^A_{d_V}$ and $R^A_{u_V}$ should deviate from each other and R^A_V in order to produce an effect that looks similar as having as large deviation in $s_{\rm W}$ reported by NuTeV. The principle is to calculate R^- in two ways:

1. For $R^-(x,Q^2,s^{\rm NuTeV}_{\rm W},R^A_{u_V}=R^A_{d_V}=R^A_V)$ we use NuTeV $s^{\rm NuTeV}_{\rm W}=0.2277$ and assume $R^A_{u_V}=R^A_{d_V}=R^A_V$.
2. For $R^-(x,Q^2,\langle s_{\rm W}\rangle,R^A_{u_V}\neq R^A_{d_V})$ we take world average $\langle s_{\rm W}\rangle = 0.2227$ and allow $R^A_{u_V}\neq R^A_{d_V}$.

The task is then to decompose R^A_V to $R^A_{d_V}$ and $R^A_{u_V}$ in such a way that the following conditions are met:

- Difference between the above two R^-s goes to zero

  $$R^-(x, Q^2, s_{\rm W}^{\rm NuTeV}, R^A_{uV} = R^A_{dV} = R^A_V) - R^-(x, Q^2, \langle s_{\rm W}\rangle, R^A_{uV} \neq R^A_{dV}) \to 0$$

- R^A_V from EKS98 is recovered

  $$R^A_V(x, Q^2) = \frac{R^A_{u_V}\, u^V_p(x, Q^2) + R^A_{d_V}\, d^V_p(x, Q^2)}{u^V_p(x, Q^2) + d^V_p(x, Q^2)}$$

- Charge and baryon number are conserved

  $$\int_0^1 dx\, R^A_{u_V} u^V_p = 2 \qquad \int_0^1 dx\, R^A_{d_V} d^V_p = 1.$$

Rather than using the double differential cross-sections we should integrate them over Bjorken-x according to the NuTeV kinematics taking heavy quark production and Cabibbo-mixing into account. Although this calculation has to be carried out numerically we can still understand the direction of the deviation analytically from the differential form of R^- in eq. (5.12): Since the quantity $h(y, s_{\rm W})$ is not very sensitive to small changes in $s_{\rm W}$ it is nearly constant $h \equiv h(y, \langle s_{\rm W}\rangle) \approx h(y, s_{\rm W}^{\rm NuTeV})$, and at given x and Q^2 we require

$$\left(\frac{1}{2} - s_{\rm W}^{\rm NuTeV}\right)\left[1 - \frac{\Delta}{A} h \frac{u^V_p - d^V_p}{u^V_p + d^V_p}\right] = \left(\frac{1}{2} - \langle s_{\rm W}\rangle\right)\left[1 - \frac{\Delta}{A} h \frac{u^V_{p/A} - d^V_{p/A}}{u^V_{p/A} + d^V_{p/A}}\right].$$

Because $s_{\rm W}^{\rm NuTeV} > \langle s_{\rm W}\rangle$ we get

$$\frac{u^V_p - d^V_p}{u^V_p + d^V_p} < \frac{u^V_{p/A} - d^V_{p/A}}{u^V_{p/A} + d^V_{p/A}} \tag{5.14}$$

which leads to a condition

$$R^A_{d_V}(x, Q^2) < R^A_V(x, Q^2) < R^A_{u_V}(x, Q^2). \tag{5.15}$$

in a region of x and Q^2 to which the NuTeV experiment is most sensitive. Interestingly, our result seems contradictory to the one by Kumano [48], who has also studied this issue.

5.2.2 Results

In the NuTeV experiment the ν and $\overline{\nu}$ cross-sections were measured over a range of beam energies $E_{\rm beam}$, virtualities Q^2 and Bjorken-x. The details about the flux and energy distribution of the incoming neutrinos rest on the Monte Carlo simulation and we cannot reproduce the actual kinematical distribution of the NuTeV data. Instead, we simply use the average values

$$\begin{aligned} \langle E_{\rm beam}\rangle &= 116\ {\rm GeV} \\ \langle Q^2\rangle &= 20.5\,{\rm GeV}^2 \end{aligned}$$

and impose the NuTeV cuts on the final state hadronic energy $yE_{\rm beam} + M$

$$E_{\rm min} \leq yE_{\rm beam} + M \leq E_{\rm max}$$

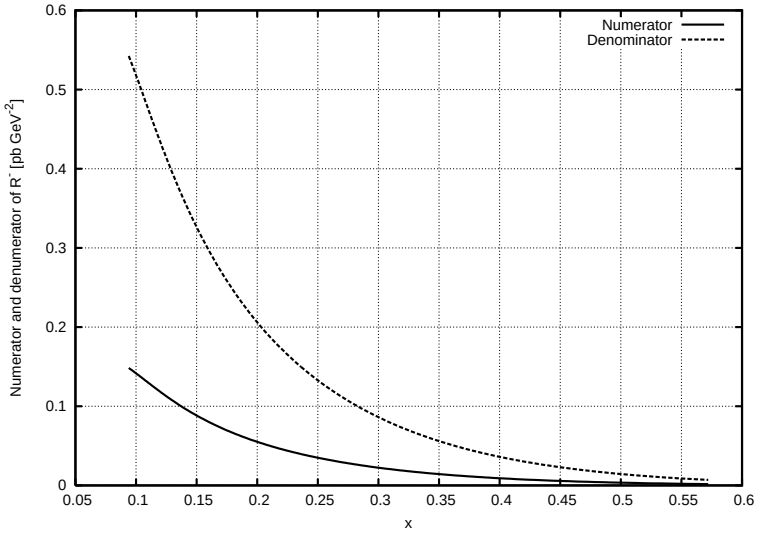

Figure 5.1: Differences of double differential neutrino and antineutrino cross-sections. In the ratio R^- the NC difference is in the numerator while the CC difference enters to the denominator. The curves are calculated for iron ($A = 56$, $\Delta = 4$) with EKS98 nuclear modifications.

with $E_{\min} = 20\,\mathrm{GeV}$ and $E_{\max} = 180\,\mathrm{GeV}$. These, together with the requirement $y \leq 1$ constrain x between

$$0.094 \approx \frac{Q^2}{2EM} = x_{\min} \leq x \leq x_{\max} = \frac{Q^2}{2(E_{\min} - M)} \approx 0.57, \tag{5.16}$$

and fixes the x-region where (5.15) must hold in order to find a solution.

To find the x-region which mostly contributes in the ratio R^- we use the double differential cross-sections and calculate the numerator and the denominator of R^- separately. The result is shown in fig. 5.1 and it is obvious that the smallest x-region is the most important one. This means that the largest differences between R_{d_V} and R_{u_V} should be introduced around $x \sim x_{\min} \sim 0.1$.

To get a crude order-of-magnitude estimate to check whether our idea is realistic or not we find a solution in which the valence-d modification $R^A_{d_V}$ is parametrized in the following, very rough manner:

$$R^A_{d_V}(x, Q^2) = \begin{cases} C_1 = \text{constant}, & \text{when } x < x_{\min} \\ C_2 = \text{constant}, & \text{when } x_{\min} \leq x \leq x_{\max} \\ R^A_V(x, Q^2) \,\text{from EKS98} & \text{when } x_{\max} < x \leq 1 \end{cases} . \tag{5.17}$$

A solution of this kind is shown in fig. (5.2). Interestingly, the deviations of $R^A_{u_V}$ and $R^A_{d_V}$ from R^A_V that would cause as much deviation in R^- as does changing mixing angle from $\langle s_{\mathrm{W}} \rangle$ to $s_{\mathrm{W}}^{\mathrm{NuTeV}}$ are only modest in $R^A_{u_V}$: **About 20% modifications in $R^A_{u_V}$ from R^A_V should be enough!**

In addition to this 'extreme' all-explaining case we consider a continuous, more 'natural-looking' parametrization for $R^A_{d_V}$. An example of such is shown

in fig. 5.3. Also in this case our conservation laws are fulfilled and the deviation induced in R^- is equivalent to a $\Delta s_{\rm W} \approx 0.0018$. This is around 36% of the whole NuTeV anomaly.

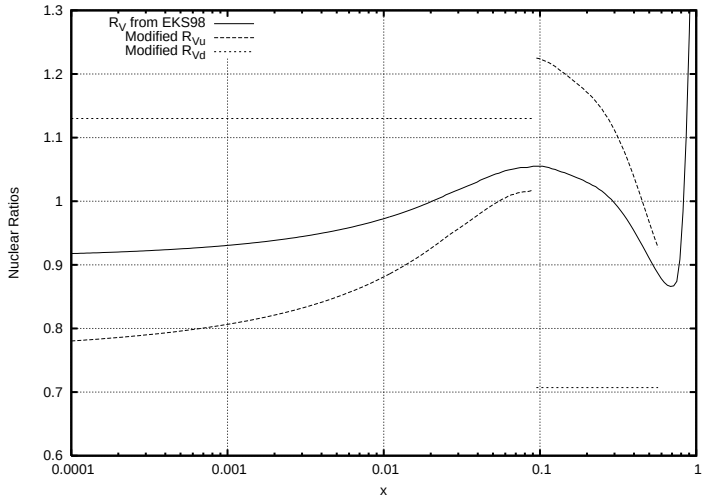

Figure 5.2: An order-of-magnitude estimate about the nuclear valence quark modifications needed to alone account for the large value of x_W reported by NuTeV. The individual modifications $R^A_{u_V}$ and $R^A_{d_V}$ for iron ($A = 56$, $\Delta = 4$) are shown as functions of x at a fixed scale $Q^2 = 20.5$ GeV^2. The average valence quark modification R^A_V is from the EKS98-parametrization [43, 44]. The coefficients in eq. (5.17) are $C_1 = 1.13$ and $C_1 = 0.7070$.

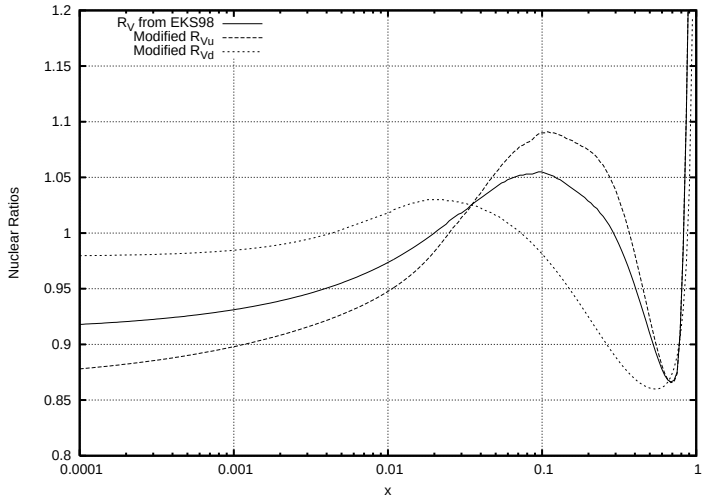

Figure 5.3: As fig. 5.2 but in this case the shown valence quark modifications would explain about third of the large value of x_W reported by NuTeV.

5.2.3 Consequences in R_{DY} and R_{F_2}

So far so good. We have shown that having $R^A_{u_V} \neq R^A_{d_V}$ affects the observed ratio R^- but we have not yet discussed the other consequences it may cause. Most importantly, we should check how largely it affects the ratios R_{F_2} and R_{DY} that are the basis for determining the nPDFs.

To make this as transparent as possible, we calculate the ratios R_{F_2} and R_{DY} for iron in two ways. First, using the EKS98 values $R^A_{u_V} = R^A_{d_V} = R^A_V$ and then with the 'extreme' modifications of fig. (5.2). The differences between these two quantities turn out to be very tiny as can be seen from fig. 5.4 where we have also added some experimental data for an iron nucleus to illustrate how small the difference resulting from having $R^A_{u_V} \neq R^A_{d_V}$ really is compared to the typical experimental uncertainties.

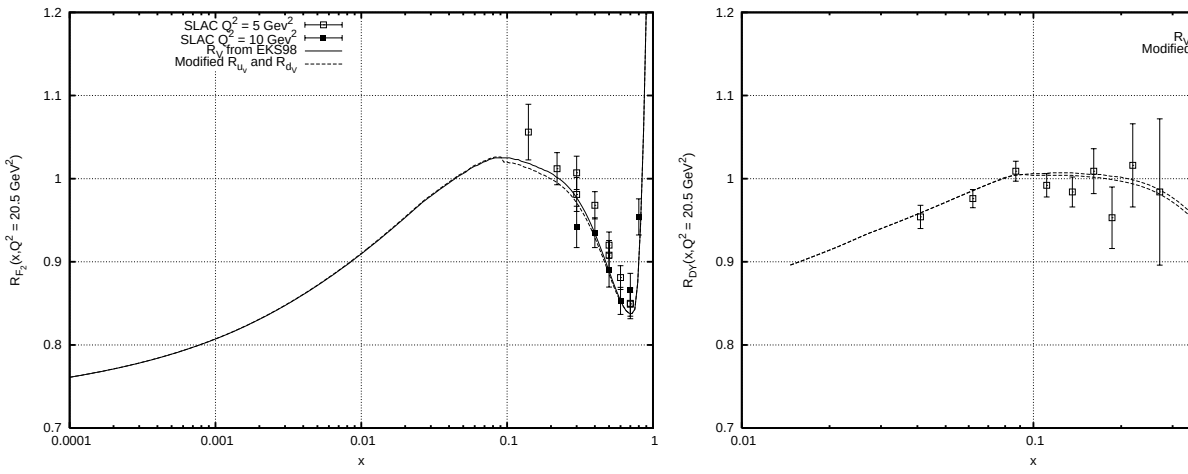

(a) $R^A_{F_2}$ (b) R_{DY}

Figure 5.4: The nuclear modification ratios $R^A_{F_2}$ and $R_{\mathrm{DY}}(Q^2 = 20.5\,\mathrm{GeV}^2)$ for iron $A = 56$ with neutron excess $\Delta = 4$ at fixed $Q^2 = 20.5\,\mathrm{GeV}^2$. The solid lines are obtained with the EKS98 modification and the dashed one results from 'extreme' modifications of eq. 5.17 and fig. 5.2. In the case of Drell-Yan ratio R_{DY} the variable x refers to the target(iron) momentum fraction. The data shown are from **FNAL-772** [29] and **SLAC** [47] experiments.

The NuTeV group has argued that all nuclear effects are correctly taken into account by their analysis since it incorporates the nPDFs that are obtained with the very same target as the one which was used in the $\sin^2\theta_{\mathrm{W}}$ experiment. We have, however, just shown that even the global analysis of nPDFs is not able to unfold the possible difference between the nuclear effects of valence-u and valence-d quarks. This indicates that if such a difference exists, the NuTeV group cannot have taken such an effect into account, either!

5.3 Conclusion an outlook

The NuTeV collaboration has measured the value of Weinberg weak mixing angle $\sin^2\theta_{\rm W}$ using deep inelastic neutrino scattering off an iron target. The extraction was made through the Paschos-Wolfenstein ratio R^- which strips away most part of the detailed parton structure effects of the iron nucleus. However, the imprint is not completely lost: iron is a non-isoscalar nucleus and R^- gets contribution from the valence distributions of up and down quarks.

The global analysis of Drell-Yan and DIS data together with sum rules, provides currently the most precise knowledge of the nuclear effects in PDFs compared to the free proton. However, even the global perturbatice QCD analysis cannot determine the nuclear corrections for the valence-d and valence-u distributions separately and without better knowledge or further constraints one usually assumes the average modification

$$R_V^A(x,Q^2) \equiv \frac{u_{p/A}^V(x,Q^2) + d_{p/A}^V(x,Q^2)}{u_p^V(x,Q^2) + d_p^V(x,Q^2)},$$

which is quite well constrained, to apply for both: $R_{u_V}^A \approx R_{d_V}^A \approx R_V^A$.

We have pointed out that the extraction of $\sin^2\theta_{\rm W}$ via Paschos-Wolfenstein ratio R^- is affected by this approximation and taking $R_{u_V}^A \neq R_{d_V}^A \neq R_V^A$ we have been able to show that changes of the order of only 20-40% can lead to modification of $R^-(Q^2 = 20.5\,\mathrm{GeV}^2)$ which is as large as would be induced by increasing the $\sin^2\theta_{\rm W}$ to the large value reported by NuTeV! As long as the modifications are made in such a way that R_V^A from the global analysis is always recovered, the charge, momentum and baryon number of a proton are also conserved. We have also explicitly demonstrated that the deviations induced to the measurable ratios R_{DY} of Drell-Yan and R_{F_2} of DIS that provide the data driven constraints for the nuclear corrections are not on a detectable level compared to the current experimental data.

Thus, it should be possible to explain the whole anomaly just by introducing mutually different nuclear corrections for valence-u and valence-d quarks and, in fact, this anomaly can be seen a as a first hint at least about the *direction* of the difference at $x \geq 0.1$. In other words, the exciting NuTeV result can be added to the list of data constraints in the global analysis of the nPDFs. The results of this thesis will be published soon [16], and to perform such an updated global analysis will be our future task.

To settle down the NuTeV anomaly, at least two independent experiments to pin down the Weinberg angle from neutrino experiments exist. The first of these, the NOMAD experiment in CERN [49], tries to extract the Weinberg angle from R^ν and is already in the stage of data analysis. In the another one, still under planning, the strategy is to measure the Weinberg angle in a reactor-based experiment [50]. In any case, this thesis shows that it is far too early to claim any appearance of beyond Standard Model physics in the NuTeV anomaly.

Bibliography

[1] D. Abbaneo *et al.* [ALEPH Collaboration], arXiv:hep-ex/0112021.

[2] G. P. Zeller *et al.* [NuTeV Collaboration], Phys. Rev. Lett. **88** (2002) 091802 [Erratum-ibid. **90** (2003) 239902] [arXiv:hep-ex/0110059].

[3] The figures are from NuTeV web page http://www-e815.fnal.gov/NuTeV.html

[4] K. S. McFarland and S. O. Moch, arXiv:hep-ph/0306052.

[5] J. T. Londergan, arXiv:hep-ph/0408243.

[6] S. Davidson, S. Forte, P. Gambino, N. Rius and A. Strumia, JHEP **0202** (2002) 037 [arXiv:hep-ph/0112302].

[7] O. Brein, B. Koch and W. Hollik, arXiv:hep-ph/0408331.

[8] E. Ma, arXiv:hep-ph/0306218.

[9] J. R. Yablon, arXiv:hep-ph/0509223.

[10] B. A. Dobrescu and R. K. Ellis, Phys. Rev. D **69** (2004) 114014 [arXiv:hep-ph/0310154].

[11] A. B. Arbuzov, D. Y. Bardin and L. V. Kalinovskaya, JHEP **0506** (2005) 078 [arXiv:hep-ph/0407203].

[12] K. P. O. Diener, S. Dittmaier and W. Hollik, Phys. Rev. D **69** (2004) 073005 [arXiv:hep-ph/0310364].

[13] G. P. Zeller *et al.* [NuTeV Collaboration], Phys. Rev. D **65** (2002) 111103 [Erratum-ibid. D **67** (2003) 119902] [arXiv:hep-ex/0203004].

[14] D. Mason [NuTeV Collaboration], arXiv:hep-ex/0405037.

[15] S. Kretzer, F. Olness, J. Pumplin, D. Stump, W. K. Tung and M. H. Reno, Phys. Rev. Lett. **93** (2004) 041802 [arXiv:hep-ph/0312322].

[16] K. J. Eskola and H. Paukkunen, paper in preparation.

[17] S. Weinberg, Phys. Rev. Lett. **19** (1967) 1264.

[18] P. T. Matthews and A. Salam, Phys. Lett. **8** (1964) 357.

[19] M. Peskin and D. Schroeder, An Introduction to Quantum Field Theory, Westview 1995

[20] H. Lehmann, K. Symanzik and W. Zimmermann, Nuovo Cim. **1** (1955) 205.

[21] R. Field, Applications of perturbative QCD, Addison Wesley (1989).

[22] C. Quigg, Gauge Theories of the Strong, Weak & Electromagnetic Interactions, HarperCollins Publishers (1997).

[23] S. Eidelman *et al.*, Phys. Lett. B **592** (2004) 1.

[24] J. D. Bjorken and E. A. Paschos, Phys. Rev. **185** (1969) 1975.

[25] W. G. Seligman, FERMILAB-THESIS-1997-21

[26] D. MacFarlane *et al.*, Z. Phys. C **26** (1984) 1.

[27] J. P. Berge *et al.*, Z. Phys. C **35** (1987) 443.

[28] S. D. Drell and T. M. Yan, Phys. Rev. Lett. **25** (1970) 316 [Erratum-ibid. **25** (1970) 902].

[29] D. M. Alde *et al.*, Phys. Rev. Lett. **64** (1990) 2479.

[30] J. D. Bjorken, Phys. Rev. **179** (1969) 1547.

[31] Y. L. Dokshitzer, "Calculation Of The Structure Functions For Deep Inelastic Scattering And E+ Sov. Phys. JETP **46** (1977) 641 [Zh. Eksp. Teor. Fiz. **73** (1977) 1216].

[32] V. N. Gribov and L. N. Lipatov, Sov. J. Nucl. Phys. **15**, 438, 675 (1972) [Yad. Fiz. **15**, 781 (1972)].

[33] G. Altarelli and G. Parisi, Nucl. Phys. B **126** (1977) 298.

[34] J. Pumplin, arXiv:hep-ph/0507093.

[35] J. Pumplin, D. R. Stump, J. Huston, H. L. Lai, P. Nadolsky and W. K. Tung, JHEP **0207** (2002) 012 [arXiv:hep-ph/0201195].

[36] M. Derrick *et al.* [ZEUS Collaboration], Z. Phys. C **72** (1996) 399 [arXiv:hep-ex/9607002].

[37] M. Arneodo *et al.* [New Muon Collaboration], Nucl. Phys. B **483** (1997) 3 [arXiv:hep-ph/9610231].

[38] A. C. Benvenuti *et al.* [BCDMS Collaboration], Phys. Lett. B **223** (1989) 485.

[39] C. Adloff *et al.* [H1 Collaboration], Eur. Phys. J. C **21** (2001) 33 [arXiv:hep-ex/0012053].

[40] L. W. Whitlow, E. M. Riordan, S. Dasu, S. Rock and A. Bodek, "Precise measurements of the proton and deuteron structure functions from a Phys. Lett. B **282** (1992) 475.

[41] S. Chekanov *et al.* [ZEUS Collaboration], Eur. Phys. J. C **21** (2001) 443 [arXiv:hep-ex/0105090].

[42] P. Amaudruz *et al.* [New Muon Collaboration], Nucl. Phys. B **441** (1995) 3 [arXiv:hep-ph/9503291].

[43] K. J. Eskola, V. J. Kolhinen and P. V. Ruuskanen, Nucl. Phys. B **535** (1998) 351 [arXiv:hep-ph/9802350].

[44] K. J. Eskola, V. J. Kolhinen and C. A. Salgado, Eur. Phys. J. C **9** (1999) 61 [arXiv:hep-ph/9807297].

[45] C. H. Llewellyn Smith, Nucl. Phys. B **228** (1983) 205.

[46] E. A. Paschos and L. Wolfenstein, Phys. Rev. D **7** (1973) 91.

[47] J. Gomez *et al.*, Phys. Rev. D **49** (1994) 4348.

[48] M. Hirai, S. Kumano and T. H. Nagai, Phys. Rev. D **71** (2005) 113007 [arXiv:hep-ph/0412284].

[49] R. Petti [NOMAD Collaboration], arXiv:hep-ex/0411032.

[50] J. M. Conrad, J. M. Link and M. H. Shaevitz, Phys. Rev. D **71**, 073013 (2005) [arXiv:hep-ex/0403048].